2023

Identifying Factors Controlling Dinophysis Spp. Feeding, Growth, And Toxin Production Through Field And Lab Studies

Vanessa R. Strohm
College of William and Mary - Virginia Institute of Marine Science, vanessastrohm04@gmail.com

Identifying Factors Controlling *Dinophysis* spp. Feeding, Growth, and Toxin Production Through Field and Lab Studies

---

A Thesis

Presented to

The Faculty of the School of Marine Science

William & Mary

In Partial Fulfillment

of the Requirements for the Degree of

Master of Science

---

by

Vanessa Reneé Strohm

May 2023

APPROVAL PAGE

This Thesis is submitted in partial fulfillment of

the requirements for the degree of

Master of Science

Vanessa Reneé Strohm

Approved by the Committee, April 2023

Juliette L. Smith, Ph.D.
Advisor

Nicole C. Millette, Ph.D.

Richard A. Snyder, Ph.D.

Lisa Campbell, Ph.D.
Texas A&M University
College Station, Texas, USA

To my parents, for always encouraging me to pursue my dreams, and supporting me every step of the way.

CONTENTS

ACKNOWLEDGEMENTS

First and foremost, I would like to thank my advisor, Dr. Juliette Smith, for her support and guidance during my graduate career. Thank you for allowing me the opportunity to come work in the Smith HAB lab. Starting graduate school during the peak of the pandemic was definitely not easy, and we both had to learn to be flexible and adapt to a changing environment. Thank you to our lab manager, Marta Sanderson, for her support with lab experiments, running the mass specs, and maintaining the IFCB. Her support and dedication to her own work, as well as students' work is greatly appreciated. I would also like to thank I-Shuo (Wade) Huang for his unwavering support and encouragement and for teaching me about the IFCB and preparing me to run it in his absence. So many hours were spent late in the lab or on zoom, during the week or on weekends, to make sure the IFCB was up and running, or I received the data I needed. Thank you to Nour Ayache for teaching me everything I know about culturing *Dinophysis* and helping me with all my culturing experiments. I would also like to thank other Smith HAB Lab members that I have worked with during my time at VIMS, including Josh Garber, Sarah Pease, Taylor Armstrong, and Jackie Friedman. I would also like to acknowledge my former REU student, Maya Casey, for her work with the IFCB maintenance and data analysis during the summer of 2021. I would also like to thank undergraduates Amy Menegay and Jordon Mercer, for their help in the lab. It has been a pleasure to work with both of you for the past year. I would also like to thank my committee members, Dr. Nicole Millette, Dr. Richard Snyder, and Dr. Lisa Campbell for their responsiveness to my questions, and their suggestions, and recommendations.

Additionally, I would like to thank the entire team at McLane for their assistance with the IFCB. I came into graduate school knowing absolutely nothing about specialized machinery like the IFCB, and without their help, would not have been able to get the IFCB up and running. Similarly, thank you to Todd Nelson for his assistance with the VIMS pier IFCB set-up and power monitoring and Tanya Ward for her technical assistance with data storage.

I would also like to acknowledge the help I received from fellow students and friends. Thank you to A. Challen Hyman for his help with data analysis for Chapter 1. Thank you to Josh Garber for being both a roommate, lab mate, and friend. Thank you to present and former Hedge House occupants for welcoming me into the family. Lastly, many thanks to Grace Molino, Jainita Patel, and Aly Hall for helping me with my research and being amazing, encouraging, supportive friends. I will always cherish our friendship.

Finally, I would like to thank the Office of Academic Studies for all they do for graduate students. Their support and dedication to graduate students is appreciated, and they truly care about the success of each and every student. Thank you to the VIMS community as a whole, for being so supportive and willing to help, even during the pandemic. I have met so many amazing people during my time at VIMS.

This work was funded by the NOAA National Centers for Coastal Ocean Science Competitive Research, ECOHAB Program (award number #NA19NOS4780182) and through VIMS fellowships: Harry & Barbara Hager Fellowship, Strickland Family Fellowship, and a Student Research Grant.

LIST OF TABLES

LIST OF FIGURES

THESIS ABSTRACT

Harmful algal blooms (HABs) and their associated phycotoxins pose a threat to both human and shellfish health around the world. *Dinophysis* spp., a causative organism of diarrhetic shellfish poisoning (DSP) in humans, and its two toxin classes: dinophysistoxins (DTXs) and pectenotoxins (PTXs), have been documented throughout the year in the Chesapeake Bay. While DTX concentrations currently remain below regulatory limits in regional seafood products, further research is needed to understand environmental drivers, both biotic and abiotic, that may be impacting *Dinophysis* spp. feeding on prey, growth, and toxin production. To characterize populations of *Dinophysis in situ*, an Imaging FlowCytobot (IFCB) was deployed off the Virginia Institute of Marine Science (VIMS) pier for five sampling seasons. The IFCB captures images of phytoplankton cells every ~20 minutes, generating large, continuous data sets that are then automatically classified using a machine learning algorithm, in this case, a convolutional neural network (CNN) framework. The IFCB-generated abundance data for the dinoflagellates *Dinophysis acuminata*, and *Prorocentrum cordatum*, as well as the ciliate *Mesodinium rubrum*, were then incorporated into an ecological predictive model along with abiotic variables such as sea surface temperature, salinity, turbidity, pH, and discharge. Given that *Dinophysis* is an obligate mixotroph, the relationship between bloom timing of the prey item *M. rubrum* and *D. acuminata* were explored by fitting models with no lag of *M. rubrum*, a 14-day lag, and a 75-day lag. Additionally, *P. cordatum* abundance was explored as a proxy for *D. acuminata* abundance. Results revealed that *D. acuminata* abundance was significantly linked with salinity, time of year, *M. rubrum* abundance with a 14-day lag, and *P. cordatum* abundance. The results of this study provide further insight into potential biotic and abiotic factors regulating *Dinophysis* populations in Chesapeake Bay.

To test another possible abiotic factor, turbulence, a culturing study was undertaken in the laboratory with four isolates of three species of *Dinophysis*: *D. acuminata*, *D. ovum*, and *D. caudata.* These isolates, from the Gulf and East Coasts of the U.S., were exposed to two levels of turbulence for six days to determine its effect on feeding, growth, and toxin production. While an effect of turbulence on ingestion rates of *M. rubrum* by *Dinophysis* was not detected, exposure to high turbulence inhibited growth of both *D. acuminata* and *D. ovum* and stimulated growth of *D. caudata*. As a result of inhibited growth, both *D. acuminata* and *D. ovum* had reduced toxin production rates, but *D. acuminata* was shown to accumulate toxin inside cells, while *D. ovum* released toxin extracellularly into the media. Conversely, the stimulation of growth for *D. caudata* resulted in decreased intracellular toxin content, but no effect on toxin production rate. While understanding phytoplankton population dynamics in the natural environment is complex, the results of these studies highlight some important environmental factors impacting *Dinophysis* spp. feeding, growth, and toxin production in the lab and field in both Chesapeake Bay and the East and Gulf Coasts of the U.S.

Identifying Factors Controlling *Dinophysis* spp. Feeding, Growth, and Toxin Production Through Field and Lab Studies

GENERAL INTRODUCTION

Harmful Algal Blooms (HABs) and Phycotoxins

Phytoplankton are an essential part of the world's water bodies, forming the base of food webs and providing food for upper trophic levels like filter-feeding bivalves (i.e., oysters, mussels, clams), crustaceans, and finfish (Hallegraeff, 1993). However, under favorable environmental conditions, "harmful algal blooms" (HABs), can form. True to their name, HABs cause harm to the surrounding environment, through either the production of toxins/harmful compounds, or through physical accumulation of cells that disrupt ecosystem functioning (Anderson et al. 2002). HABs can be detrimental to a system by causing water discoloration and odor, oxygen depletion leading to hypoxia or anoxia, ichthyotoxicity to fish and invertebrates, and their production of potent toxins (phycotoxins) is also a threat to wildlife, domestic animals, and human health (Hallegraeff, 1993, Anderson et al. 2002, Grattan et al. 2016 and references therein). Decades of research have linked nutrient availability (naturally derived nutrients) and eutrophication (anthropogenically derived nutrients) to HABs (Anderson et al. 2002, Sellner et al. 2003, Anderson et al. 2008, Glibert, 2017, Wurtsbaugh et al. 2019). With the rapid growth and expansion of the world's population, more nutrients and pollutants are entering waterways, degrading water quality, and contributing to favorable conditions for HABs (Anderson et al. 2008, Wurtsbaugh et al. 2019). Eutrophication is considered to be a natural phenomenon that was first described as increases in phytoplankton abundance compared to nutrient-poor water bodies; anthropogenic eutrophication is instead linked to human sources of nutrients such as wastewater discharge, fertilizer runoff, and has more recently been referred to as "cultural eutrophication" (Anderson et al. 2008, Glibert, 2017, Wurtsbaugh et al. 2019).

HAB species that produce phycotoxins occur along the freshwater to marine continuum and can be dangerous to human health. There are six recognized phycotoxin syndromes, including ciguatera fish poisoning (CFP), paralytic shellfish poisoning (PSP), neurotoxic shellfish poisoning (NSP), amnesic shellfish poisoning (ASP), diarrhetic shellfish poisoning (DSP), and azaspiracid shellfish poisoning (Satake, 1998, Grattan et al. 2016). Freshwater cyanobacteria can also produce toxins (cyanotoxins) that have hepatotoxic, neurotoxic, and dermatoxic effects in humans and other mammals (Merel et al. 2013). There is evidence to suggest that cyanotoxins can be transported to marine environments through rivers, streams, and other inland water bodies (Gibble et al. 2016, Peacock et al. 2018, Onofrio et al. 2021, Howard et al. 2022). Humans can be exposed to freshwater and marine phycotoxins through several different routes including unsafe drinking water, aerosolized toxins, aquatic recreational or occupational activity, and consumption of fish or shellfish that have bioaccumulated phycotoxins (Grattan et al. 2016).

Dinophysis and mixotrophy

One toxigenic HAB genus of particular interest is the kleptoplastidic mixotrophic dinoflagellate *Dinophysis* (Reguera et al. 2012). Of the over 100 species that have been assigned to this genus, 12 have been found to produce toxins (Reguera et al. 2012). Park et al. (2006) successfully established the first *Dinophysis* monoculture in 2006 through a three-step feeding regime: the cryptophyte *Teleaulax* sp. is fed to the mixotrophic ciliate *Mesodinium rubrum,* which is then fed to the mixotrophic dinoflagellate, *Dinophysis*. Among the four types of mixotrophy described by Stoecker (1998), *Dinophysis* is considered a Model IIIB mixotroph, meaning it is primarily phagotrophic and harbors cryptophyte prey plastids obtained from the mixotrophic ciliate *Mesodinium rubrum* (Reguera et al. 2012). In a follow-up study that built on

these classifications of mixotrophy, Mitra et al. (2016) described both *Dinophysis* and *Mesodinium* as plastidic specialist non-constitutive mixotrophs (pSNCMs), meaning these species have developed a need to acquire a capacity for photosynthesis from a specific prey source. In this case, *Mesodinium* feeds on several different cryptophyte prey types, but acquires plastids from only specific cryptophyte clades (*Geminigera*/*Teleaulax)* (Johnson et al. 2013), while *Dinophysis* relies on cryptophyte plastids acquired through ingestion of *Mesodinium* prey to survive (Park et al. 2006). *Dinophysis* is considered an obligate mixotroph, meaning it needs prey and light for long-term survival (Smith et al. 2012). In the absence of prey, *Dinophysis* cultures have been shown to maintain stationary phase for up to two months when irradiated (65 µmol photons $m^{-2}s^{-1}$), while in the absence of light, cultures began to decline after one month (Smith et al. 2012). This highlights the need for *Dinophysis* to acquire phototrophy through sequestration and maintenance of cryptophyte plastids (a.k.a. organelle retention) (Johnson, 2011).

Dinophysis displays a complex feeding behavior in which a *Dinophysis* cell slowly approaches a resting *M. rubrum* cell and links itself to its prey with a peduncle or capture filament. *Dinophysis* will then tow the attached *M. rubrum* cell around and eventually transfer the cell contents into its own cell, and digest them, retaining only the plastids from the *M. rubrum* cell (Park et al. 2006, Jiang et al. 2018). *Mesodinium rubrum* was recently shown to also be an ambush predator (Jiang & Johnson, 2021). A high-speed microscale imaging system (HSMIS) captured *M. rubrum* using its oral tentacles to poke the ventral posterior of its cryptophyte prey up to 16 times in ~1s, potentially using extrusomes to aid in prey capture (Jiang & Johnson, 2021). After ingestion, *M. rubrum* cells contain a single prey nucleus and several

smaller nuclei that are distributed around the periphery of the cell and are passed to new cells during division (Fiorendino et al. 2020).

Phycotoxins and Diarrhetic Shellfish Poisoning (DSP)

Although relatively rare in phytoplankton assemblages (10^{-4} -10^{-2} cells L^{-1}), 12 species of *Dinophysis* produce a class of potent lipophilic toxins called diarrhetic shellfish toxins (DSTs) that can accumulate in filter feeders (Reguera et al. 2012, Trainer et al. 2013, Deeds et al. 2020). DSTs consist of okadaic acid (OA), dinophysistoxins (DTXs), and their derivatives, which are acidic polyethers that inhibit protein phosphatases (Cohen et al. 1990). These toxins are the causative agents of global diarrhetic shellfish poisoning (DSP) in humans (Yasumoto et al. 1985, Dominguez et al. 2010). Symptoms are characterized by gastrointestinal illness including diarrhea, nausea, and vomiting. Symptoms typically appear 3 to 12 hours after ingestion of contaminated shellfish, with a recovery time of around 3 days (Aune & Yndestad 1993, Hallegraeff, 2003, Blanco et al. 2005). The first reports of a gastrointestinal illness occurring after consumption of cooked mussels were documented in the Netherlands in 1961; however, the causative organism was not identified (Reguera et al. 2014). It wasn't until the late 1970's that DSP was described (Yasumoto et al. 1985) and okadaic acid, previously isolated from a sponge *Halichondria okadai*, was identified as the toxin responsible for DSP outbreaks (Reguera et al. 2014). Along with oysters and mussels, other bivalves that have been found to accumulate DSTs include varnish clams, California mussels, Pacific oysters, and manilla clams (Trainer et 2013). An additional, and likely underestimated source of DSTs and DSP is the epiphytic/epibenthic dinoflagellate *Prorocentrum lima* (Morton et al. 1999). In 1998, *P. lima* was suspected to be responsible for cases of gastroenteritis in Maine, but additional research demonstrated that

accumulation of DSTs in shellfish did not pose a significant human health risk (Maranda et al. 2007a, b).

Pectenotoxins (PTXs) are a second class of toxins, polyether-lactones, that are produced by species of *Dinophysis* and have been shown to be hepatotoxic to mice via intraperitoneal injection (Miles et al. 2004a). Their impacts on human health have been debated (Reguera et al. 2012), and as such, PTXs are not regulated in the U.S. or the EU (European Commission, 2021). However, PTXs may pose a threat to shellfish health and aquaculture sustainability; in particular, younger life stages of bivalves have been shown to be vulnerable to PTXs (Gaillard et al. 2020, Pease et al. 2022).

History of *Dinophysis* on U.S. Coasts

Dinophysis is globally distributed, with reported DSP events in Japan, Europe, Asia, Chile, Canada, and New Zealand (Reguera et al. 2012). In the U.S., *Dinophysis* spp. cells and DSTs have been detected (below U.S. Food and Drug Administration (FDA) guidance levels of 160 ng g^{-1} OA equivalence in shellfish meat) as far back as the 1980s in Narragansett Bay, Rhode Island, and Maine, but reports of DSP illnesses are sparse, and the causative organisms could not be confirmed (Anderson et al. 2021). A precautionary shellfish bed closure was implemented in the Potomac and Rappahannock rivers of Virginia in 2002 in response to a *Dinophysis* bloom with peak concentrations of 236,000 cells L^{-1} (Wolny et al. 2020), but DSTs were not found above FDA guidance levels (Tango et al. 2004). In 2008, a bloom (> 200,000 cells L^{-1}) of *D. ovum* in the Gulf of Mexico, Texas led to harvesting closures and product recall after concentrations of DSTs in Eastern oyster meat (*Crassostrea virginica*) exceeded FDA guidance levels (Campbell et al. 2010, Deeds et al. 2010), marking the first official DSP event in the U.S. (Anderson et al. 2021). Since the emergence of DSP in the U.S., research has focused on the bloom dynamics of

D. ovum along the Texan coastline, concluding that the bloom originated offshore and was advected into coastal bays and estuaries, where high cell concentrations resulted in toxin accumulation in oysters (Campbell et al. 2010, Swanson et al. 2010). Additionally, early *Mesodinium* blooms may be necessary for the formation of a *D. ovum* bloom and, as such, could be used as an indicator of potential *D. ovum* blooms (Harred & Campbell 2014, Fiorendino et al. 2020). However, the authors also cautioned that no clear *in situ* predator-prey relationships could be quantified between the two species.

The first confirmed DSP illnesses in the U.S. occurred 3 years later, on the West Coast, in Washington State, where three individuals became ill after consuming mussels harvested from Sequim Bay State Park (Lloyd et al. 2013, Trainer et al. 2013). A follow-up monitoring study that collected shellfish and phytoplankton samples from WA coastal waters revealed DSTs were widespread in the study area, and California mussel, varnish clam, manila clam, and Pacific oyster samples exceeded the regulatory limit of 160 ng g^{-1} OA equivalence in shellfish tissue (Trainer et al. 2013). On the California coast, a four-year time series study showed that *Dinophysis* spp. are present in background concentrations throughout the year (754 cells L^{-1} on average) and toxin concentrations in mussel samples exceeded guidance level thresholds 10% of the time (Shultz et al. 2019). Over the four-year period, the study also demonstrated that detectable (background) concentrations of DSTs were found in 61% of weekly non-commercial mussel samples. As in TX, researchers in CA have very recently linked ciliate abundance to *Dinophysis* cell abundance, using prey as a predictor of predator abundance. Models run in the study identified ciliate abundance as an important predictor of *Dinophysis* abundance, with higher abundance of ciliates linked to an increase in *Dinophysis* abundance (Kenitz et al. 2023).

On the East Coast of the U.S., *Dinophysis* species have historically been recorded in plankton assemblages (Mulford, 1972, Maranda & Shimizu, 1987, Anderson et al. 2021), but Hattenrath-Lehmann et al. (2013) reported the first significant bloom of *D. acuminata* along this coastline. In their study, plankton and shellfish samples were collected over a four-year period (2008-2011) in the region in Northport Bay, Long Island Sound, New York, and cell concentrations reached extraordinary highs, nearing 1.3 million cells L^{-1} in 2011. Toxins detected in sieved samples included OA, DTX-1, PTX-2, PTX-11, and isomers; softshell clams and ribbed mussels collected during the study contained DSTs above U.S. regulatory limits. Additionally, the authors reported observations of *Dinophysis* blooms in other bays along Long Island Sound reaching similar maximum concentrations. In a follow-up study, Hattenrath-Lehmann et al. (2018) collected samples of concentrated cells and blue mussels (*Mytilus edulis*), and deployed passive samplers to track DSTs throughout a *Dinophysis* bloom. In the particulate fraction (concentrated cells), PTX was the dominant toxin in profiles, while in contrast, blue mussels had higher concentrations of esterified DSTs than PTXs. Within the extracts of passive samplers, free DSTs: OA and DTX-1 were most abundant, demonstrating the lack of biotransformation of DSTs compared to what was observed in mussel samples. Additionally, elevated concentrations of DSTs exceeding FDA guidelines have been found in shellfish collected off the New England coast in Massachusetts and Maine (Anderson et al. 2021). Similar to the Gulf and West Coasts, preliminary studies in this region have linked *D. acuminata* cell abundance to *Mesodinium* spp. abundance (Hattenrath-Lehmann et al. 2013, Hattenrath-Lehmann et al. 2015).

In Virginia and Maryland, over 13 species of *Dinophysis* have been identified (Marshall, 1980, 1982, Marshall et al. 1981), and based on modern morphological and molecular analyses,

Wolny et al. (2020) identified *D. acuminata* and *D. norvegica* as the dominant species. The authors also noted an additional "small *Dinophysis* sp." that can be morphologically separated from other species, but not molecularly distinguished from the *D. acuminata*-complex (*D. acuminata*, *D. ovum*, *D. sacculus*). These findings contrast with the earlier work of Marshall, and could reflect changes in *Dinophysis* populations over time, or advancement in laboratory identification techniques. Through the establishment of the Chesapeake Bay Program's phytoplankton monitoring program, data between 1999 to 2016 show that *Dinophysis acuminata* occurred annually throughout the VA portion of Chesapeake Bay at an average concentration of 403 cells L^{-1} (Wolny et al. 2020). While this average concentration in the Bay can be considered relatively low, and *Dinophysis* spp. rare in the overall phytoplankton assemblage, *Dinophysis* produces potent toxins that can lead to detectable levels of accumulation in shellfish at just a few hundred cells per liter (Campbell et al. 2010). DSTs have also been shown to be present year-round in Bay waters (Onofrio et al. 2021, Pease 2021); with OA, DTX-1 and esterified forms, and PTX-2 being the only analogues identified *in situ* thus far (Wolny et al. 2020, Pease 2021).

When passive samplers were deployed at twelve sites in the Chesapeake Bay and VA coastal bays, OA and DTX-1 were detected in all samples (n = 321), and PTX-2 in all but one sample (Onofrio et al. 2021), showing their ubiquitous distribution over time and space. Additionally, there were differences in toxin profile and timing of peak toxin concentrations between the Chesapeake Bay and coastal bays, with the coastal bays peaking in toxin concentrations two months earlier than the Chesapeake Bay sites (Onofrio et al. 2021). Recent work has also quantified a suite of phycotoxins in oyster meat in the Bay, including DSTs (Pease 2021). Results show that OA and DTX-1, toxins responsible for DSP, were rarely detected in oyster samples, and when they were, they occurred in trace amounts (well below regulatory limit),

despite being detected consistently in other environmental matrices within the study (Pease, 2021). Based on these previous studies, it has been established that multiple species of *Dinophysis* and their toxins (OA, DTX-1, PTX-2) are present in the Bay year-round, but do not pose a current risk to public health based on their relatively low concentrations (Onofrio et al. 2021, Pease, 2021). However, additional baseline data are needed to further understand the environmental drivers of *Dinophysis* abundance under current conditions in this region so extrapolations can be made for future climate change scenarios.

Biological and Environmental Controls on *Dinophysis* spp.

Since the pivotal work by Park and coauthors (2006), monocultures have been used to investigate growth of *Dinophysis* species in response to variations in environmental conditions such as nutrients, temperature, light, and most recently, salinity (Tong et al. 2011, Smith et al. 2012, Nielson et al. 2012, Tong et al. 2015, Hattenrath-Lehmann & Gobler 2015, Fiorendino et al. 2020, Gaillard et al. 2021). Some culturing studies go further, to characterize toxin profiles and toxin production rates related to species or strain differences, or in response to the above environmental parameters (Deeds et al. 2010, Fux et al. 2011, Smith et al. 2012, Deeds et al. 2020, Wolny et al. 2020). *Dinophysis acuminata* preferentially utilizes ammonium and urea as opposed to nitrate (Hattenrath-Lehmann & Gobler 2015, Hattenrath-Lehmann et al. 2015, García-Portela et al. 2020, Hattenrath-Lehmann et al. 2021), and does not directly assimilate dissolved phosphate (Tong et al. 2015). Cultures of *D. ovum* and *D. acuminata* have been found to grow best at moderate temperatures (18-24˚C) (Fiorendino et al. 2020), while Basti et al. (2015) found that the cell density of a *D. caudata* culture increased significantly with increasing temperature, and was highest under 27, 30, and 32.5˚C. Irradiance levels above 100 µmol quanta $m^{-2}s^{-1}$ did not have a significant impact on the growth of the *D. acuminata* or *D. ovum* isolates

used in the experiment (Fiorendino et al. 2020). Similarly, Tong et al. (2011) found that light intensities between 65 to 284 μmol photons $m^{-2}s^{-1}$ had no significant impact on *D. acuminata* growth or toxin content. Nielson et al. (2012) determined that growth of a *D. acuminata* culture increased with increasing irradiance levels between 7 to 130 μmol photons $m^{-2}s^{-1}$, but the cellular toxin content only increased slightly between treatments, demonstrating the decoupling of toxin content and irradiance in *Dinophysis* cultures. In regard to salinity, Fiorendino et al. (2020) found optimal growth conditions for *D. ovum* isolated from Surfside Beach, TX, and *D. acuminata* isolated from Nassawadox, VA to be between 22-26. In a short-term salinity stress experiment, Gaillard et al. (2021) found cultures of *D.* cf *sacculus* to have high tolerance to abrupt changes in salinity (salinity values of 25, 35, and 42).

An additional environmental variable, turbulence, is ubiquitous in aquatic systems and can thus potentially influence phytoplankton population dynamics (Guadayol et al. 2009). Phytoplankton cells are subject to both large-scale and small-scale turbulence either directly or indirectly, and changes in water column position due to turbulent mixing can result in different nutrient concentrations, light intensities, and prey availability (Mann & Lazier 1991, Peters & Marrasé 2000, García-Portela et al. 2019). Due to their size, phytoplankton interact more directly with small-scale turbulence (Kolmogorov scales) (Estrada and Berdalet 1998). The kinetic energy generated by wind and waves is transferred to smaller eddies until viscous forces – "related to internal resistance of the fluid molecules" as explained by Estrada & Berdalet (1998), convert it to heat (Sullivan et al. 2003). Thus, phytoplankton in the water column perceive turbulence as laminar shear (Thomas et al. 1995, Estrada & Berdalet 1998). Margalef (1978) suggested a conceptual model or "Mandala" to explain the succession of phytoplankton species according to two factors: nutrients and turbulence. According to the theory, turbulent conditions

with high nutrient concentrations favor diatoms and coccolithophorids, while low turbulence, and nutrient-poor waters favor dinoflagellates. Building on Margalef's Mandala, Glibert (2016) proposed an updated mandala that incorporates twelve variables/traits that influence phytoplankton including preference for chemically reduced or oxidized nitrogen, adaptation to light and tendency to be autotrophic vs. mixotrophic, environmental turbulence, production of toxins or reactive oxygen species (ROS), growth rate, etc., in hopes of further elucidating the variables that control phytoplankton abundance. Given that dinoflagellates, especially harmful algal bloom-forming species, are associated with a calm, stratified water column (Berdalet et al. 2007), several researchers have conducted laboratory and field studies to determine the response of dinoflagellates to small-scale turbulence. Many have found species-specific responses that may include changes in morphology (Zirbel et al. 2000), swimming behavior (Estrada et al. 1987, Chen et al. 1998, Karp-Boss et al. 2000), growth rates (Pollingher & Zemel, 1981, Havskum et al. 2005, Stoecker et al. 2006), and changes in cellular toxin content (Juhl et al. 2001, Bolli et al. 2007). Recently, García-Portela et al. (2019) investigated the effect of small-scale turbulence on two species of *Dinophysis*: *D. acuminata* and *D. acuta* (isolated from Spain). The study demonstrated a species-specific growth response to turbulence, i.e., *D. acuta* was more sensitive to small-scale turbulence than *D. acuminata*. While both species had significantly lower growth rates in high turbulence treatments compared to controls, *D. acuminata* grew (i.e., positive growth rate) under high turbulence, while *D. acuta* did not grow (i.e., negative growth rate) when exposed to high turbulence, and did not resume growth during the 2-day recovery period. These different responses to turbulence likely explain their seasonal distribution *in situ*. There are limited data on the effects of turbulence on *Dinophysis* sp. toxin production, but a field study by Díaz et al. (2019) did quantify toxin samples (OA) that were collected during a cruise in

the Galician Rías of Vigo and Pontevedra; however, researchers did not find any pattern between toxin accumulation per cell and circadian pattern (i.e., a peak in newly dividing cells causing a decline in content per cell).

Scientists have had great interest in examining the impact of turbulence on phytoplankton communities, in general, but the use of many different turbulence-generating systems and lack of quantification of turbulence in early studies has made comparison of results difficult (Arnott et al. 2021). The most common set-ups used to generate turbulence include aeration systems, Couette cylinders, oscillating grid systems, and shaker tables. While oscillating grid systems have dominated experimental set-ups in recent years (Arnott et al. 2021), Guadayol et al. (2009) compared turbulence generation suitability between oscillating grid systems and shaker tables, and found that both systems produced fairly isotropic conditions (i.e. turbulent forces have no preferred direction) (McGillicuddy Jr & Franks, 2019), and deemed them both sufficient for environmentally realistic turbulence generation, with a few stipulations for turbulence generation with shaker tables. Isotropy can be lost while using shaker tables in low turbulence/energy conditions, so the authors recommend avoiding oscillation frequencies below 1Hz to ensure isotropy is maintained. Additionally, there is the potential for a gradient of dissipation in the experimental flasks, where energy dissipation rates (ε) can vary by an order of magnitude between the wall and the center of the flask. To limit the interference of these two caveats, it is recommended to avoid oscillation frequencies below 1Hz (equivalent to 40rpm on shaker table) and to use small and narrow culture flasks (125-mL Erlenmeyer flasks, also used in Zirbel et al. 2000) to maintain homogeneity of the turbulent forces.

Advances in Technology to Track HABs and Phycotoxins

Tools have been adapted from other disciplines or new technologies developed to aid in the early detection of HAB cells and toxins *in situ*. Due to laborious and expensive phytoplankton monitoring programs, and time-consuming extraction of samples, tools are now being employed that greatly reduce the amount of manpower necessary to collect valuable information. One such technology is solid phase adsorption toxin tracking (SPATT) discs. SPATTs are passive samplers that contain resin capable of passively adsorbing lipophilic phycotoxins from ambient water that may occur in low concentrations (Makenzie et al. 2004, Roué et al. 2018). Since its application to HAB toxin monitoring by Makenzie et al. (2004), SPATT technology has been used all over the world, in a variety of systems, to track and understand phycotoxin abundance and dynamics (Roué et al. 2018). Of the variety of resins that have been used in SPATTs, the consensus is that HP-20 resin is the most effective resin for use in SPATTs, with high adsorption of DSTs and PTXs, and detection of a suite of phycotoxins (Makenzie et al. 2004, Hattenrath-Lehmann et al. 2018, Roué et al. 2018, Onofrio et al., 2021). SPATTs have been widely used to monitor DSTs in a variety of systems, and research has been done to determine if SPATTs can be used as an early warning tool to detect DSTs prior to their accumulation in shellfish, with varying results (Pizzaro et al. 2013, Hattenrath-Lehmann et al. 2018, Roué et al. 2018). Hattenrath-Lehmann et al. (2018) found that SPATTs detected DSTs in the water column three-to-four weeks earlier than deployed mussels and were better at predicting shellfish toxicity than *Dinophysis* cell densities or particulate toxin concentrations. This agrees with Li et al. (2016) and Makenzie et al. (2004), who both found that SPATTs were capable of adsorbing and detecting DSTs 1-2 weeks before levels peaked in scallops and mussels, respectively. In contrast, Pizzaro et al. (2013) deployed SPATTs for one week in aquaculture growing areas in Ría de Pontevedra

and discovered a lag between detection of *Dinophysis* cells in the water column, and detection of DSTs on SPATTs. Ultimately, they concluded that *Dinophysis* cell abundance was a better predictor of shellfish toxicity that SPATTs. Additionally, the authors found that SPATTs may overestimate expected toxin concentrations in shellfish. They proposed several explanations for why this may be the case, including the fact that SPATTs do not carry out biotransformation of toxins or include a loss term, represent an "average" of toxins throughout the entire water column (when it has been observed that *Dinophysis* occurs in thin layers), and can accumulate toxins even when no *Dinophysis* cells are present. Depending on the research question at hand, accumulation of toxin in the absence of cells may be very informative. Onofrio et al. (2021) was interested in documenting the distribution of phycotoxins in the Chesapeake Bay, and deployed SPATTs at numerous locations throughout the Bay. Using SPATTs, the authors were able to detect DSTs and PTXs year-round, in the absence of *Dinophysis* cells. This application proved to be useful for establishing baseline DST and PTX data and observing seasonal trends in DST and PTX distribution. SPATTs have a variety of applications and can be used in a variety of systems to track phycotoxin abundance and distribution. The pros and cons associated with SPATTs depend on the questions a researcher is aiming to answer. SPATTs are inexpensive and easy to make, can adsorb a variety of phycotoxins with high sensitivity, and require a much simpler extraction process than traditional shellfish samples (Makenzie et al. 2004). Overall, SPATTs are a valuable monitoring tool for the detection and monitoring of phycotoxins in the aquatic environment but should be used to supplement traditional phytoplankton monitoring techniques (i.e., water sampling and shellfish tissue extraction).

In addition to detecting and tracking phycotoxins, it is also important to track phytoplankton and HAB species abundance spatially and temporally. This is made possible through utilization

of an Imaging FlowCytobot (IFCB). The Imaging FlowCytobot (IFCB) is an invaluable monitoring tool that replaces the laborious process of manual microscopic identification of phytoplankton communities (Olson & Sosik 2007, Sosik & Olson 2007). The IFCB uses a combination of flow cytometry and high-resolution photography to capture images of individual phytoplankton cells between 10-150 μm, while also providing peripheral data, e.g., chlorophyll fluorescence or biovolume, for each image (Olson & Sosik 2007). The instrument will draw a 5-mL water sample every ~20 minutes, generating large, continuous data sets when deployed for several months at a time. Then, a supervised machine learning system (i.e., artificial intelligence) is used to "train" the IFCB to automatically identify, classify and categorize pictures into algal taxa. The long-term deployment capabilities of the IFCB make it ideal for early detection of HABs like *Dinophysis*, with its ability to produce toxins at a few hundred cells per liter (Campbell et al. 2010).

Since becoming commercially available in 2013, researchers from all over the U.S. and the world have utilized the IFCB for a variety of phytoplankton and HAB applications. The IFCB is extremely versatile in that it can be submerged in the water and operate autonomously or be used on research cruises or in the lab. This versatility has allowed researchers the freedom to explore a variety of research questions that would otherwise not be possible. When combined with environmental data (e.g., sea surface temperature, salinity, discharge rate, nutrients, etc.), the IFCB can be used to study an entire phytoplankton assemblage and its response to changes in these environmental variables. For example, Fischer et al. (2020) used large data sets generated from the IFCB, in combination with other historical environmental data, to investigate the shift from diatom to dinoflagellate abundance in Monterey Bay, CA. Additionally, Kramer et al. (2020) deployed the IFCB on a research cruise during the Thomas Fire to explore the impacts of

the fire (i.e., ash influx) on phytoplankton community composition. The IFCB can also be used to examine phytoplankton community response to severe weather events; Anglés et al. (2015) documented changes in phytoplankton community composition after the passage of four tropical cyclones in the Gulf of Mexico. Strong winds, storm surge, and flooding substantially changed the salinity of the system, thus leading to significant changes in phytoplankton composition (diatoms versus dinoflagellates). The IFCB has also been shown to be extremely beneficial for early detection of HABs. The first substantial *Dinophysis* bloom in the U.S. was detected via an IFCB in the Mission-Aransas estuary (Campbell et al. 2010). The early warning from the IFCB prevented a significant number of DSP illnesses that could have happened at the Rockport/Fulton Oyster Festival if *Dinophysis* cells had not been detected, prompting toxins to be quantified in shellfish (Deeds et al. 2010). The IFCB continues to provide an early warning for HABs found on the Texas coast, including *Karenia brevis*, *Dinophysis ovum*, and *Prorocentrum texanum* (Campbell et al. 2013, Henrichs et al. 2021). The IFCB is also becoming more accessible through collaborations between academic, federal, and state institutions that use the IFCB to track HABs that occur on all coasts of the U.S. and around the world.

Project Objectives

The overarching goal of my research was to investigate biological and environmental drivers of Dinophysis growth and toxin production. I addressed this goal through two objectives: (1) to investigate the role of biotic and abiotic factors in *Dinophysis* abundance *in situ*, and (2) to conduct culturing experiments to understand the role of turbulence in *Dinophysis* feeding on prey, growth, and toxin production.

Under my first objective, ***I hypothesized*** that a combination of abiotic and biotic factors would influence *Dinophysis* abundance. I accomplished this objective by combining IFCB-

generated data for *Dinophysis* and *Mesodinium* with environmental variables (i.e., sea surface temperature, salinity, pH, turbidity, and discharge) to determine any significant predictors of *Dinophysis* in the York River, Chesapeake Bay via ecological modeling.

Given the limited information on *Dinophysis* growth and toxin production in response to turbulence, ***I hypothesized*** that continuous exposure to moderate turbulence would increase *Dinophysis/Mesodinium* encounter rates, thus increasing *Dinophysis* growth and toxin production in culturing experiments. However, continuous exposure to high turbulence was expected to disrupt the complex feeding behavior of *Dinophysis*, reducing overall growth. Additionally, ***I hypothesized*** that increased turbulence would stress or lyse *Dinophysis* cells, leading to an increase in extracellular toxin in treatment flasks. I accomplished this objective by conducting a preliminary range-finding experiment, and a second experiment exposing four strains of *Dinophysis* to two levels of continuous turbulence for 6 days.

REFERENCES

Anderson, D. M., Burkholder, J. M., Cochlan, W. P., Glibert, P. M., Gobler, C. J., Heil, C. A., Kudela, R. M., Parsons, M. L., Rensel, J. E. J., Townsend, D. W., Trainer, V. L., & Vargo, G. A. (2008). Harmful algal blooms and eutrophication: Examining linkages from selected coastal regions of the United States. *Harmful Algae*, *8*(1), 39–53. https://doi.org/10.1016/j.hal.2008.08.017

Anderson, D. M., Fensin, E., Gobler, C. J., Hoeglund, A. E., Hubbard, K. A., Kulis, D. M., Landsberg, J. H., Lefebvre, K. A., Provoost, P., Richlen, M. L., Smith, J. L., Solow, A. R., & Trainer, V. L. (2021). Marine harmful algal blooms (HABs) in the United States: History, current status and future trends. *Harmful Algae*, *102*, 101975. https://doi.org/10.1016/j.hal.2021.101975

Anderson, D. M., Glibert, P. M., & Burkholder, J. M. (2002). Harmful algal blooms and eutrophication: Nutrient sources, composition, and consequences. *Estuaries*, *25*(4), 704–726. https://doi.org/10.1007/BF02804901

Anglès, S., Jordi, A., & Campbell, L. (2015). Responses of the coastal phytoplankton community to tropical cyclones revealed by high-frequency imaging flow cytometry: Phytoplankton responses to tropical cyclones. *Limnology and Oceanography*, *60*(5), 1562–1576. https://doi.org/10.1002/lno.10117

Arnott, R. N., Cherif, M., Bryant, L. D., & Wain, D. J. (2021). Artificially generated turbulence: A review of phycological nanocosm, microcosm, and mesocosm experiments. *Hydrobiologia*, *848*(5), 961–991. https://doi.org/10.1007/s10750-020-04487-5

Aune, T., Yndestad, M., 1993. Diarrhetic shellfish poisoning. In: Falconer, I.R. (Ed.), Algal Toxins in Seafood and Drinking Water. Academic Press, New York, pp. 87–104.

Badjeck, M.-C., Allison, E. H., Halls, A. S., & Dulvy, N. K. (2010). Impacts of climate variability and change on fishery-based livelihoods. *Marine Policy*, *34*(3), 375–383. https://doi.org/10.1016/j.marpol.2009.08.007

Basti, L., Uchida, H., Matsushima, R., Watanabe, R., Suzuki, T., Yamatogi, T., & Nagai, S. (2015). Influence of Temperature on Growth and Production of Pectenotoxin-2 by a Monoclonal Culture of *Dinophysis caudata*. *Marine Drugs*, *13*(12), 7124–7137. https://doi.org/10.3390/md13127061

Blanco, J., Moroño, Á., & Fernández, M. L. (2005). *Toxic Episodes In Shellfish, Produced By Lipophilic Phycotoxins: An Overview*.

Bolli, L., Llaveria, G., Garces, E., Guadayol, O., van Lenning, K., Peters, F., & Berdalet, E. (2007). Modulation of ecdysal cyst and toxin dynamics of two *Alexandrium* (Dinophyceae) species under small-scale turbulence.

Campbell, L., Henrichs, D. W., Olson, R. J., & Sosik, H. M. (2013). Continuous automated imaging-in-flow cytometry for detection and early warning of *Karenia brevis* blooms in the Gulf of Mexico. *Environmental Science and Pollution Research*, *20*(10), 6896–6902. https://doi.org/10.1007/s11356-012-1437-4

Campbell, L., Olson, R. J., Sosik, H. M., Abraham, A., Henrichs, D. W., Hyatt, C. J., & Buskey, E. J. (2010). First Harmful *Dinophysis* (Dinophyceae, Dinophysiales) Bloom In The U.S. Is Revealed By Automated Imaging Flow Cytometry1: Dinophysis Dynamics From Imaging Flowcytobot. *Journal of Phycology*, *46*(1), 66–75. https://doi.org/10.1111/j.1529-8817.2009.00791.x

Chen, D., K. Muda, K. Jones, J. Leftly & P. Stansby, 1998. Effect of shear on growth and motility of *Alexandrium minutum* Halim, a red-tide dinoflagellate. In Reguera, B., J. Blanco,

M. L. Fernández & T. Wyatt (eds), Harmful algae. Xunta de Galicia and Intergovernmental Oceanographic Commision of UNESCO, Vigo: 352–355.
Cohen P, Holmes CF, Tsukitani Y. Okadaic acid: a new probe for the study of cellular regulation. Trends Biochem Sci. 1990 Mar;15(3):98-102. doi: 10.1016/0968-0004(90)90192-e. PMID: 2158158.
Deeds, J. R., Whitney L. Stutts, Mary Dawn Celiz, Jill MacLeod, Amy E. Hamilton, Bryant J. Lewis, David W. Miller, Kohl Kanwit, Juliette L. Smith, David M. Kulis, Pearse McCarron, Carlton D. Rauschenberg, Craig A. Burnell, Stephen D. Archer, Jerry Borchert, & Shelley K. Lankford. (2020). Dihydrodinophysistoxin-1 Produced by *Dinophysis norvegica* in the Gulf of Maine, USA and Its Accumulation in Shellfish. *Toxins*, *12*(533), 1–19.
Deeds, J. R., Wiles, K., Heideman, G. B., White, K. D., & Abraham, A. (2010). First U.S. report of shellfish harvesting closures due to confirmed okadaic acid in Texas Gulf coast oysters. *Toxicon*, *55*(6), 1138–1146. https://doi.org/10.1016/j.toxicon.2010.01.003
Díaz, P. A., Ruiz-Villarreal, M., Mouriño-Carballido, B., Fernández-Pena, C., Riobó, P., & Reguera, B. (2019). Fine scale physical-biological interactions during a shift from relaxation to upwelling with a focus on Dinophysis acuminata and its potential ciliate prey. *Progress in Oceanography*, *175*, 309–327. https://doi.org/10.1016/j.pocean.2019.04.009
Dominguez, H.J., Paz, B., Daranas, A.H., Norte, M., Franco, J.M., Fernández, J.J., 2010. Dinoflagellate polyether within the yessotoxin, pectenotoxin and okadaic acid toxin groups: Characterization, analysis and human health implications. Toxicon 56, 191–217. https://doi.org/10.1016/j.toxicon.2009.11.005
Estrada, M., Alcaraz, M., & Marrasé, C. (1987). Effects of turbulence on the composition of phytoplankton assemblages in marine microcosms. *Marine Ecology Progress Series*, *38*(3), 267–281.
Estrada, M., & Berdalet, E. (1998). Effects of Turbulence on Phytoplankton. *Physiological Ecology of Harmful Algal Blooms*, *41*.
European Commission, 2021. Commission Implementing Regulation (EU) 2021/1709 of 23 September 2021 amending Implementing Regulation (EU) 2019/627 as regards uniform practical arrangements for the performance of official controls on products of animal origin.
Fiorendino, J. M., Smith, J. L., & Campbell, L. (2020). Growth response of *Dinophysis*, *Mesodinium*, and *Teleaulax* cultures to temperature, irradiance, and salinity. *Harmful Algae*, *98*, 101896. https://doi.org/10.1016/j.hal.2020.101896
Fischer, A. D., Hayashi, K., McGaraghan, A., & Kudela, R. M. (2020). Return of the "age of dinoflagellates" in Monterey Bay: Drivers of dinoflagellate dominance examined using automated imaging flow cytometry and long-term time series analysis. *Limnology and Oceanography*, *65*(9), 2125–2141. https://doi.org/10.1002/lno.11443
Fux, E., Smith, J. L., Tong, M., Guzmán, L., & Anderson, D. M. (2011). Toxin profiles of five geographical isolates of *Dinophysis* spp. From North and South America. *Toxicon*, *57*(2), 275–287. https://doi.org/10.1016/j.toxicon.2010.12.002
Gaillard, S., Le Goïc, N., Malo, F., Boulais, M., Fabioux, C., Zaccagnini, L., Carpentier, L., Sibat, M., Réveillon, D., Séchet, V., Hess, P., Hégaret, H. (2020). Cultures of *Dinophysis sacculus*, *D. acuminata* and pectenotoxin 2 affect gametes and fertilization success of the Pacific oyster, *Crassostrea gigas*. *Environ. Pollut*. 265. https://doi.org/10.1016/j.envpol.2020.114840
Gaillard, S., Réveillon, D., Danthu, C., Hervé, F., Sibat, M., Carpentier, L., Hégaret, H., Séchet, V., & Hess, P. (2021). Effect of a short-term salinity stress on the growth, biovolume, toxins,

osmolytes and metabolite profiles on three strains of the *Dinophysis acuminata*-complex (*Dinophysis* cf. *Sacculus*). *Harmful Algae*, *107*, 102009. https://doi.org/10.1016/j.hal.2021.102009

García-Portela, M., Reguera, B., Ribera d'Alcalà, M., Rodríguez, F., & Montresor, M. (2019). Effects of small-scale turbulence on two species of *Dinophysis*. *Harmful Algae*, *89*, 101654. https://doi.org/10.1016/j.hal.2019.101654

García-Portela, M., Reguera, B., Gago, J., Le Gac, M., & Rodríguez, F. (2020). Uptake of Inorganic and Organic Nitrogen Sources by *Dinophysis acuminata* and *D. acuta*. *Microorganisms*, *8*(2), 187. https://doi.org/10.3390/microorganisms8020187

Gibble, C. M., Peacock, M. B., & Kudela, R. M. (2016). Evidence of freshwater algal toxins in marine shellfish: Implications for human and aquatic health. *Harmful Algae*, *59*, 59–66. https://doi.org/10.1016/j.hal.2016.09.007

Glibert, P. M. (2016). Margalef revisited: A new phytoplankton mandala incorporating twelve dimensions, including nutritional physiology. *Harmful Algae*, *55*, 25–30. https://doi.org/10.1016/j.hal.2016.01.008

Glibert, P. M. (2017). Eutrophication, harmful algae and biodiversity—Challenging paradigms in a world of complex nutrient changes. *Marine Pollution Bulletin*, *124*(2), 591–606. https://doi.org/10.1016/j.marpolbul.2017.04.027

Grattan, L. M., Holobaugh, S., & Morris, J. G. (2016). Harmful algal blooms and public health. *Harmful Algae*, *57*, 2–8. https://doi.org/10.1016/j.hal.2016.05.003

Guadayol, Ò., Peters, F., Stiansen, J. E., Marrasé, C., & Lohrmann, A. (2009). Evaluation of oscillating grids and orbital shakers as means to generate isotropic and homogeneous small-scale turbulence in laboratory enclosures commonly used in plankton studies: Turbulence in laboratory containers. *Limnology and Oceanography: Methods*, *7*(4), 287–303. https://doi.org/10.4319/lom.2009.7.287

Hallegraeff, G. M. (1993). A review of harmful algal blooms and their apparent global increase. *Phycologia*, *32*(2), 79–99. https://doi.org/10.2216/i0031-8884-32-2-79.1

Hallegraeff, G. M.,(2003). Harmful algal blooms: a global overview. In: Hallegraeff, G.M., Anderson, D.M., Cembella, A.D. (Eds.), *Manual on harmful marine microalgae* (2nd rev. ed). UNESCO Publishing, Landais, France, 25-40.

Harred, L. B., & Campbell, L. (2014). Predicting harmful algal blooms: A case study with *Dinophysis ovum* in the Gulf of Mexico. *Journal of Plankton Research*, *36*(6), 1434–1445. https://doi.org/10.1093/plankt/fbu070

Hattenrath-Lehmann, T. K., Marcoval, M. A., Berry, D. L., Fire, S., Wang, Z., Morton, S. L., & Gobler, C. J. (2013). The emergence of *Dinophysis acuminata* blooms and DSP toxins in shellfish in New York waters. *Harmful Algae*, *26*, 33–44. https://doi.org/10.1016/j.hal.2013.03.005

Hattenrath-Lehmann, T., & Gobler, C. J. (2015). The contribution of inorganic and organic nutrients to the growth of a North American isolate of the mixotrophic dinoflagellate, *Dinophysis acuminata*: The effects of nutrients on a culture of Dinophysis. *Limnology and Oceanography*, *60*(5), 1588–1603. https://doi.org/10.1002/lno.10119

Hattenrath-Lehmann, T. K., Marcoval, M. A., Mittlesdorf, H., Goleski, J. A., Wang, Z., Haynes, B., Morton, S. L., & Gobler, C. J. (2015). Nitrogenous Nutrients Promote the Growth and Toxicity of *Dinophysis acuminata* during Estuarine Bloom Events. *PLOS ONE*, 22.

Hattenrath-Lehmann, T., Lusty, M., Wallace, R., Haynes, B., Wang, Z., Broadwater, M., Deeds, J., Morton, S., Hastback, W., Porter, L., Chytalo, K., & Gobler, C. (2018). Evaluation of

Rapid, Early Warning Approaches to Track Shellfish Toxins Associated with *Dinophysis* and *Alexandrium* Blooms. *Marine Drugs*, *16*(1), 28. https://doi.org/10.3390/md16010028

Hattenrath-Lehmann, T. K., Nanjappa, D., Zhang, H., Yu, L., Goleski, J. A., Lin, S., & Gobler, C. J. (2021). Transcriptomic and isotopic data reveal central role of ammonium in facilitating the growth of the mixotrophic dinoflagellate, *Dinophysis acuminata*. *Harmful Algae*, *104*, 102031. https://doi.org/10.1016/j.hal.2021.102031

Havskum, H., Hansen, P. J., & Berdalet, E. (2005). Effect of turbulence on sedimentation and net population growth of the dinoflagellate *Ceratium tripos* and interactions with its predator, *Fragilidium subglobosum*. *Limnology and Oceanography*, *50*(5), 1543–1551. https://doi.org/10.4319/lo.2005.50.5.1543

Henrichs, D. W., Anglès, S., Gaonkar, C. C., & Campbell, L. (2021). Application of a convolutional neural network to improve automated early warning of harmful algal blooms. *Environmental Science and Pollution Research*, *28*(22), 28544–28555. https://doi.org/10.1007/s11356-021-12471-2

Howard, M. D. A., Smith, J., Caron, D. A., Kudela, R. M., Loftin, K., Hayashi, K., Fadness, R., Fricke, S., Kann, J., Roethler, M., Tatters, A., & Theroux, S. (2022). Integrative monitoring strategy for marine and freshwater harmful algal blooms and toxins across the freshwater-to-marine continuum. *Integrated Environmental Assessment and Management*, *00*(00), 1–19.

Jiang, H., Kulis, D. M., Brosnahan, M. L., & Anderson, D. M. (2018). Behavioral and mechanistic characteristics of the predator-prey interaction between the dinoflagellate *Dinophysis acuminata* and the ciliate *Mesodinium rubrum*. *Harmful Algae*, *77*, 43–54. https://doi.org/10.1016/j.hal.2018.06.007

Jiang, H., & Johnson, M. (2021). Swimming behavior of cryptophyte prey affects prey preference of the ambush-feeding ciliate *Mesodinium rubrum*. *Aquatic Microbial Ecology*, *86*, 169–184. https://doi.org/10.3354/ame01964

Johnson, M. D. (2011). The acquisition of phototrophy: Adaptive strategies of hosting endosymbionts and organelles. *Photosynthesis Research*, *107*(1), 117–132. https://doi.org/10.1007/s11120-010-9546-8

Johnson, M. D., Stoecker, D. K., & Marshall, H. G. (2013). Seasonal dynamics of *Mesodinium rubrum* in Chesapeake Bay. *Journal of Plankton Research*, *35*(4), 877–893. https://doi.org/10.1093/plankt/fbt028

Juhl, A. R., Trainer, V. L., & Latz, M. I. (2001). Effect of fluid shear and irradiance on population growth and cellular toxin content of the dinoflagellate *Alexandrium fundyense*. *Limnology and Oceanography*, *46*(4), 758–764.

Karp-Boss, L., Boss, E., & Jumars, P., A. (2000). Motion of dinoflagellates in a simple shear flow. *Limnology and Oceanography*, *45*(7), 1594–1602.

Kramer, S. J., Bisson, K. M., & Fischer, A. D. (2020). Observations of Phytoplankton Community Composition in the Santa Barbara Channel During the Thomas Fire. *Journal of Geophysical Research: Oceans*, *125*(12). https://doi.org/10.1029/2020JC016851

Kenitz, K. M., Anderson, C. R., Carter, M. L., Eggleston, E., Seech, K., Shipe, R., Smith, J., Orenstein, E. C., Franks, P. J. S., Jaffe, J. S., & Barton, A. D. (2023). Environmental and ecological drivers of harmful algal blooms revealed by automated underwater microscopy. *Limnology and Oceanography*, lno.12297. https://doi.org/10.1002/lno.12297

Li, F.-L., Li, Z.-X., Guo, M.-M., Wu, H.-Y., Zhang, T.-T., & Song, C.-H. (2016). Investigation of diarrhetic shellfish toxins in Lingshan Bay, Yellow Sea, China, using solid-phase

adsorption toxin tracking (SPATT). *Food Additives and Contaminants: Part A*, *33*(8), 1367–1373.
Lloyd, J. K., Duchin, J. S., Borchert, J., Quintana, H. F., & Robertson, A. (2013). Diarrhetic Shellfish Poisoning, Washington, USA, 2011. *Emerging Infectious Diseases*, *19*(8), 1314–1316. https://doi.org/10.3201/eid1908.121824
MacKenzie, L., Beuzenberg, V., Holland, P., McNabb, P., & Selwood, A. (2004). Solid phase adsorption toxin tracking (SPATT): A new monitoring tool that simulates the biotoxin contamination of filter feeding bivalves. *Toxicon*, *44*(8), 901–918. https://doi.org/10.1016/j.toxicon.2004.08.020
Mann, K.H., Lazier, J.R.N., 1991. Dynamics of Marine Ecosystems. Biological-physical Interactions in the Oceans. Blackwell Scientific Publications, Boston
Margalef, R. (1978). Life-forms of phytoplankton as survival alternatives in an unstable environment. *Oceanol.*, *1*, 493–509.
Maranda, L., & Shimizu, Y. (1987). Diarrhetic Shellfish Poisoning in Narragansett Bay. *Estuaries*, *10*(4), 298. https://doi.org/10.2307/1351887
Maranda, L., Corwin, S., & Hargraves, P. E. (2007). Prorocentrum lima (Dinophyceae) in northeastern USA coastal waters I. Abundance and distribution. *Harmful Algae*.
Maranda, L., Corwin, S., Dover, S., & Morton, S. L. (2007). *Prorocentrum lima* (Dinophyceae) in northeastern USA coastal waters II: Toxin load in the epibiota and in shellfish. *Harmful Algae*.
Marshall, H. G. (1980). Seasonal Phytoplankton Composition in the Lower Chesapeake Bay and Old Plantation Creek, Cape Charles, Virginia. *Estuaries*, *3*(3), 207. https://doi.org/10.2307/1352071
Marshall, H. G., Nesius, K. K. & Cibik, S. J. 1981. Phytoplankton studies within the Virginia Barrier Islands. II. Seasonal study of phytoplankton within the barrier island channels. Castanea 46:89–99.
Marshall, H. G. 1982. The composition of phytoplankton within the Chesapeake Bay Plume and adjacent waters off the Virginia coast, USA. *Estuar. Coast. Shelf Sci*. 15:29–43.
McGillicuddy, D. J., & Franks, P. J. S. (2019). Models of Plankton Patchiness. In *Encyclopedia of Ocean Sciences* (pp. 536–546). Elsevier. https://doi.org/10.1016/B978-0-12-409548-9.11610-0
Merel, S., Walker, D., Chicana, R., Snyder, S., Baurès, E., & Thomas, O. (2013). State of knowledge and concerns on cyanobacterial blooms and cyanotoxins. *Environment International*, *59*, 303–327. https://doi.org/10.1016/j.envint.2013.06.013
Miles, C.O., Wilkins, A.L., Munday, R., Dines, M.H., Hawkes, A.D., Briggs, L.R., Sandvik, M., Jensen, D.J., Cooney, J.M., Holland, P.T., Quilliam, M.A., MacKenzie, A.L., Beuzenberg, V., Towers, N.R., 2004a. Isolation of pectenotoxin-2 from *Dinophysis acuta* and its conversion to pectenotoxin-2 seco acid, and preliminary assessment of their acute toxicities. *Toxicon*. 43, 1–9. https://doi.org/10.1016/j.toxicon.2003.10.003
Mitra, A., Flynn, K. J., Tillmann, U., Raven, J. A., Caron, D., Stoecker, D. K., Not, F., Hansen, P. J., Hallegraeff, G., Sanders, R., Wilken, S., McManus, G., Johnson, M., Pitta, P., Våge, S., Berge, T., Calbet, A., Thingstad, F., Jeong, H. J., … Lundgren, V. (2016). Defining Planktonic Protist Functional Groups on Mechanisms for Energy and Nutrient Acquisition: Incorporation of Diverse Mixotrophic Strategies. *Protist*, *167*(2), 106–120. https://doi.org/10.1016/j.protis.2016.01.003

Morton, S. L., Leighfield, T. A., Haynes, B. L., Petitpain, D. L., Busman, M. A., Moeller, P. D. R., Bean, L., McGowan, J., Hurst Jr, J. W., & Van Dolah, F. (1999). Evidence of diarrhetic shellfish poisoning along the coast of Maine. *Journal of Shellfish Research*, *18*(2), 681–686.

Mulford, R. A. (1972). An Annual Plankton Cycle on the Chesapeake Bay in the Vicinity of Calvert Cliffs, Maryland June 1969-May 1970. *Academy of Natural Sciences*, *124*, 17–40.

Nielsen, L., Krock, B., & Hansen, P. (2012). Effects of light and food availability on toxin production, growth and photosynthesis in *Dinophysis acuminata*. *Marine Ecology Progress Series*, *471*, 37–50. https://doi.org/10.3354/meps10027

Olson, R. J., & Sosik, H. M. (2007). A submersible imaging-in-flow instrument to analyze nano- and microplankton: Imaging FlowCytobot: In situ imaging of nano- and microplankton. *Limnology and Oceanography: Methods*, *5*(6), 195–203. https://doi.org/10.4319/lom.2007.5.195

Onofrio, M. D., Egerton, T. A., Reece, K. S., Pease, S. K. D., Sanderson, M. P., Iii, W. J., Yeargan, E., Roach, A., DeMent, C., Wood, A., Reay, W. G., Place, A. R., & Smith, J. L. (2021). Spatiotemporal distribution of phycotoxins and their co-occurrence within nearshore waters. *Harmful Algae*, *103*, 101993. https://doi.org/10.1016/j.hal.2021.101993

Park, M., Kim, S., Kim, H., Myung, G., Kang, Y., & Yih, W. (2006). First successful culture of the marine dinoflagellate *Dinophysis acuminata*. *Aquatic Microbial Ecology*, *45*, 101–106. https://doi.org/10.3354/ame045101

Peacock, M. B., Gibble, C. M., Senn, D. B., Cloern, J. E., & Kudela, R. M. (2018). Blurred lines: Multiple freshwater and marine algal toxins at the land-sea interface of San Francisco Bay, California. *Harmful Algae*, *73*, 138–147. https://doi.org/10.1016/j.hal.2018.02.005

Pease, Sarah., K.D. (2021). *Co-occurring HAB species and phycotoxins: Interactions with oysters*. PhD Thesis. William & Mary.

Pease, S. K. D., Brosnahan, M. L., Sanderson, M. P., & Smith, J. L. (2022). Effects of Two Toxin-Producing Harmful Algae, *Alexandrium catenella* and *Dinophysis acuminata* (Dinophyceae), on Activity and Mortality of Larval Shellfish. *Toxins*, *14*(5), 335. https://doi.org/10.3390/toxins14050335

Peters, F., & Marrasé, C. (2000). Effects of turbulence on plankton: An overview of experimental evidence and some theoretical considerations. *Marine Ecology Progress Series*, *205*, 291–306. https://doi.org/10.3354/meps205291

Pizarro, G., Moroño, Á., Paz, B., Franco, J., Pazos, Y., & Reguera, B. (2013). Evaluation of Passive Samplers as a Monitoring Tool for Early Warning of *Dinophysis* Toxins in Shellfish. *Marine Drugs*, *11*(10), 3823–3845. https://doi.org/10.3390/md11103823

Pollingher, U., & Zemel, E. (1981). In situ and experimental evidence of the influence of turbulence on cell division processes of *Peridinium cinctum* forma *westii* (Lemm.) Lefèvre. *British Phycological Journal*, *16*(3), 281–287. https://doi.org/10.1080/00071618100650301

Pratchett, M. S., Munday, P. L., Wilson, S. K., Graham, N. A. J., Cinner, J. E., Bellwood, D. R., Jones, G. P., Polunin, N. V. C., & McClanahan, T. R. (2008). Effects of climate -induced coral bleaching on coral -reef fishes—Ecological and economic consequences. In *Oceanography and Marine Biology* (0 ed., Vol. 46, pp. 251–296). CRC Press. https://doi.org/10.1201/9781420065756-8

Reguera, B., Riobó, P., Rodríguez, F., Díaz, P., Pizarro, G., Paz, B., Franco, J., & Blanco, J. (2014). Dinophysis Toxins: Causative Organisms, Distribution and Fate in Shellfish. *Marine Drugs*, *12*(1), 394–461. https://doi.org/10.3390/md12010394

Reguera, B., Velo-Suárez, L., Raine, R., & Park, M. G. (2012). Harmful *Dinophysis* species: A review. *Harmful Algae*, *14*, 87–106. https://doi.org/10.1016/j.hal.2011.10.016

Roué, M., Darius, H., & Chinain, M. (2018). Solid Phase Adsorption Toxin Tracking (SPATT) Technology for the Monitoring of Aquatic Toxins: A Review. *Toxins*, *10*(4), 167. https://doi.org/10.3390/toxins10040167

Satake, M., Ofuji, K., Naoki, H., James, K. J., Furey, A., McMahon, T., Silke, J., & Yasumoto, T. (1998). Azaspiracid, a New Marine Toxin Having Unique Spiro Ring Assemblies, Isolated from Irish Mussels, *Mytilus edulis*. *Journal of the American Chemical Society*, *120*(38), 9967–9968. https://doi.org/10.1021/ja981413r

Sellner, K. G., Doucette, G. J., & Kirkpatrick, G. J. (2003). Harmful algal blooms: Causes, impacts and detection. *Journal of Industrial Microbiology and Biotechnology*, *30*(7), 383–406. https://doi.org/10.1007/s10295-003-0074-9

Shultz, D., Campbell, L., & Kudela, R. M. (2019). Trends in *Dinophysis* abundance and diarrhetic shellfish toxin levels in California mussels (*Mytilus californianus*) from Monterey Bay, California. *Harmful Algae*, *88*, 101641. https://doi.org/10.1016/j.hal.2019.101641

Smith, J. L., Tong, M., Fux, E., & Anderson, D. M. (2012). Toxin production, retention, and extracellular release by *Dinophysis acuminata* during extended stationary phase and culture decline. *Harmful Algae*, *19*, 125–132. https://doi.org/10.1016/j.hal.2012.06.008

Sosik, H. M., & Olson, R. J. (2007). Automated taxonomic classification of phytoplankton sampled with imaging-in-flow cytometry: Phytoplankton image classification. *Limnology and Oceanography: Methods*, *5*(6), 204–216. https://doi.org/10.4319/lom.2007.5.204

Stoecker, D. K. (1998). Conceptual models of mixotrophy in planktonic protists and some ecological and evolutionary implications. *European Journal of Protistology*, *34*(3), 281–290. https://doi.org/10.1016/S0932-4739(98)80055-2

Stoecker, D. K., Long, A., Suttles, S. E., & Sanford, L. P. (2006). Effect of small-scale shear on grazing and growth of the dinoflagellate Pfiesteria piscicida. *Harmful Algae*, *5*(4), 407–418. https://doi.org/10.1016/j.hal.2005.11.009

Sullivan, J. M., Swift, E., Donaghay, P. L., & Rines, J. E. B. (2003). Small-scale turbulence affects the division rate and morphology of two red-tide dinoflagellates. *Harmful Algae*, *2*(3), 183–199. https://doi.org/10.1016/S1568-9883(03)00039-8

Swanson, K. M., Flewelling, L. J., Byrd, M., Nunez, A., & Villareal, T. A. (2010). The 2008 Texas *Dinophysis ovum* bloom: Distribution and toxicity. *Harmful Algae*, *9*(2), 190–199. https://doi.org/10.1016/j.hal.2009.10.001

Tango, P., Butler, W., Lacouture, R., Goshorn, D., Magnien, R., Michael, B., Hall, S., Brohawn, K., Wittman, R., & Beatty, W. (n.d.). An unprecedented bloom of *Dinophysis acuminata* in Chesapeake Bay. *In Steidinger, K. A., Landsberg, J. H., Tomas, C. R. & Vargo, G. A. [Eds.] Harmful Algae 2002. Florida Fish and Wildlife Conservation Commission, Florida Institute of Oceanography, and Intergovernmental Oceanographic Commission of UNESCO*, 358–360.

Thomas, W. H., Vernet, M., & Gibson, C. H. (1995). Effects Of Small-Scale Turbulence On Photosynthesis, Pigmentation, Cell Division, And Cell Size In The Marine Dinoflagellate *Gonyaulax polyedra* (Dinophyceae)[1]. *Journal of Phycology*, *31*(1), 50–59. https://doi.org/10.1111/j.0022-3646.1995.00050.x

Tong, M., Kulis, D. M., Fux, E., Smith, J. L., Hess, P., Zhou, Q., & Anderson, D. M. (2011). The effects of growth phase and light intensity on toxin production by *Dinophysis acuminata*

from the northeastern United States. *Harmful Algae*, *10*(3), 254–264. https://doi.org/10.1016/j.hal.2010.10.005

Tong, M., Smith, J., Kulis, D., & Anderson, D. (2015). Role of dissolved nitrate and phosphate in isolates of *Mesodinium rubrum* and toxin-producing *Dinophysis acuminata*. *Aquatic Microbial Ecology*, *75*(2), 169–185. https://doi.org/10.3354/ame01757

Trainer, V., Moore, L., Bill, B., Adams, N., Harrington, N., Borchert, J., da Silva, D., & Eberhart, B.-T. (2013). Diarrhetic Shellfish Toxins and Other Lipophilic Toxins of Human Health Concern in Washington State. *Marine Drugs*, *11*(6), 1815–1835. https://doi.org/10.3390/md11061815

Wolny, J. L., Egerton, T. A., Handy, S. M., Stutts, W. L., Smith, J. L., Whereat, E. B., Bachvaroff, T. R., Henrichs, D. W., Campbell, L., & Deeds, J. R. (2020). Characterization of *Dinophysis* spp. (Dinophyceae, Dinophysiales) from the mid-Atlantic region of the United States [1]. *Journal of Phycology*, *56*(2), 404–424. https://doi.org/10.1111/jpy.12966

Wurtsbaugh, W. A., Paerl, H. W., & Dodds, W. K. (2019). Nutrients, eutrophication and harmful algal blooms along the freshwater to marine continuum. *WIREs Water*, *6*(5). https://doi.org/10.1002/wat2.1373

Yasumoto, T., Murata, M., Oshima, Y., Sano, M., Matsumoto, G. K., & Clardy, J. (1985). Diarrhetic Shellfish Toxins. *Tetrahedron*, *41*(6), 1019–1025.a

Zirbel, M. J., Veron, F., & Latz, M. I. (2000). The reversible effect of flow on the morphology of *ceratocorys horrida* (PERIDINIALES, DINOPHYTA) [*]. *Journal of Phycology*, *36*(1), 46–58. https://doi.org/10.1046/j.1529-8817.2000.98088.x

CHAPTER 1:

IDENTIFYING DRIVERS OF *DINOPHYSIS* ABUNDANCE IN CHESAPEAKE BAY USING HIGH-RESOLUTION IMAGING FLOWCYTOBOT (IFCB) AND ENVIRONMENTAL DATA

ABSTRACT

The mixotrophic dinoflagellate *Dinophysis* and its two classes of toxin, dinophysistoxins (DTXs) and pectenotoxins (PTXs), have been increasingly found on U.S. coasts within the past several decades. *Dinophysis* and DTXs is a causative organism of diarrhetic shellfish poisoning (DSP) in humans while PTXs have been linked to shellfish and finfish illness. In Chesapeake Bay, *Dinophysis* cells and toxins have been found year-round in coastal waters and shellfish meat, and while DTXs have remained below regulatory limits thus far, further research is needed to characterize and understand *Dinophysis* bloom dynamics given this region's lucrative oyster and northern quahog (hard clam) aquaculture. An Imaging FlowCytobot (IFCB) was deployed off the Virginia Institute of Marine Science (VIMS) pier for five sampling seasons from 2017 through 2022, and generated abundance data for *Dinophysis acuminata*, *Mesodinium rubrum*, and *Prorocentrum cordatum* (formerly *Prorocentrum minimum*). In addition to these biotic variables, abiotic variables (i.e., sea surface temperature (SST), salinity, turbidity, pH, discharge) were also included in a generalized additive model (GAM) with an autoregressive (AR1) covariance structure, with the goal of further understanding *Dinophysis* bloom dynamics in this region. Lagging *M. rubrum* abundance in relation to *D. acuminata* abundance was explored by fitting several different models, as a relationship between the predator and prey have been documented in previous literature. The models revealed that *D. acuminata* abundance was strongly linked to salinity, time of year, *M. rubrum* abundance with a 14-day lag, and *P. cordatum* abundance in this system. While the models may be improved by incorporating different predictor variables or including a larger data set, the results of this study provide regulatory agencies with other species that may serve as early indicators of *D. acuminata* abundance in Chesapeake Bay.

INTRODUCTION

The mixotrophic dinoflagellate *Dinophysis* produces lipophilic toxins, known as diarrhetic shellfish toxins (DSTs), that can accumulate in filter feeders and lead to diarrhetic shellfish poisoning (DSP) in humans (Yasumoto et al. 1985, Dominguez et al. 2010, Reguera et al. 2014). Symptoms of DSP are characterized by gastrointestinal illness including diarrhea, nausea, and vomiting. Symptoms typically appear 3 to 12 hours after ingestion of contaminated shellfish, with a recovery time of around 3 days (Aune & Yndestad 1993, Hallegraeff, 2004, Blanco et al. 2005). *Dinophysis* spp. can also produce pectenotoxins (PTXs), which are polyether lactones that have been shown to negatively affect shellfish and finfish health (Miles et al. 2004, Rountos et al. 2019, Gaillard et al. 2020, Pease et al. 2022, Gaillard et al. 2023), but potential human health impacts are still debated (Reguera et al. 2014). Since Park et al. (2006) established the first *Dinophysis* cultures through a three-step feeding regime involving the cryptophyte *Teleaulax* and the ciliate *Mesodinium rubrum*, lab experiments have been carried out to determine the response of *Dinophysis* cultures to a variety of environmental factors including changes in temperature, salinity, and prey availability (Kamiyama et al. 2010, Hattenrath-Lehmann et al. 2015, Tong et al. 2015, Basti et al. 2018, Smith et al. 2018, Fiorendino et al. 2020, Gaillard et al. 2021).

Cultures of *D. ovum* and *D. caudata* have been found to grow best at moderate temperatures (18-24˚C) (Fiorendino et al. 2020), while Basti et al. (2015) found that cell density of a *D. caudata* culture increased significantly with increasing temperature, reaching maximum densities under 27, 30, and 32.5˚C. Similarly, Kamiyama et al. (2010) found an increase in cell abundance, as well as increases in toxin content, when *D. acuminata* culture was exposed to increasing temperatures (10, 14, 18, and 22˚C). Research involving the impact of salinity on

Dinophysis spp. growth and toxin production are relatively limited, but Fiorendino et al. (2020) found optimal growth conditions for *D. ovum* isolated from Surfside Beach, TX, and *D. acuminata* isolated from Nassawadox, VA to be between 22-26. Cultures of *D.* cf *sacculus* have been shown to have a high tolerance to abrupt changes in salinity (Gaillard et al. 2021). *Dinophysis* is also an obligate mixotroph, requiring the presence of light and prey to reach maximal growth rates (Park et al. 2006, Kim et al, 2008, Riisgaard & Hansen, 2009). Smith et al. (2018) found that prey strain, nutritional content, and biovolume impacted a *D. acuminata* culture; *D. acuminata* exhibited a higher growth rate, biovolume, toxin quota and toxin per mL of culture when fed a larger, more nutritious strain of *M. rubrum*. These culturing studies have provided valuable information about *Dinophysis* growth, physiology, and toxin production in response to various environmental conditions in a controlled laboratory setting.

In combination with culturing studies, research has also focused on studying field populations of *Dinophysis* spp. to better understand the influence of local and long-term hydrodynamic conditions on growth and toxin production in different regions. *Dinophysis* is globally distributed (Reguera et al. 2012), and the systems in which *Dinophysis* blooms occur are often vastly different. However, some common themes have emerged from the literature that describe *Dinophysis* physiology and population dynamics *in situ*. Several studies, ranging from the Galician Rías Baixas (NW Spain) to the Swedish west coast, have highlighted the importance of large-scale hydrological forcings on *Dinophysis* populations, particularly the role of winds, advection, and upwelling (Godhe et al. 2002, Díaz et al. 2013, Díaz et al. 2019). The Galician Rías Baixas experiences upwelling-downwelling cycles, and these transitions can have a significantly negative impact on *Dinophysis* populations through direct physical effects (i.e., dispersion and advection out of coastal areas) or indirect effects (i.e., disturbance of cells via

turbulence and a rapid decrease in temperature in surface waters) (Díaz et al. 2019). Godhe et al. (2016) found that salinity and wind (both of which can contribute to stratification), were important factors in *Dinophysis* abundance on the Swedish west coast. Like other studies, the authors deduced that the observed *Dinophysis* population was not endemic to the study area and was instead advected into the region via wind and currents (Campbell et al. 2010). Studies have shown that *Dinophysis*, like other dinoflagellates, has a patchy distribution and has also been shown to form thin vertical layers (sometimes at depth) in the water column (Escalera et al. 2012, Reguera et al. 2012).

Along with physical forcings, another important controller of *Dinophysis* population dynamics *in situ* is prey availability. As an obligate mixotroph, *Dinophysis* requires ciliate prey and light to survive (Park et al. 2006, Kim et al. 2008, Riisgaard & Hansen, 2009). Field studies have shown that *Dinophysis* and its prey, *M. rubrum*, co-occur spatiotemporally and at depth (Sjöqvist & Lindholm, 2011, Reguera et al. 2012). Evidence from the Northern Baltic Sea revealed that while *D. acuminata* did not exhibit daily vertical migration, staying within the upper 9 m, *M. rubrum* migrated from the surface to 20 m (Sjöqvist & Lindholm 2011). In the Gulf of Mexico, U.S., Harred and Campbell (2014) analyzed *D. ovum* and *M. rubrum* abundance and environmental data over a 5-year period and found a positive time-lagged correlation between *Mesodinium* and *Dinophysis* of up to 60 days, suggesting that *Mesodinium* abundance could potentially serve as an early indicator of a *D. ovum* bloom. However, the authors could not identify a strong predator-prey relationship in periods when both *M. rubrum* and *D. ovum* overlapped. A recent study conducted in the Southern California Bight (SBC) found links between ciliate abundance and *Dinophysis* spp. cell abundance, with predictive models identifying ciliate abundance as an important predictor of *Dinophysis* abundance (i.e., higher

abundance of ciliates leads to higher abundance of *Dinophysis* spp.); however, this study included ciliates as a general category, not just *M. rubrum* (Kenitz et al. 2023). Other studies from around the world have found that peaks in *M. rubrum* abundance can precede peaks of *Dinophysis* spp. by weeks to months (Yih et al. 2013, Moita et al. 2016, Anschütz et al. 2022). Some studies have also found correlations between *Dinophysis* abundance and nutrients (i.e., N:P ratios), dissolved oxygen (DO), sea surface temperature (SST), and total suspended solids (TSS) (Singh et al. 2014, Ajani et al. 2016). The wide range of significant environmental variables reported reflects the specificity needed to determine *Dinophysis* population dynamics from region to region.

An Imaging FlowCytobot (IFCB) was regularly deployed off the Virginia Institute of Marine Science (VIMS) pier from 2017-2022. The IFCB is an invaluable monitoring tool that uses flow cytometry and high-resolution photography to capture images of individual phytoplankton cells between 10-150 μm, while also providing peripheral data, e.g., chlorophyll fluorescence or biovolume, for each image (Olson & Sosik 2007, Sosik & Olson 2007). Due to its frequency of sampling (approximately every 20 minutes) and long-term deployment capabilities (6 months at a time), the IFCB is ideal for the early detection of relatively low-abundance harmful algal blooms (HABs). *Dinophysis* is one such genus that does not discolor the water during blooms, and yet is able to cause shellfish closures when present at just a few hundred cells per liter (Campbell et al. 2010). The current study utilized six years, five sampling seasons, of high-resolution data for several abiotic factors (pH, salinity, SST, turbidity, discharge), as well as biological data generated from the IFCB (daily cell concentrations, cells mL^{-1}, for *D. acuminata*, *M. rubrum*, and *P. cordatum*), to: (1) identify abiotic and/or biotic

factors driving *D. acuminata* abundance; and (2) develop ecological models to predict the relative abundance of *Dinophysis acuminata* in the York River, Chesapeake Bay.

MATERIALS AND METHODS

2.1 Study site

The York River estuary is the fifth largest tributary in Chesapeake Bay, with a flow and watershed area on the order of 6900 km^2 (2662 mi^2) (Reay & Moore, 2009) (Figure 1). The two major tributaries of the York River include the Mattaponi and Pamunkey Rivers, whose

Figure 1 Map of the Chesapeake Bay (inset) and the study site (Virginia Institute of Marine Science (VIMS) pier (37.247333˚N, 76.499427˚W). Symbol indicates approximate location of VIMS pier where IFCB was deployed.

confluence is located around West Point (37.5315˚N, 76.7964˚W) (Lin & Kuo, 2001). The combination of freshwater inputs from the above tributaries and saltwater inputs from the Atlantic Ocean create a salinity gradient in the York River (Reay, 2009). It is also classified as a microtidal, partially mixed estuary (Reay & Moore, 2009). Stratification and vertical mixing of the water column are both present and oscillate depending on seasonal and tidal cycles (Haas,

1977, Sharples et al. 1994). Freshwater inputs, reduced mixing during neap tides, and local surface water heating can induce water column stratification, while turbulent mixing from storms and tides can promote water column mixing (Reay, 2009). The York River represents a unique continuum of freshwater to estuarine habitat, and as such, boasts a diverse phytoplankton assemblage including diatoms, chlorophytes, cyanobacteria, cryptomonads, euglenophytes, and dinoflagellates (Marshall, 2009).

2.2 Data acquisition

An Imaging FlowCytobot (IFCB, McLane Research Laboratories, Inc., Falmouth, MA) was deployed off the Virginia Institute of Marine Science (VIMS) pier in the York River, Chesapeake Bay, from 2018 – 2022 (37.247333˚N, 76.499427˚W) (Figure 1). The IFCB uses a combination of flow cytometry and high-resolution photography to capture images of individual phytoplankton cells between 10-150 μm, while also providing peripheral data, e.g., chlorophyll fluorescence or biovolume, for each image (Olson & Sosik, 2007). The red diode laser within the IFCB causes chlorophyll-containing cells to fluoresce, which then triggers the xenon flash lamp to illuminate the flow cell before an image is captured (Olson & Sosik, 2007). The instrument draws a 5-mL water sample every ~20 minutes, thus generating large, continuous data sets when deployed for several months at a time. Before a sample enters the IFCB, it first passes through a 130-μm Nitex screen that is surrounded by 1-mm copper mesh. To prevent biofouling within the instrument, a sodium azide solution and/or detergent is added internally approximately daily (Olson & Sosik, 2007). After image acquisition, the data were transferred from the onboard CPU to a server at VIMS every 4 hours. Between 2017 and 2022, deployment efforts were focused on November 1st through June 1st.

2.3 Convolutional Neural Network (CNN) classifier development

An inception v3 model was constructed to identify phytoplankton taxa present in the IFCB image time series from the York River, Chesapeake Bay from 2017 – 2022 (https://github.com/WHOIGit/ifcb_classifier). Inception v3 is a type of convolutional neural network model that resolves image features at a variety of scales while also balancing model complexity and computational cost for model application (Szegedy et al. 2016). The model was built from a total of 129 training set classes provided by M. Brosnahan and H. Sosik (Woods Hole Oceanographic Institute, WHOI). Of these, 116 defined taxa were to genus or species level with no less than 50 images. An additional 5 classes defined other cell types and 8 defined other common particle types (beads, detritus, camera spots, etc.). Region-specific images were added to the training set using VIMS pier deployment data: small and large *Mesodinium rubrum*, *Prorocentrum cordatum*, *Fragilariopsis*, *Gymnodinium*, and *Navicula*. After the first v3 model iteration, ~3 syringes per month were manually annotated over the 6 years of data, with a focus on *Dinophysis* spp., *Mesodinium rubrum*, *Prorocentrum*, *Prorocentrum cordatum*, *Prorocentrum dentatum*, *Prorocentrum micans*, and *Prorocentrum triestinum* using the WHOI IFCB annotate software (https://ifcb-annotate.whoi.edu, https://github.com/LouisK130/IFCB-Annotate). It was hypothesized that *Prorocentrum* spp. abundance, due to its ability to form high biomass blooms and observed co-occurrence with *Dinophysis* spp., may be able to be used as a proxy for *Dinophysis* spp. abundance. As such the five different *Prorocentrum* groups were included in the v3 model. After additional CNN model development, several *Prorocentrum* categories were excluded (*Prorocentrum* (general), *Prorocentrum micans*, *Prorocentrum dentatum*, *Prorocentrum triestinum*) due to low cell abundances throughout the sampling seasons. To evaluate the accuracy and precision of the classifier, histograms comparing true positive (TP)

and false positives (FP) produced by the classifier were made (Figure S1, S2); a correction factor was applied to cell abundance data based on the FP to TP ratio. The accuracy/precision histograms were also used to determine a threshold where the classifier had the highest probability for the lowest number of false positives; the threshold chosen for all classes in this study was 0.95 (Figure S1, S2). Additionally, the raw cell abundance data was corrected for the volume (mL) analyzed per day prior to model analysis, providing an average abundance for each taxa per day.

2.4 Environmental data

High-resolution environmental data for SST, salinity, pH, and turbidity were collected every 15 minutes from the Virginia Estuarine and Coastal Observing System (VECOS) Gloucester Point Continuous Monitoring Station (YRK005.40, 37.247284˚N N, 76.499369˚W) located north of the York River channel, ~5.4 nautical miles upstream from the mouth of the river in southeastern Virginia (http://vecos.vims.edu) (Table 1). The continuous monitoring station includes a fixed YSI 6600 data sonde, operated by the Chesapeake Bay National Estuarine Research Reserve (CBNERR), that is positioned 0.5 meters from the bottom of the river. Six years of data (2017 – 2022) were downloaded from the VECOS site. Any data that were marked as rejected due to mechanical malfunctions or sonde failures by VECOS were excluded from the analysis. Additionally, high-resolution discharge data were also downloaded for the Mattaponi (USGS site 01674500, 37.883889˚N, 77.165278˚W) and Pamunkey (USGS site 01673000, 37.7675˚N, 77.3325˚W) Rivers for the same time period from the United States Geological Survey (USGS) National Water Information System website (https://waterdata.usgs.gov/nwis/uv?) (Table 1). Discharge data from these two sites were averaged together. The high-resolution data for each abiotic variable were averaged over each day and are presented as an average per day.

2.5 Ecological model development

To begin, all biotic and abiotic data were sorted, and only days where paired abiotic and biotic data were available were used in analysis (n = 156). The data were also separated into sampling seasons between November 1 and June 1, the period when *Dinophysis* spp. abundance is elevated in Chesapeake Bay according to IFCB data. Initially, six years of data (2017 – 2022) were explored. However, data from 2017 and 2019 were excluded from the ecological model due to either gaps in the data from the IFCB being out of the water (2019), or rejection of environmental data due to equipment failures or malfunctions (2017); all data, however, are presented in figures. The IFCB was only deployed for one month (March) in 2019 due to an extensive troubleshooting period, i.e., sedimentation and internal biofouling.

Table 1 Variables used in ecological model development, along with their frequency, units, and source.

Type of data	Frequency	Variable	Units	Source
Biological	25 min	Phytoplankton taxa abundance	cells mL^{-1}	Imaging FlowCytobot (IFCB)
Hydrological	15 min	Sea surface temperature	˚C	VECOS, http://vecos.vims.edu
	15 min	Salinity	ppt	VECOS, http://vecos.vims.edu
	15 min	pH	Standard unit, SU	VECOS, http://vecos.vims.edu
	15 min	Turbidity	Nephelometric turbidity unit, NTU	VECOS, http://vecos.vims.edu
	15 min	Discharge	ft^3s^{-1}	USGS, https://waterdata.usgs.gov/

Analysis

All data transformations, visualizations, and analyses were conducted using the R language for statistical computing (R Core Team 2023). Prior to analysis, IFCB-generated abundance data for *Dinophysis*, *Mesodinium*, and *Prorocentrum* were log(x + 1) transformed (x = cells mL^{-1}) to meet normality assumptions of parametric analyses. Sampling dates were represented as integers by converting them to their corresponding Julian date.

The model framework for ln *Dinophysis* abundance/volume sampled (herein, ln *Dinophysis* abundance) is expressed as:

$$y \sim MVN(\mu, \Sigma)$$

$$\mu = f\left(x_p\right)$$

$$\Sigma_{ij} = \sigma_\epsilon \phi^{t_{ij}}$$

Here, the response variable *y* is a 1 x T vector of ln *Dinophysis* abundance. Covariance of sequential timesteps was modeled using continuous AR1 covariance matrix Σ where covariance of sequential observations is a function of random noise σ_ε^2 and autocorrelation parameter ϕ raised to t_{ij}, the temporal lag between observation i and observation j. The benefit of this covariance structure is its ability to model dependence among highly correlated, unequally spaced data generated from high-resolution time series. Meanwhile, μ denoted the mean expected ln *Dinophysis* abundance and was a function of predictors x_p (either linear or smoothed).

Several statistical model structures were employed to examine relationships between *Dinophysis* abundance and predictors of interest. Relationships between ln *Dinophysis* abundance and predictor variables (SST (˚C), salinity (ppt), pH, turbidity (Nephelometric

Turbidity Unit, NTU), discharge (ft^3s^{-1}), *Mesodinium* abundance (cells mL^{-1}), *Prorocentrum* abundance (cells mL^{-1})) were initially explored in a linear model framework including all predictor variables (Model 1a) (Table 2). Preliminary results from the initial model indicated that several predictors (discharge, SST, and pH) were not statistically significant, and consequently, a second linear model with a reduced set of predictors was subsequently fit with informative predictors (Model 2a) (Table 2). In addition, to explore potential non-linear relationships between *Dinophysis* abundance and predictor variables, a generalized additive model (GAM) framework was used, modeling predictors as weighted smoothed functions $f_p(x_p) = \sum_{k=1}^{Kp} \beta_{pk} b_{pk}(x_p)$ where $b_{pk}(x_p)$ are basis functions for predictor x_p for both full and reduced predictors (Models 3a and 4a) (Table 2). In Models 3a and 4a, all continuous predictor variables were fit with a smoothing function, while the categorical predictor variable (month) was not.

Additionally, previous studies that have modeled *Dinophysis* bloom dynamics have revealed that lagging *Mesodinium* abundance by up to 3 months relative to *Dinophysis* improved prediction of *Dinophysis* abundance (Yih et al. 2013, Harred & Campbell, 2014, Moita et al. 2016, Anschütz et al. 2022). To test this hypothesis in the current study, each of the four models from above (Models 1a, 2a, 3a, 4a) were run with no lag of *Mesodinium* abundance, a 14-day lag of *Mesodinium* (Models 1b, 2b, 3b, 4b), and a 75-day lag of *Mesodinium* (Models 1c, 2c, 3c, 4c). (Table 2). *P. cordatum* abundance and all other abiotic variables (i.e., SST, salinity, pH, discharge, turbidity) were not tested for lags with *Dinophysis* abundance given that we were most interested in understanding which of these factors coincided with elevated *Dinophysis* abundance.

In total, 12 statistical models were developed and evaluated within an Information Theoretic framework (Anderson & Burnham, 2002). For each model, AICc (Akaike's

Information Criterion) was employed to evaluate the degree of statistical support for each model. AIC is a metric that estimates the predictive performance of a model, and a lower AIC value indicates a better predictive performance. AIC penalizes for model complexity, thus lowering the risk of overfitting the model to the data, and AIC_c accounts for small sample size (Kenitz et al. 2023). Weighted model probabilities (w_i) based on Δ_i values, the difference between the AIC score of the best fitting model and model i, were used to determine the probability that a particular model was the best-fitting model in a set (Anderson, 2008). Likelihood ratio X^2 tests were then used to further evaluate models with comparable AIC_c scores to determine their importance (Anderson & Burnham, 2002). When two models had comparable AIC_c scores and likelihood ratio X^2 tests did not suggest significant differences in explanatory power, the simpler model was chosen as the more appropriate model under the principle of parsimony.

Table 2 Information theoretic analysis of 12 statistical models using SST (T), salinity (S), turbidity (Turb), month (M), discharge (D), *Mesodinium rubrum* abundance with no lag (Me), a 14-day lag (Me14), and a 75-day lag (Me75), and *Prorocentrum cordatum* abundance (P). AIC_c is the Akaike information criterion corrected for small sample size, Δ_i is the difference between any model and the best model in the set, and w_i is the weighted model probability that a given model is the best among the set considered. Values from the best model are shown in bold font.

Model	Formula	AICc	Δ_i	w_i
M1a	T + S + Turb + M + D + Me + P	327.56	38.07	0
M1b	T + S + Turb + M + D + Me14 + P	326.54	37.05	0
M1c	T + S + Turb + M + D + Me75 + P	331.44	41.95	0
M2a	S + M + Me + P	296.17	6.68	0.03
M2b	S + M + Me14 + P	296.63	7.14	0.02
M2c	S + M + Me75 + P	300.87	11.38	0
M3a	s(T) + s(S) + s(Turb) + M + s(D) + s(Me) + s(P)	310.32	20.83	0
M3b	s(T) + s(S) + s(Turb) + M + s(D) + s(Me14) + s(P)	302.84	13.35	0
M3c	s(T) + s(S) + s(Turb) + M + s(D) + s(Me75) + s(P)	310.44	20.95	0
M4a	s(S) + M + s(Me) + s(P)	293.41	3.92	0.11
M4b	**s(S) + M + s(Me14) + s(P)**	**289.49**	**0**	**0.79**
M4c	s(S) + M + s(Me75) + s(P)	295.22	5.73	0.05

RESULTS

3.1 Fluctuations in abiotic and biotic predictor variables during the study period

During the study period, average discharge from the Mattaponi and Pamunkey Rivers varied widely, with one precipitation event causing a maximum discharge rate of 16,195 $ft^3\ s^{-1}$; the lowest discharge rate during the study period was 121 $ft^3\ s^{-1}$ (Figure 2). The 2018 – 2019 and 2020 – 2021 sampling seasons had similar discharge rates, between 1737 $ft^3\ s^{-1}$ and 1760 $ft^3\ s^{-1}$, followed by the 2017 – 2018 sampling season (815 $ft^3\ s^{-1}$), 2019 – 2020 sampling season (606 $ft^3\ s^{-1}$), and 2021 – 2022 sampling season (555 $ft^3\ s^{-1}$) (Figure 2). Like discharge, turbidity in the York River was also variable during the study period, with a maximum of 40 NTU and a minimum of 1 NTU (Figure 2). When averaging across all sampling seasons, however, there was little difference (< 2 NTU) in turbidity between them (Figure 2). The maximum pH in the York River during the study period was 8.8, while the minimum was 7.4 (Figure 2). The 2018 – 2019 sampling season seemed to have the most variability, while the pH in the other sampling seasons remained fairly stable (Figure 2). SST in the York River was also variable; during all sampling seasons, the peak in SST was reached in early June, with a recorded maximum of 25˚C during the 2019 – 2020 sampling season (Figure 2). The lowest recorded SST during the study period was 0.2˚C in early January of the 2017 – 2018 sampling season (Figure 2).

Salinity fluctuated ~14ppt over the entire sampling period at the study site. The lowest recorded salinity was 10 ppt, and the highest was 24 ppt (Figure 2). The average salinity during the 2018 – 2019 sampling season was the lowest (13 ppt), while the highest average salinity was observed during the 2017 – 2018 sampling season (20 ppt) (Figure 2). Salinity during the 2017 -

2018, 2019 – 2020, and 2021 – 2022 sampling seasons appeared to steadily decline from November to June, while salinity was more consistent during 2018 – 2019 and 2020 – 2021 sampling seasons (Figure 2).

The bloom timing and magnitude of *M. rubrum* varied widely from year to year. The concentrations of *M. rubrum* ranged from ~ 7 cells mL^{-1} to over 400 cells mL^{-1} over the entire sampling period. The highest concentration of *Mesodinium* was recorded on March 16th, 2019, at 571 cells mL^{-1} (Figure 3). The earliest peak in *M. rubrum* occurred in December 2017, and the latest peak occurred in May 2022 (Figure 3). During the 2019 – 2020 and 2020 – 2021 sampling seasons, *M. rubrum* peaked between mid-February and mid-March (Figure 3).

The bloom timing of *P. cordatum* was more consistent from year to year, with the highest concentrations being observed between March and June (Figure 3). The highest concentration of *P. cordatum* was recorded on May 25th, 2018, at 607 cells mL^{-1} (Figure 3). A peak in *P. cordatum* concentration also occurred in June 2022, but was two orders of magnitude lower than 2018 (11 cells mL^{-1}) (Figure 3). During 2019 – 2020 *P. cordatum* peaked earlier in the season, around mid-April; the peak in *P. cordatum* occurred around late April during the 2020 – 2021 sampling season (Figure 3).

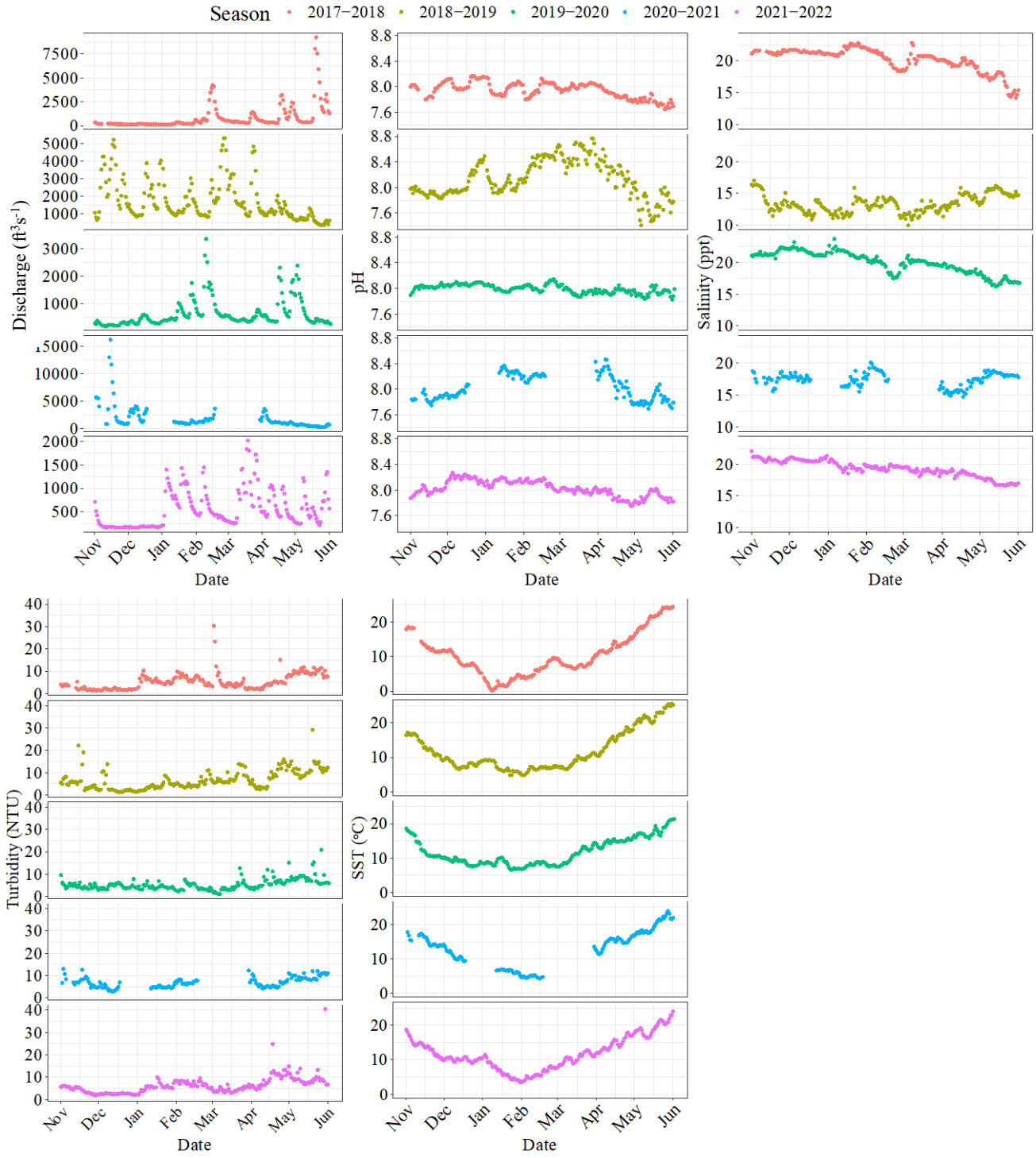

Figure 2 Panel of abiotic factors collected from a CBNERR sonde located in the York River across the five sampling seasons. Each line represents a sampling season.

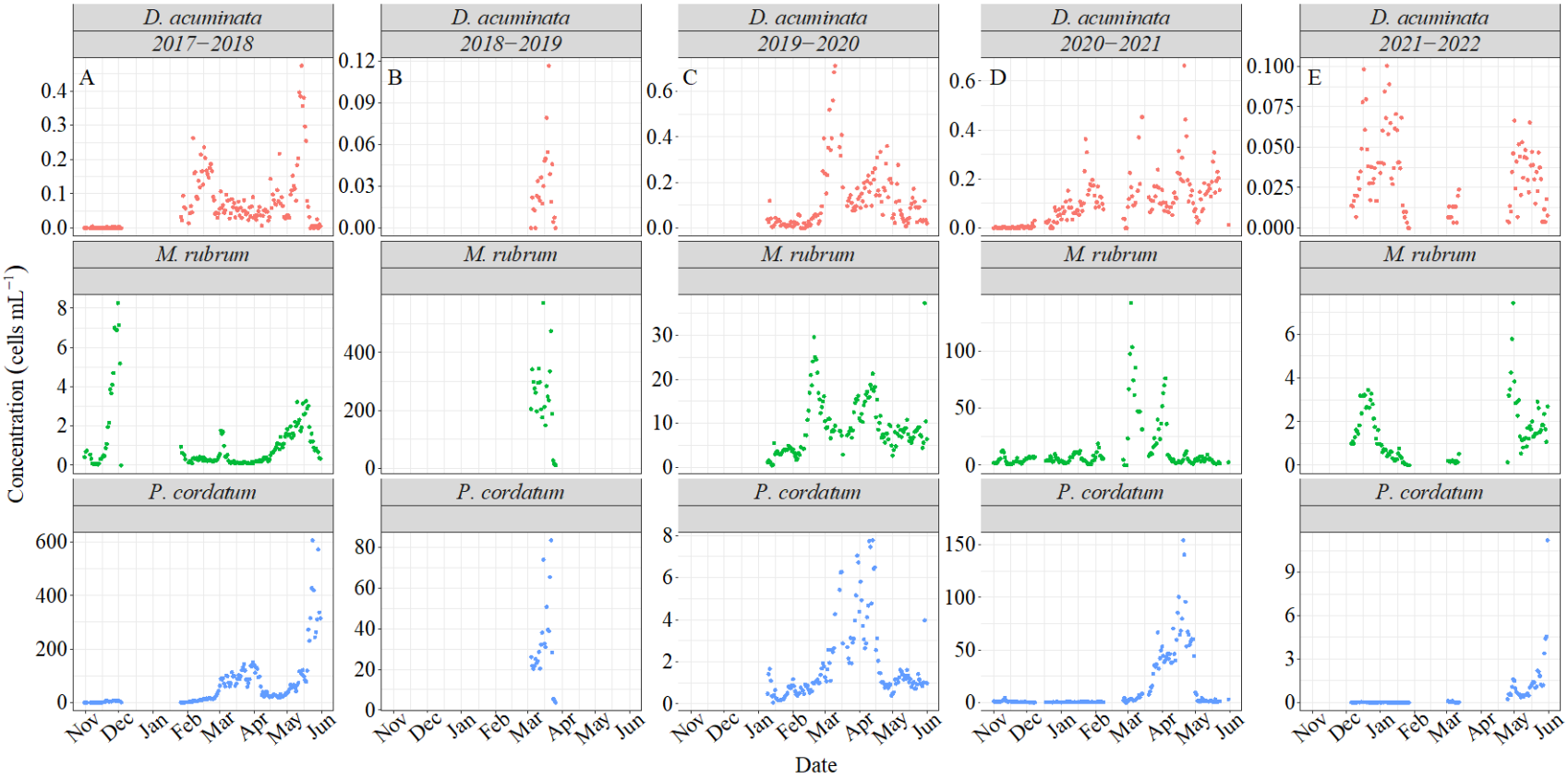

Figure 3 Panel of IFCB-generated abundance data (cells mL^{-1}) for *D. acuminata*, *M. rubrum*, and *P. cordatum* for the 2017 – 2018 (A), 2018 – 2019 (B), 2019 – 2020 (C), 2020 – 2021 (D), and 2021 – 2022 (E) sampling seasons.

3.2 Ecological model comparison and diagnostics

The best ecological model was Model 4b, a reduced generalized additive model with month, salinity, *M. rubrum* abundance with 14-day lag and *P. cordatum* abundance as predictors (AICc = 289.49, Table 2). Analysis of coefficients of smoothed terms for Model 4b indicated effective degrees of freedom for all smoothed terms except for salinity were 1, indicating the effects of the predictors were linear. As such, an additional model (Model 5) was created that was identical to Model 4b, but *M. rubrum* and *P. cordatum* abundance were not converted to smoothed functions. Log likelihood X^2 to test for the difference between these two models indicated they had equivalent statistical support ($p = 0.63$), and under the principle of parsimony, Model 5 was chosen. The value of phi (ϕ), a measure of autocorrelation, for Model 5 was 0.61 (min: 0.44, max: 0.75). Results herein will refer to Model 5.

3.3 Significant drivers of *Dinophysis* abundance

The timing and magnitude of *Dinophysis acuminata* varied from year to year, but *D. acuminata* abundance never exceeded 1 cell mL^{-1} between 2017 and 2022 (Figure 3). The highest concentration of *D. acuminata* during the study period occurred on March 10th, 2020, with a peak concentration of 0.7 cells mL^{-1} (Figure 3). The peak timing of *D. acuminata* abundance ranged from January during the 2021 – 2022 sampling season, to March during 2019 – 2020, and May during 2017 – 2018 and 2020 into 2021 (Figure 3). The IFCB was only deployed for the month of March during 2018 – 2019, but *Dinophysis* was detected during this month at concentrations less than 0.1 cells mL^{-1} (Figure 3).

Time of year had a negative effect on *D. acuminata* abundance, with higher concentrations of *D. acuminata* observed in January through May compared to November and June (Table 3, Figure 3). *Mesodinium rubrum* abundance with a 14-day lag and *P. cordatum*

abundance both had a positive effect on *D. acuminata* abundance (Table 3), with model coefficients of 0.35 ± 0.07, 0.22 ± 0.06, respectively. Salinity was included as a smoothed term in the final model and as such, there was a linear relationship with ln(*D. acuminata*) abundance up to ~ 17 ppt before the effect of salinity reached an asymptote and no longer had an effect on *D. acuminata* abundance (Figure 4).

Table 3 Model estimates and 95% confidence intervals for two biotic and one abiotic variable included in the final model (Model 5).

Variable	Minimum	Mean	Maximum
(Intercept)	-3.36	-2.61	-1.87
ln(*M. rubrum* abundance – 14 day lag)	0.20	0.35	0.50
ln(*P. cordatum* abundance)	0.11	0.22	0.34
Month2	-1.47	-0.56	0.35
Month3	-2.47	-1.25	-0.03
Month4	-1.70	-0.84	0.01
Month5	-2.11	-1.31	-0.50
Month6	-4.29	-2.93	-1.57
Month11	-4.24	-3.26	-2.28

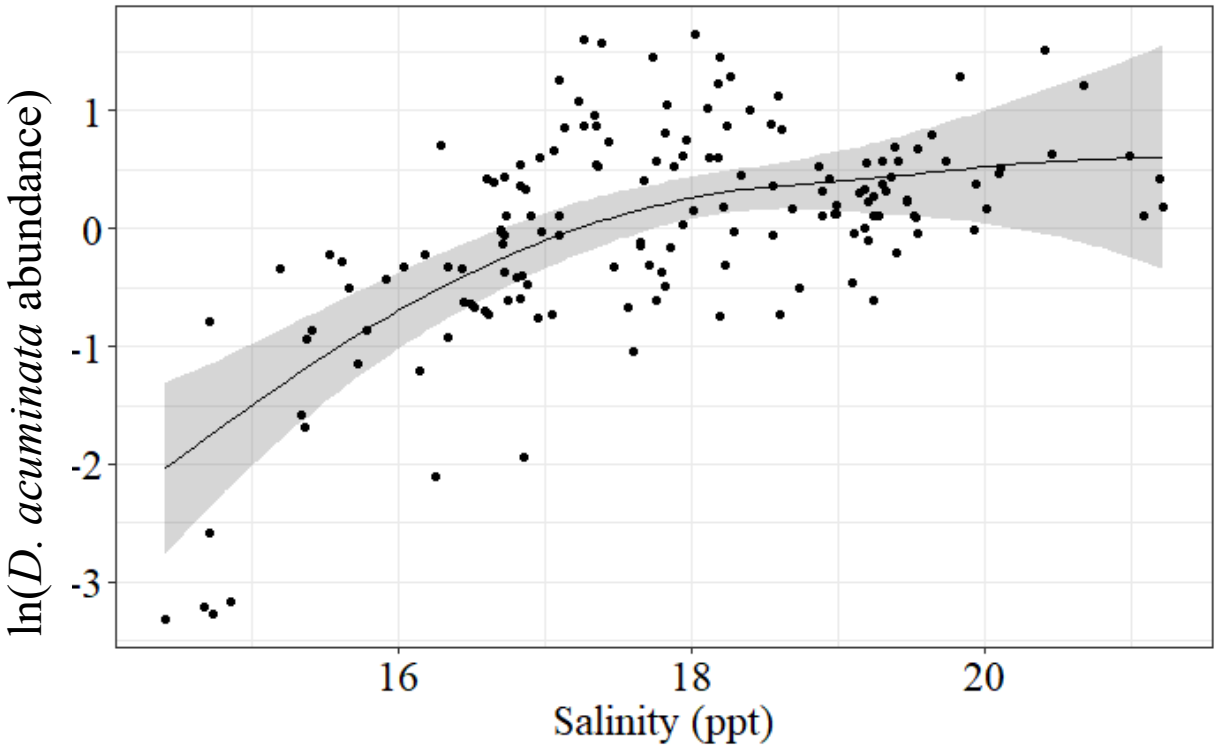

Figure 4 Plot of predicted values versus residuals of salinity (ppt) and ln(*Dinophysis acuminata* abundance) from the final model, Model 5. The gray band represents standard error.

DISCUSSION

The goal of the current study was to develop a predictive model for *Dinophysis acuminata* abundance in the York River, Chesapeake Bay, to better understand the relationship between *D. acuminata* abundance and a variety of abiotic and biotic factors. Important abiotic factors in the ecological model included salinity and time of year (month), while important biotic factors included *Mesodinium rubrum* abundance (the ciliate prey of *Dinophysis*), as well as *Prorocentrum cordatum* abundance. The relationship between predator and prey was explored by fitting additional models that each incorporated a different time-lag of *M. rubrum* abundance (no lag, 14-day, and 75-day lag). Ultimately, a 14-day lag of *M. rubrum* was incorporated into the final model, demonstrating the ciliate peak precedes *D. acuminata* by two weeks. The relationship between *M. rubrum* and *D. acuminata* has been well-documented in previous literature, but this is the first time a modeling study of this nature has been conducted in the Chesapeake Bay, with important implications for *D. acuminata* bloom dynamics in the York River. *Prorocentrum cordatum* was shown to be a co-occurring species with *D. acuminata*, lending potential for the higher-abundance HAB (3 orders of magnitude) to be investigated as a proxy or indicator of low-abundance *Dinophysis* blooms in future efforts towards forecasting of DSP and/or incorporation of satellite products.

4.1 Abiotic drivers

The two abiotic factors that were important predictors of *D. acuminata* abundance in the model were salinity and time of year (month). Salinity was included as a smoothed term in the model, meaning its effect on *D. acuminata* abundance was shown to be non-linear. Figure 4 demonstrates that there does appear to be a threshold where salinity will have a positive effect on *D. acuminata* abundance; after that threshold is reached, salinity no longer influences *D.*

acuminata abundance. Recent culturing studies have shown some *Dinophysis* isolates (*D. acuminata* and *D. ovum*) can only tolerate a narrow salinity range (22-26), while other isolates appear to be more tolerant of abrupt changes in salinity (*D.* cf *sacculus*), ranging from 25 up to 42 (Fiorendino et al. 2020, Gaillard et al. 2021). In the field, Harred and Campbell (2014) also proposed a narrow optimal salinity range in the Gulf of Mexico for bloom initiation of both *D. ovum* (28-33) and the ciliate prey item *M. rubrum* (30-34). In Japanese waters, *D. fortii* and *D. acuminata* were shown to appear at similar salinities (34 and 33, respectively) (Hoshiai et al. 2003). In the present study, the maximum salinity observed over the study period was 23.71 ± 0.49, which falls within the range proposed by Fiorendino et al. (2020) but is below the proposed range of Harred and Campbell (2014) and Hoshiai et al. (2003). In the York River, Chesapeake Bay, salinity appeared to have a positive effect on *D. acuminata* abundance up to a threshold of ~17 ppt, demonstrating that the salinity range in this system is lower compared to some of the previously reported studies, and growth of the *D. acuminata* population may require a relatively narrow salinity range.

Modeling and observational studies that aim to identify important drivers of *Dinophysis* spp. abundance have also included salinity as a predictor variable. Ajani et al. (2016) found that salinity was significantly associated with the abundance of *D. caudata*, but not *D. acuminata*, in Berowra Creek, southeastern Australia. Another study that investigated the influence of biotic and abiotic factors on *Dinophysis* spp. abundance and concentration of diarrhetic shellfish toxins (DSTs) in plankton populations identified salinity as one of the principal variables influencing the concentration of DSTs in plankton; salinity was inversely related to *Dinophysis* spp. abundance and diarrhetic shellfish toxin (DST) concentration (Godhe et al. 2002). Additionally, Bouquet et al. (2022) used two different methods to predict the effect of environmental factors

(i.e., SST, salinity, and turbidity) on *Dinophysis* and *Alexandrium* abundance, and the authors found that salinities less than 27.8 ppt posed the highest risk for the formation of a *Dinophysis* bloom in two French Mediterranean lagoons.

While salinity may directly control *Dinophysis* spp. and *M. rubrum* abundance, it may also exert an indirect influence through the promotion of water column stratification. Dinoflagellates are typically associated with stratified, nutrient-poor waters (Margalef, 1978), and *Dinophysis* abundance has also been associated with a stable, stratified water column (Reguera et al. 2012, Díaz et al. 2013). In the Reloncaví Fjord in southern Chile, seasonal field surveys identified saline stratification as an important factor promoting sustained *D. acuminata* populations in the inner portions of the fjords (Alves-de-Souza et al. 2018). The current study site, York River, Chesapeake Bay, is a dynamic system, whose salinities range from tidal freshwater to polyhaline regimes (Reay & Moore, 2009). The IFCB was deployed in the lower York River, which tends to be more stratified than the upper York due to deeper depths and weaker tidal currents (Friedrichs, 2009). However, the VIMS pier is located nearshore in the lower York, where the water is shallower and may be more well-mixed (Friedrichs, 2009). As such, the influence of stratification on *D. acuminata* populations in the York River cannot be fully explained without further study, or incorporation of a different metric of stratification other than discharge.

The other important abiotic predictor of *D. acuminata* abundance in the model was time of year (month). In the current study, the mean abundance of *D. acuminata* varied monthly in the lower York. It was generally not detected earlier in the year (November – December), before increasing in abundance in January and reaching peak concentrations in April and May (Figure 3). A similar seasonal pattern in *Dinophysis* abundance was documented in the Southern

California Bight and Australia, with peak *Dinophysis* spp. abundances being recorded in the spring and autumn months, and minimum cell abundances being recorded in winter months (Ajani et al. 2013, Ajani et al. 2016, Kenitz et al. 2023). Other systems have documented differences in bloom timing; for example, *D. acuminata* in the Galician Rías (off the Iberian coast) has been shown to persist throughout the upwelling season (spring and summer), while *Dinophysis acuta* appears later, when water column stratification is maximal (Escalera et al. 2006, Díaz et al. 2016). In addition, *D. acuminata* blooms have been documented in colder SSTs (10-5-14.8˚C) in Greek waters, and as high as 19˚C in the northwestern coast of the Netherlands (Peperzak et al. 1996, Koukaras & Nikolaidis, 2004, Ajani et al. 2016). The variability in bloom initiation under different temperatures suggests that temperature may not be the main driver of *Dinophysis* abundance in most systems. This agrees with the current study, as SST did not have a significant effect on *D. acuminata* abundance in the York River, Chesapeake Bay; SST ranged from ~ 5˚C to 20˚C between January through May across the five sampling seasons and reached a minimum of ~ 0˚C during the 2017- 2018 sampling season. However, it is important to note that SST may be indirectly influencing *Dinophysis* bloom dynamics by promoting a more stable stratified water column, increasing metabolic rates, or directly impacting its prey by accelerating growth, thus resulting in a shorter time frame for interaction with prey (Anschütz et al. 2022).

4.2 Biotic drivers

The two biotic factors that were important predictors of *D. acuminata* abundance included *M. rubrum* abundance and *P. cordatum* abundance. The relationship between *Dinophysis* and its prey item, the ciliate *Mesodinium rubrum*, has been well documented in field and lab studies, beginning with the first successful cultivation of a *Dinophysis acuminata* culture by Park et al. (2006). *Dinophysis* displays a complex feeding behavior, in which a *Dinophysis*

cell slowly approaches a resting *M. rubrum* cell, links itself to its prey with a peduncle or capture filament and tows the *M. rubrum* cell around. Eventually, *Dinophysis* transfers the *M. rubrum* cell contents into its own cell, where it digests them and only retains the *M. rubrum* plastids (Park et al. 2006, Jiang et al. 2018). *Dinophysis* is considered an obligate mixotroph, meaning it needs prey and light for long-term survival (Park et al. 2006, Smith et al. 2012).

In the field, several studies from different regions have shown that a peak in *M. rubrum* abundance may precede a peak in *Dinophysis* spp. abundance by weeks to several months (Yih et al. 2013, Harred & Campbell, 2014, Moita et al. 2016, Anschütz et al. 2022). For example, when documenting the occurrence of *M. rubrum* in Korean coastal waters, Yih et al. (2013) found that a population of *D. acuminata* peaked in abundance seven days after that of *M. rubrum*. Data from two monitoring stations in northwest Portugal and Galicia, Spain suggest a two-to-three-week delay between maxima of *M. rubrum* and *D. acuta*, while the population maxima of *D. acuminata* was coincident with that of *M. rubrum* (Moita et al. 2016). In the U.S., Harred and Campbell (2014) modeled the relationship between *M. rubrum* and *D. ovum* in the Gulf of Mexico, Texas, and found the highest positive correlation between *D. ovum* and *M. rubrum* abundance when *M. rubrum* abundance was lagged by up to one-to-two months. However, due to these lag times of up to 60 days, the authors hesitated to conclude that the peaks in *M. rubrum* abundance were a direct cause of the subsequent increases in *D. ovum* abundance. Additionally, a recent modeling study investigating the bloom dynamics of the *Teleaulax*-*Mesodinium*-*Dinophysis* (TMD) complex proposed that timing of prey availability has a significant effect on TMD bloom dynamics (Anschütz et al. 2022). As *M. rubrum* itself is an obligate mixotroph (Mitra et al. 2016), the timing in peaks of its prey item, cryptophytes belonging to the *Geminigera*/*Teleaulax* clades (Johnson et al. 2013), is also an important factor in this

complicated food web (Anschütz et al. 2022). The authors also emphasized that *M. rubrum*, as both an important grazer of cryptophyte populations as well as a prey source for *Dinophysis*, will have the biggest impact on the overall bloom dynamics of the TMD complex compared to other organisms in the system (Anschütz et al. 2022). In the current study, the peak in *M. rubrum* abundance was seen prior to that of *D. acuminata*, particularly in the 2017 – 2018, 2019- 2020, and 2020 – 2021 sampling seasons (Figure 3). In the 2017-2018 sampling season, the peak in *M. rubrum* occurred around December, and *D. acuminata* started to increase in abundance around February, before reaching a maximum in mid-May (i.e., 2 – 4.5-month lag). The peaks between the species were closer in time during 2019 – 2020, with the peak in *M. rubrum* occurring in late February, and the peak in *D. acuminata* occurring ~1 month later in mid-March (Figure 3). In 2020 – 2021, a peak in *M. rubrum* occurred in early March, with a subsequent peak in *D. acuminata* approximately 2 months later in mid – late April (Figure 3). In contrast, the *D. acuminata* peak in 2021 – 2022 appeared to be coincident with that of *M. rubrum* (Figure 3). As such, the model with the 14-day lag of *Mesodinium* was the best fit for the data compared to no lag and a 75-day lag. This agrees with the above studies, and suggests that like other systems, *M. rubrum* peak abundances in the York River, Chesapeake Bay may be an important factor driving *D. acuminata* abundances.

In addition to *M. rubrum* abundance, the abundance of *Prorocentrum cordatum* was also an important biological predictor of *D. acuminata* in the model. Given its propensity to form high-biomass blooms, *P. cordatum* abundance was included with the goal of potentially using *P. cordatum* abundance as a proxy for *D. acuminata* abundance. Since *Dinophysis* can "bloom" and produce toxins at extremely low cell concentrations (1-25 cells mL^{-1} in the U.S.) and typically does not discolor the water (Maestrini, 1998, Campbell et al. 2010, Trainer et al. 2013, Shultz et

al. 2019) or produce a detectable signal via satellite imagery, identifying another species that regulatory agencies could track as a predictor of *Dinophysis* spp. is especially relevant. *Dinophysis acuminata* and *P. cordatum* peaks did occur at similar times during the 2017 – 2018, 2018 – 2019, and 2019 – 2020 sampling seasons. However, during the 2020 – 2021 and 2021 – 2022 sampling seasons, co-occurrence was less evident, with *P. cordatum* detection occurring at the same time or even later than *D. acuminata* (Figure 3). The use of *P. cordatum* as an indicator of *D. acuminata* may, therefore, be most relevant during the spring months (March - June) when the peaks of both species tend to overlap (Figure 3). Given the results of this study, further research into the relationship between *P. cordatum* and *D. acuminata* in Chesapeake Bay is warranted.

Prorocentrum cordatum, also considered a HAB, is a member of the class Dinophyceae that is globally distributed and commonly found in temperate and sub-tropical regions (Heil et al. 2005). High-biomass blooms of *P. cordatum* have been recorded in a variety of ecosystems, and their associated ecosystem effects include anoxic/hypoxic events, fish and shellfish mortality, and submerged aquatic vegetation (SAV) loss (Tango et al. 2005). Additionally, *P. cordatum* poses a threat to shellfish health, with immune system effects reported for juvenile oysters, *Crassostrea virginica*, after exposure to a *P. cordatum* in the laboratory and in the field (Hegaret & Wikfors, 2005a, b). In the Chesapeake Bay, *P. cordatum* is a recurrent bloom-forming species that has been shown to reach peak abundances in late spring and summer (Brownlee et al. 2005). Blooms of *P. cordatum* can exceed 3,000 cells mL^{-1} and are locally referred to as “mahogany tides” (Brownlee et al. 2005, Tango et al. 2005). *Prorocentrum cordatum* can tolerate a wide range of temperatures (12 – 28˚C) and salinities (4.5 – 12.8 ppt) (Johnson, 2014). *Prorocentrum cordatum* is also a mixotroph, and in a controlled lab experiment, a Chesapeake Bay isolate was

shown to ingest two different strains of the cryptophyte *Teleaulax amphioxeia*, like the ciliate *M. rubrum* (Johnson, 2014).

4.3 Future studies

The goal of the current study was to identify biotic and abiotic factors driving *D. acuminata* blooms in the York River, Chesapeake Bay, to further understand bloom dynamics in this system. While salinity, time of year, *M. rubrum* abundance, and *P. cordatum* abundance were all significant in the model, future models will need to be further refined to solidify the relationships between these biotic and abiotic variables and *D. acuminata* abundance. As the relationships between environmental variables and HABs in the field is complex, especially for this mixotrophic HAB, future models should consider other variables that were not included in the current study. For example, the potential relationship between *Dinophysis* abundance and thermal or haline stratification has been previously discussed (Reguera et al. 1993, Reguera et al. 1995, Escalera et al. 2006, Reguera et al. 2012, Díaz et al. 2016). In the current study, discharge from the Mattaponi and Pamunkey Rivers into the York River was used as a proxy for stratification. Future studies should include another proxy for stratification, or should directly quantify stratification in the York River, to further explore this relationship. Additionally, investigating local as well as large-scale physicochemical and climatological processes in the York River or Chesapeake Bay system using longer term data sets may also prove to be important (Fischer et al. 2020). In this study, model fitting was challenging due to occasional gaps in either biotic or abiotic data sets. The value of phi (ϕ) was high for this model (0.61, min: 0.44, max: 0.75), which was expected due to the autocorrelation between data points that is typical of high-resolution time series analysis.

It may also be important to distinguish between small and large cells of *Mesodinium* spp., as previous studies have documented the presence of small and large cell sizes in their respective systems (Harred & Campbell, 2014, Moita et al. 2016). Harred and Campbell (2014) reported *M. rubrum* cell sizes (cross-sectional area) ranging from 224 to 4415 μm^2 in Gulf of Mexico, Texas, and hypothesized that there may be other species of *Mesodinium* present in the system; the ranges in cell size could also be due to nutrient and prey availability (Montagnes et al. 2008). In northwest Portugal and Galicia, Spain, *Mesodinium* cell size was also variable, and the authors again hypothesized that the smaller cell form was most likely *M. rubrum*, while the large form may have been a new species, *M. major*, that is very similar in characteristics and appearance to *M. rubrum* (Moita et al. 2016). In a lab study, the biovolume and nutritional status of two *M. rubrum* strains were shown to have the greatest impact on *D. acuminata* growth, ingestion, and biovolume (Smith et al. 2018). As such, accounting for the variations in *M. rubrum* cell size or biovolume may have important implications for *Dinophysis* growth and toxicity; this concept should be explored in future modeling studies.

To further investigate the relationship between *D. acuminata* and the genus *Prorocentrum*, it may be advantageous to include all *Prorocentrum* spp. that were quantified by the CNN model. The other species of *Prorocentrum* that were included in the original CNN classifier (*Prorocentrum* (general), *P. micans*, *P. dentatum*, *P. triestinum*) were ultimately excluded from the prediction model due to low cell abundances that would not be relevant as a proxy for *D. acuminata*. Instead of just *P. cordatum*, future research should investigate adding all *Prorocentrum* spp. abundances together and including that as a predictor in the model.

CONCLUSION

This study is the first attempt to predict the relationship between *D. acuminata* and biotic and abiotic factors in the York River, Chesapeake Bay. The IFCB proved to be an invaluable tool for detecting cells of *Dinophysis*, that are known to be rare in phytoplankton assemblages. Additionally, several biotic and abiotic factors were identified as potential drivers of *D. acuminata* abundance. In addition, a 14-day lag of the prey item *M. rubrum* was also incorporated into the model, in agreement with previous modeling studies. Future research should incorporate longer-term data sets, or other environmental variables, to further elucidate the factors influencing *D. acuminata* abundance in the York River, Chesapeake Bay ecosystem. For regulatory agencies, the relationship between *P. cordatum* and *D. acuminata*, and using *P.cordatum* as a proxy for *D. acuminata* should also be investigated further.

Acknowledgements

Thank you to I-Shuo (Wade) Huang, Marta Sanderson, Joshua Garber, Todd Nelson, and Tanya Ward for their assistance with deploying, recovering, and maintaining the IFCB. Thank you to A. Challen Hyman for his help with ecological model development and R assistance. Additionally, thank you to Michael Brosnahan, Mrunmayee Pathare, Heidi Sosik, and Emily Peacock from Woods Hole Oceanographic Institute (WHOI) for their help with IFCB data analysis and classifier development. Thank you to Grace Molino for providing a map of the study area. Many thanks to Maya Casey for her help with classifier development and data analysis for the 2020 sampling season. This work was funded by the National Oceanic and Atmospheric Administration (NOAA) National Centers for Coastal Ocean Science Competitive Research, ECOHAB Program under award #NA19NOS4780182 to Juliette L. Smith, and the NOAA Monitoring and Event Response (MERHAB) Program under award # NA19NOS4780186 to Michael L. Brosnahan.

REFERENCES

Ajani, P., Brett, S., Krogh, M., Scanes, P., Webster, G., & Armand, L. (2013). The risk of harmful algal blooms (HABs) in the oyster-growing estuaries of New South Wales, Australia. *Environmental Monitoring and Assessment*, *185*(6), 5295–5316. https://doi.org/10.1007/s10661-012-2946-9

Ajani, P., Larsson, M. E., Rubio, A., Bush, S., Brett, S., & Farrell, H. (2016). Modelling bloom formation of the toxic dinoflagellates *Dinophysis acuminata* and *Dinophysis caudata* in a highly modified estuary, south eastern Australia. *Estuarine, Coastal and Shelf Science*, *183*, 95–106. https://doi.org/10.1016/j.ecss.2016.10.020

Alves-de-Souza, C., Iriarte, J. L., & Mardones, J. I. (2019). Interannual Variability of *Dinophysis acuminata* and *Protoceratium reticulatum* in a Chilean Fjord: Insights from the Realized Niche Analysis. *Toxins*, *11*(1), 19. https://doi.org/10.3390/toxins11010019

Anderson, D. R., & Burnham, K. P. (2002). Avoiding Pitfalls When Using Information-Theoretic Methods. *The Journal of Wildlife Management*, *66*(3), 912. https://doi.org/10.2307/3803155

Anderson, D. R. (2008). Model-Based Inference in the Life Sciences: A primer on evidence.

Anschütz, A.-A., Flynn, K. J., & Mitra, A. (2022). Acquired Phototrophy and Its Implications for Bloom Dynamics of the *Teleaulax-Mesodinium-Dinophysis*-Complex. *Frontiers in Marine Science*, *8*, 799358. https://doi.org/10.3389/fmars.2021.799358

Aune, T., Yndestad, M., 1993. Diarrhetic shellfish poisoning. In: Falconer, I.R. (Ed.), Algal Toxins in Seafood and Drinking Water. Academic Press, New York, pp. 87–104.

Basti, L., Suzuki, T., Uchida, H., Kamiyama, T., & Nagai, S. (2018). Thermal acclimation affects growth and lipophilic toxin production in a strain of cosmopolitan harmful alga *Dinophysis acuminata*. *Harmful Algae*, *73*, 119–128. https://doi.org/10.1016/j.hal.2018.02.004

Basti, L., Uchida, H., Matsushima, R., Watanabe, R., Suzuki, T., Yamatogi, T., & Nagai, S. (2015). Influence of Temperature on Growth and Production of Pectenotoxin-2 by a Monoclonal Culture of *Dinophysis caudata*. *Marine Drugs*, *13*(12), 7124–7137. https://doi.org/10.3390/md13127061

Blanco, J., Moroño, Á., & Fernández, M. L. (2005). Toxic Episodes In Shellfish, Produced By Lipophilic Phycotoxins: An Overview. *Revista Galega de Recursos Mariños (Monog.)*, *1*, 1–70.

Bouquet, A., Laabir, M., Rolland, J. L., Chomérat, N., Reynes, C., Sabatier, R., Felix, C., Berteau, T., Chiantella, C., & Abadie, E. (2022). Prediction of *Alexandrium* and *Dinophysis* algal blooms and shellfish contamination in French Mediterranean Lagoons using decision trees and linear regression: A result of 10 years of sanitary monitoring. *Harmful Algae*, *115*, 102234. https://doi.org/10.1016/j.hal.2022.102234

Brownlee, E. F., Sellner, S. G., & Sellner, K. G. (2005). *Prorocentrum minimum* blooms: Potential impacts on dissolved oxygen and Chesapeake Bay oyster settlement and growth. *Harmful Algae*, *4*(3), 593–602. https://doi.org/10.1016/j.hal.2004.08.009

Campbell, L., Olson, R. J., Sosik, H. M., Abraham, A., Henrichs, D. W., Hyatt, C. J., & Buskey, E. J. (2010). First Harmful *Dinophysis* (Dinophyceae, Dinophysiales) Bloom In The U.S. Is Revealed By Automated Imaging Flow Cytometry1: *Dinophysis* Dynamics From Imaging Flowcytobot. *Journal of Phycology*, *46*(1), 66–75. https://doi.org/10.1111/j.1529-8817.2009.00791.x

Chesapeake Bay National Estuarine Research Reserve in Virginia, Virginia Institute of Marine Science (CBNERR-VA VIMS), 2022. Virginia Estuarine and Coastal Observing System (VECOS). Data accessed from VECOS website: http://vecos.vims.edu; accessed 1 Nov 2022.

Díaz, P. A., Ruiz-Villarreal, M., Mouriño-Carballido, B., Fernández-Pena, C., Riobó, P., & Reguera, B. (2019). Fine scale physical-biological interactions during a shift from relaxation to upwelling with a focus on *Dinophysis acuminata* and its potential ciliate prey. *Progress in Oceanography*, *175*, 309–327. https://doi.org/10.1016/j.pocean.2019.04.009

Díaz, P. A., Ruiz-Villarreal, M., Pazos, Y., Moita, T., & Reguera, B. (2016). Climate variability and *Dinophysis acuta* blooms in an upwelling system. *Harmful Algae*, *53*, 145–159. https://doi.org/10.1016/j.hal.2015.11.007

Díaz, P., Reguera, B., Ruiz-Villarreal, M., Pazos, Y., Velo-Suárez, L., Berger, H., & Sourisseau, M. (2013). Climate Variability and Oceanographic Settings Associated with Interannual Variability in the Initiation of *Dinophysis acuminata* Blooms. *Marine Drugs*, *11*(8), 2964–2981. https://doi.org/10.3390/md11082964

Dominguez, H.J., Paz, B., Daranas, A.H., Norte, M., Franco, J.M., Fernández, J.J., 2010. Dinoflagellate polyether within the yessotoxin, pectenotoxin and okadaic acid toxin groups: Characterization, analysis and human health implications. Toxicon 56, 191–217. https://doi.org/10.1016/j.toxicon.2009.11.005.

Escalera, L., Pazos, Y., Dolores Doval, M., & Reguera, B. (2012). A comparison of integrated and discrete depth sampling for monitoring toxic species of *Dinophysis. Marine Pollution Bulletin*, *64*(1), 106–113. https://doi.org/10.1016/j.marpolbul.2011.10.015

Escalera, L., Reguera, B., Pazos, Y., Moroño, A., & Cabanas, J. (2006). Are different species of *Dinophysis* selected by climatological conditions? *African Journal of Marine Science*, *28*(2), 283–288. https://doi.org/10.2989/18142320609504163

Fiorendino, J. M., Smith, J. L., & Campbell, L. (2020). Growth response of *Dinophysis*, *Mesodinium*, and *Teleaulax* cultures to temperature, irradiance, and salinity. *Harmful Algae*, *98*, 101896. https://doi.org/10.1016/j.hal.2020.101896

Fischer, A. D., Hayashi, K., McGaraghan, A., & Kudela, R. M. (2020). Return of the "age of dinoflagellates" in Monterey Bay: Drivers of dinoflagellate dominance examined using automated imaging flow cytometry and long-term time series analysis. *Limnology and Oceanography*, *65*(9), 2125–2141. https://doi.org/10.1002/lno.11443

Friedrichs, C. T. (2009). York River Physical Oceanography and Sediment Transport. *Journal of Coastal Research*, *10057*, 17–22. https://doi.org/10.2112/1551-5036-57.sp1.17

Gaillard, S., Le Goïc, N., Malo, F., Boulais, M., Fabioux, C., Zaccagnini, L., Carpentier, L., Sibat, M., Réveillon, D., Séchet, V., Hess, P., & Hégaret, H. (2020). Cultures of *Dinophysis sacculus*, *D. acuminata* and pectenotoxin 2 affect gametes and fertilization success of the Pacific oyster, *Crassostrea gigas*. *Environmental Pollution*, *265*, 114840. https://doi.org/10.1016/j.envpol.2020.114840

Gaillard, S., Réveillon, D., Danthu, C., Hervé, F., Sibat, M., Carpentier, L., Hégaret, H., Séchet, V., & Hess, P. (2021). Effect of a short-term salinity stress on the growth, biovolume, toxins, osmolytes and metabolite profiles on three strains of the *Dinophysis acuminata*-complex (*Dinophysis* cf. *sacculus*). *Harmful Algae*, *107*, 102009. https://doi.org/10.1016/j.hal.2021.102009

Gaillard, S., Réveillon, D., Mason, P. L., Ayache, N., Sanderson, M., Smith, J. L., Giddings, S., McCarron, P., Séchet, V., Hégaret, H., Hess, P., & Vogelbein, W. K. (2023). Mortality and

histopathology in sheepshead minnow (Cyprinodon variegatus) larvae exposed to pectenotoxin-2 and Dinophysis acuminata. *Aquatic Toxicology*, *257*.
García-Portela, M., Reguera, B., Gago, J., Le Gac, M., & Rodríguez, F. (2020). Uptake of Inorganic and Organic Nitrogen Sources by *Dinophysis acuminata* and *D. acuta*. *Microorganisms*, *8*(2), 187. https://doi.org/10.3390/microorganisms8020187
Godhe, A., Svensson, S., & Rehnstam-Holm, A. (2002). Oceanographic settings explain fluctuations in *Dinophysis* spp. And concentrations of diarrhetic shellfish toxin in the plankton community within a mussel farm area on the Swedish west coast. *Marine Ecology Progress Series*, *240*, 71–83. https://doi.org/10.3354/meps240071
Haas, L. W. (1977). The effect of the spring-neap tidal cycle on the vertical salinity structure of the James, York and Rappahannock Rivers, Virginia, U.S.A. *Estuarine and Coastal Marine Science*, *5*(4), 485–496. https://doi.org/10.1016/0302-3524(77)90096-2
Hallegraeff, G. M., Anderson, D. M., Cembella, A. D., & Enevoldsen, H. O. (2004). Harmful algal blooms: A global overview. *Manual on harmful marine microalgae* (2nd rev. ed). UNESCO.
Harred, L. B., & Campbell, L. (2014). Predicting harmful algal blooms: A case study with *Dinophysis ovum* in the Gulf of Mexico. *Journal of Plankton Research*, *36*(6), 1434–1445. https://doi.org/10.1093/plankt/fbu070
Hattenrath-Lehmann, T., & Gobler, C. J. (2015). The contribution of inorganic and organic nutrients to the growth of a North American isolate of the mixotrophic dinoflagellate, *Dinophysis acuminata*: The effects of nutrients on a culture of *Dinophysis*. *Limnology and Oceanography*, *60*(5), 1588–1603. https://doi.org/10.1002/lno.10119
Hattenrath-Lehmann, T. K., Marcoval, M. A., Mittlesdorf, H., Goleski, J. A., Wang, Z., Haynes, B., Morton, S. L., & Gobler, C. J. (2015). Nitrogenous Nutrients Promote the Growth and Toxicity of *Dinophysis acuminata* during Estuarine Bloom Events. *PLOS ONE*, 22.
Hattenrath-Lehmann, T. K., Nanjappa, D., Zhang, H., Yu, L., Goleski, J. A., Lin, S., & Gobler, C. J. (2021). Transcriptomic and isotopic data reveal central role of ammonium in facilitating the growth of the mixotrophic dinoflagellate, *Dinophysis acuminata*. *Harmful Algae*, *104*, 102031. https://doi.org/10.1016/j.hal.2021.102031
Hégaret, H., & Wikfors, G. H. (2005a). Time-dependent changes in hemocytes of eastern oysters, Crassostrea virginica, and northern bay scallops, Argopecten irradians irradians, exposed to a cultured strain of Prorocentrum minimum. *Harmful Algae*, *4*(2), 187–199. https://doi.org/10.1016/j.hal.2003.12.004
Hégaret, H., & Wikfors, G. H. (2005b). Effects of natural and field-simulated blooms of the dinoflagellate Prorocentrum minimum upon hemocytes of eastern oysters, Crassostrea virginica, from two different populations. *Harmful Algae*, *4*(2), 201–209. https://doi.org/10.1016/j.hal.2003.12.005
Heil, C. A., Glibert, P. M., & Fan, C. (2005). *Prorocentrum minimum* (Pavillard) Schiller, A review of harmful algal bloom species of growing worldwide importance. *Harmful Algae*, *4*(3), 449–470. https://doi.org/10.1016/j.hal.2004.08.003
Hoshiai, G., Suzuki, T., Kamiyama, T., Yamasaki, M., & Ichimi, K. (2003). Water temperature and salinity during the occurrence of *Dinophysis fortii* and D. acuminata in Kesennuma Bay, northern Japan. *Fisheries Science*, *69*(6), 1303–1305. https://doi.org/10.1111/j.0919-9268.2003.00760.x
Jiang, H., Kulis, D. M., Brosnahan, M. L., & Anderson, D. M. (2018). Behavioral and mechanistic characteristics of the predator-prey interaction between the dinoflagellate

Dinophysis acuminata and the ciliate *Mesodinium rubrum*. *Harmful Algae*, *77*, 43–54. https://doi.org/10.1016/j.hal.2018.06.007

Johnson, M. D. (2015). Inducible Mixotrophy in the Dinoflagellate *Prorocentrum minimum*. *Journal of Eukaryotic Microbiology*, *62*(4), 431–443. https://doi.org/10.1111/jeu.12198

Johnson, M. D., Stoecker, D. K., & Marshall, H. G. (2013). Seasonal dynamics of *Mesodinium rubrum* in Chesapeake Bay. *Journal of Plankton Research*, *35*(4), 877–893. https://doi.org/10.1093/plankt/fbt028

Kamiyama, T., Nagai, S., Suzuki, T., & Miyamura, K. (2010). Effect of temperature on production of okadaic acid, dinophysistoxin-1, and pectenotoxin-2 by Dinophysis acuminata in culture experiments. *Aquatic Microbial Ecology*, *60*(2), 193–202. https://doi.org/10.3354/ame01419

Kenitz, K. M., Anderson, C. R., Carter, M. L., Eggleston, E., Seech, K., Shipe, R., Smith, J., Orenstein, E. C., Franks, P. J. S., Jaffe, J. S., & Barton, A. D. (2023). Environmental and ecological drivers of harmful algal blooms revealed by automated underwater microscopy. *Limnology and Oceanography*, lno.12297. https://doi.org/10.1002/lno.12297

Kim, S., Kang, Y., Kim, H., Yih, W., Coats, D., & Park, M. (2008). Growth and grazing responses of the mixotrophic dinoflagellate *Dinophysis acuminata* as functions of light intensity and prey concentration. *Aquatic Microbial Ecology*, *51*, 301–310. https://doi.org/10.3354/ame01203

Koukaras, K. (2004). *Dinophysis* blooms in Greek coastal waters (Thermaikos Gulf, NW Aegean Sea). *Journal of Plankton Research*, *26*(4), 445–457. https://doi.org/10.1093/plankt/fbh042

Lin, J., & Kuo, A. Y. (2001). Secondary Turbidity Maximum in a Partially Mixed Microtidal Estuary. *Estuaries*, *24*(5), 707. https://doi.org/10.2307/1352879

Maestrini, S. Y. (1998). Bloom dynamics and ecophysiology of *Dinophysis* spp. In:(D.M. Anderson, A.D. Cembella and G.M. Hallegraeff, eds.). *Physiological Ecology of Harmful Algal Blooms*, *G41*, 243–265.

Margalef, R. (1978). Life-forms of phytoplankton as survival alternatives in an unstable environment. *Oceanol.*, *1*, 493–509.

Marshall, H. G. (2009). Phytoplankton of the York River. *Journal of Coastal Research*, *10057*, 59–65. https://doi.org/10.2112/1551-5036-57.sp1.59

Miles, C.O., Wilkins, A.L., Munday, R., Dines, M.H., Hawkes, A.D., Briggs, L.R., Sandvik, M., Jensen, D.J., Cooney, J.M., Holland, P.T., Quilliam, M.A., MacKenzie, A.L., Beuzenberg, V., Towers, N.R., 2004a. Isolation of pectenotoxin-2 from *Dinophysis acuta* and its conversion to pectenotoxin-2 seco acid, and preliminary assessment of their acute toxicities. Toxicon 43, 1–9. https://doi.org/10.1016/j.toxicon.2003.10.003.

Moita, M. T., Pazos, Y., Rocha, C., Nolasco, R., & Oliveira, P. B. (2016). Toward predicting *Dinophysis* blooms off NW Iberia: A decade of events. *Harmful Algae*, *53*, 17–32. https://doi.org/10.1016/j.hal.2015.12.002

Montagnes, J., Allen, J., Brown, L., Bulit, C., Davidson, R., Díaz-Ávalos, C., Fielding, S., Heath, M., Holliday, N. P., Rasmussen, J., Sanders, R., Waniek, J., J., & Wilson, D. (2008). Factors Controlling the Abundance and Size Distribution of the Phototrophic Ciliate *Myrionecta rubra* in Open Waters of the North Atlantic. *Journal of Eukaryotic Microbiology*, *55*(5), 457–465.

Olson, R. J., & Sosik, H. M. (2007). A submersible imaging-in-flow instrument to analyze nano- and microplankton: Imaging FlowCytobot: In situ imaging of nano- and microplankton.

Limnology and Oceanography: Methods, *5*(6), 195–203. https://doi.org/10.4319/lom.2007.5.195

Park, M., Kim, S., Kim, H., Myung, G., Kang, Y., & Yih, W. (2006). First successful culture of the marine dinoflagellate *Dinophysis acuminata*. *Aquatic Microbial Ecology*, *45*, 101–106. https://doi.org/10.3354/ame045101

Pease, S. K. D., Brosnahan, M. L., Sanderson, M. P., & Smith, J. L. (2022). Effects of Two Toxin-Producing Harmful Algae, *Alexandrium catenella* and *Dinophysis acuminata* (Dinophyceae), on Activity and Mortality of Larval Shellfish. *Toxins*, *14*(5), 335. https://doi.org/10.3390/toxins14050335

Peperzak, L., Dijkema, R., Gieskes, W. W. C., Joordens, J., Peeters, J. C. H., Schol, C., Vrieling, E. G., & Zevenboom, W. (1996). Development Of A *Dinophysis Acuminata* Bloom In The River Rhine Plume (North Sea). *Intergovernmental Oceanographic Commission of UNESCO 1996*.

R Core Team (2023). R: A language and environment for statistical computing. R Foundation for Statistical Computing, Vienna, Austria. URL https://www.R-project.org/.

Reay, W. G. (2009). Water Quality within the York River Estuary. *Journal of Coastal Research*, *10057*, 23–39. https://doi.org/10.2112/1551-5036-57.sp1.23

Reay, W. G., & Moore, K. A. (2009). Introduction to the Chesapeake Bay National Estuarine Research Reserve in Virginia. *Journal of Coastal Research*, *10057*, 1–9. https://doi.org/10.2112/1551-5036-57.sp1.1

Reguera, B., Mariño, J., Campos, J., Bravo, I., Fraga, S., 1993. Trends in the occurrence of Dinophysis spp. in Galician waters. In: Smayda, T., Shimizu, Y. (Eds.), Toxic Phytoplankton Blooms in the Sea. Elsevier Science Publishers B.V., Amsterdam, Netherland,pp.559–564.

Reguera, B., Bravo, I., & Fraga, S. (1995). Autoecology and some life history stages of *Dinophysis acuta* Ehrenberg. *Journal of Plankton Research*, *17*(5), 999–1015. https://doi.org/10.1093/plankt/17.5.999

Reguera, B., Riobó, P., Rodríguez, F., Díaz, P., Pizarro, G., Paz, B., Franco, J., & Blanco, J. (2014). *Dinophysis* Toxins: Causative Organisms, Distribution and Fate in Shellfish. *Marine Drugs*, *12*(1), 394–461. https://doi.org/10.3390/md12010394

Reguera, B., Velo-Suárez, L., Raine, R., & Park, M. G. (2012). Harmful *Dinophysis* species: A review. *Harmful Algae*, *14*, 87–106. https://doi.org/10.1016/j.hal.2011.10.016

Riisgaard, K., & Hansen, P. (2009). Role of food uptake for photosynthesis, growth and survival of the mixotrophic dinoflagellate *Dinophysis acuminata*. *Marine Ecology Progress Series*, *381*, 51–62. https://doi.org/10.3354/meps07953

Rountos, K. J., Kim, J. J., Hattenrath-Lehmann, T. K., & Gobler, C. J. (2019). Effects of the harmful algae, Alexandrium catenella and Dinophysis acuminata, on the survival, growth, and swimming activity of early life stages of forage fish. *Marine Environmental Research*, *148*, 46–56. https://doi.org/10.1016/j.marenvres.2019.04.013

Sharples, J., Simpson, J. H., & Brubaker, J. M. (1994). Observations and Modelling of Periodic Stratification in the Upper York River Estuary, Virginia. *Estuarine, Coastal and Shelf Science*, *38*, 301–312.

Shultz, D., Campbell, L., & Kudela, R. M. (2019). Trends in *Dinophysis* abundance and diarrhetic shellfish toxin levels in California mussels (*Mytilus californianus*) from Monterey Bay, California. *Harmful Algae*, *88*, 101641. https://doi.org/10.1016/j.hal.2019.101641

Singh, A., Hårding, K., Reddy, H. R. V., & Godhe, A. (2014). An assessment of *Dinophysis* blooms in the coastal Arabian Sea. *Harmful Algae*, *34*, 29–35. https://doi.org/10.1016/j.hal.2014.02.006

Sjöqvist, C. O., & Lindholm, T. J. (2011). Natural Co-occurrence of *Dinophysis acuminata* (Dinoflagellata) and *Mesodinium rubrum* (Ciliophora) in Thin Layers in a Coastal Inlet: Layers of *D. acuminata* And *M. rubrum*. *Journal of Eukaryotic Microbiology*, *58*(4), 365–372. https://doi.org/10.1111/j.1550-7408.2011.00559.x

Smith, J. L., Tong, M., Fux, E., & Anderson, D. M. (2012). Toxin production, retention, and extracellular release by *Dinophysis acuminata* during extended stationary phase and culture decline. *Harmful Algae*, *19*, 125–132. https://doi.org/10.1016/j.hal.2012.06.008

Smith, J. L., Tong, M., Kulis, D., & Anderson, D. M. (2018). Effect of ciliate strain, size, and nutritional content on the growth and toxicity of mixotrophic *Dinophysis acuminata*. *Harmful Algae*, *78*, 95–105. https://doi.org/10.1016/j.hal.2018.08.001

Sosik, H. M., & Olson, R. J. (2007). Automated taxonomic classification of phytoplankton sampled with imaging-in-flow cytometry: Phytoplankton image classification. *Limnology and Oceanography: Methods*, *5*(6), 204–216. https://doi.org/10.4319/lom.2007.5.204

Szegedy, C., Vanhoucke, V., Ioffe, S., Shlens, J., & Wojna, Z. (2015). *Rethinking the Inception Architecture for Computer Vision* (arXiv:1512.00567). arXiv. http://arxiv.org/abs/1512.00567

Tango, P. J., Magnien, R., Butler, W., Luckett, C., Luckenbach, M., Lacouture, R., & Poukish, C. (2005). Impacts and potential effects due to *Prorocentrum minimum* blooms in Chesapeake Bay. *Harmful Algae*, *4*(3), 525–531. https://doi.org/10.1016/j.hal.2004.08.014

Tong, M., Smith, J., Kulis, D., & Anderson, D. (2015). Role of dissolved nitrate and phosphate in isolates of *Mesodinium rubrum* and toxin-producing *Dinophysis acuminata*. *Aquatic Microbial Ecology*, *75*(2), 169–185. https://doi.org/10.3354/ame01757

Trainer, V., Moore, L., Bill, B., Adams, N., Harrington, N., Borchert, J., da Silva, D., & Eberhart, B.-T. (2013). Diarrhetic Shellfish Toxins and Other Lipophilic Toxins of Human Health Concern in Washington State. *Marine Drugs*, *11*(6), 1815–1835. https://doi.org/10.3390/md11061815

U.S. Department of the Interior, U.S. Geological Survey. USGS Current Conditions for the Nation. https://waterdata.usgs.gov/nwis/uv?.

Wikfors, G. H. (2005). A review and new analysis of trophic interactions between *Prorocentrum minimum* and clams, scallops, and oysters. *Harmful Algae*, *4*(3), 585–592. https://doi.org/10.1016/j.hal.2004.08.008

Yasumoto, T., Murata, M., Oshima, Y., Sano, M., Matsumoto, G.K., Clardy, J., 1985. Diarrhetic shellfish toxins. Tetrahedron 41, 1019–1025. https://doi.org/10.1016/S0040-4020(01)96469-5.

Yih, W., Kim, H. S., Myung, G., Park, J. W., Yoo, Y. D., & Jeong, H. J. (2013). The red-tide ciliate *Mesodinium rubrum* in Korean coastal waters. *Harmful Algae*, *30*, S53–S61. https://doi.org/10.1016/j.hal.2013.10.006

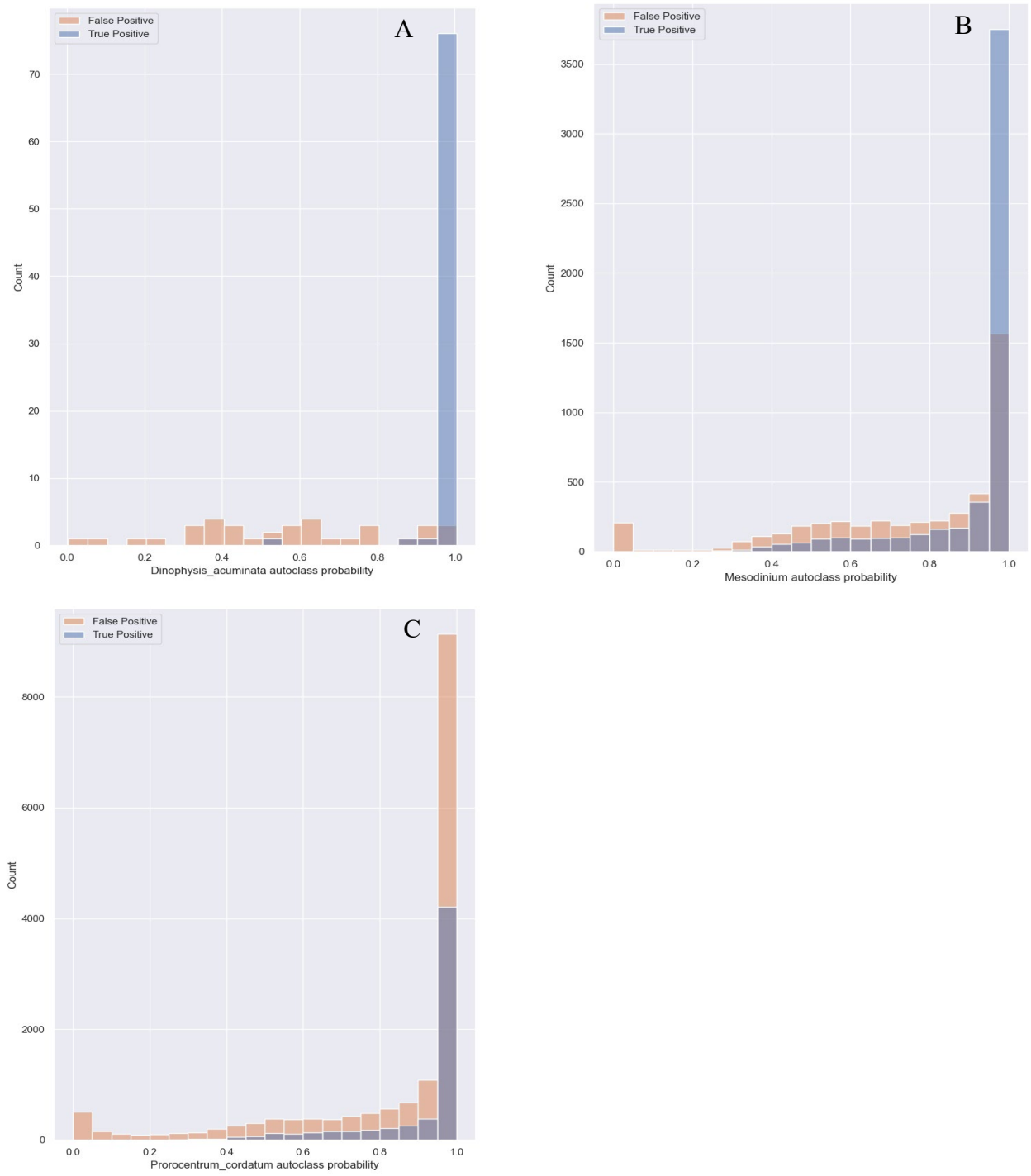

Figure S1 Precision/accuracy histograms for *D. acuminata* (A), *M. rubrum* (B), and *P. cordatum* (C) classes as a result of CNN automatic classification.

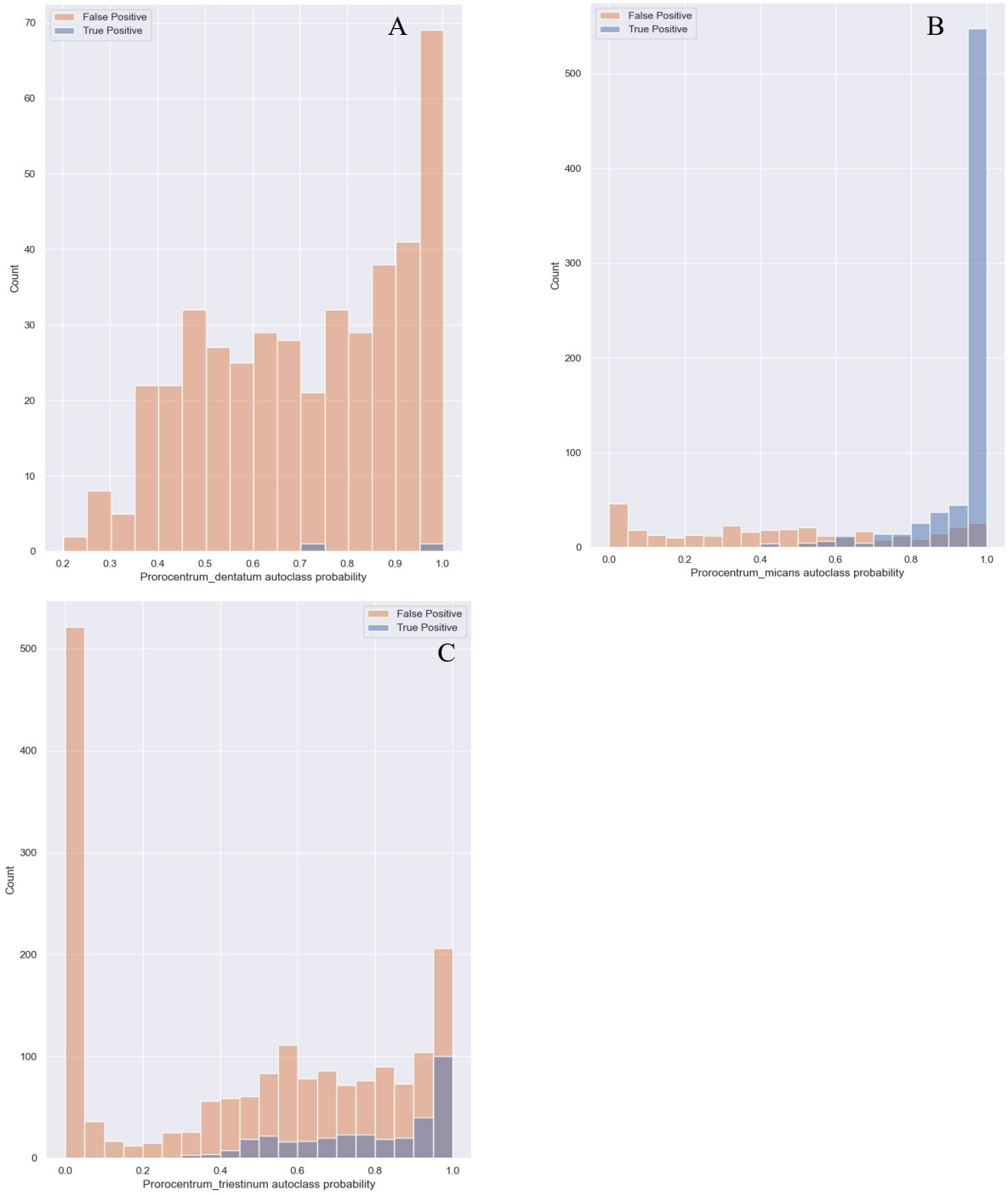

Figure S2 Precision/accuracy histograms for *P. dentatum* (A), *P. micans* (B), and *P. triestinum* (C) classes as a result of CNN automatic classification.

CHAPTER 2:

ROLE OF TURBULENCE IN *DINOPHYSIS* SPP. FEEDING, GROWTH, AND TOXIN PRODUCTION

ABSTRACT

Dinophysis, a mixotrophic dinoflagellate that is known to prey on the ciliate *Mesodinium rubrum*, is responsible for diarrhetic shellfish poisoning (DSP) in humans and has been identified on all U.S. coasts. Monocultures of *Dinophysis* have been used to investigate the growth of *Dinophysis* species in response to variations in environmental conditions, however, little is known about the roles of system stability (turbulence) and mixotrophy in the growth and toxin production of *Dinophysis* species. We performed 6-d culturing experiments with three species, four isolates, of *Dinophysis*, that included co-incubation (*Dinophysis* + *Mesodinium*) and prey-only (*Mesodinium)* flasks to explore the impact of high and low levels of turbulence on *Dinophysis* growth, feeding, and production of two toxin groups: okadaic acid and derivatives (diarrhetic shellfish toxins, DSTs) and pectenotoxins (PTXs). High turbulence slowed growth in both *D. acuminata* and *D. ovum* isolates (DAVA 01 = 0.04 ± 0.19, DANY1 = -0.02 ± 0.12, and DOSS 2206 = 0.02 ± 0.13) and increased the intracellular DST and PTX toxin content in *D. acuminata* isolates, but decreased toxin production. Turbulence also appeared to promote leaking of toxins extracellularly, as *Dinophysis ovum* also had significantly more extracellular DSTs found in the medium under high turbulence when compared to the control. The opposite pattern was observed for the *D. caudata* strain (DCSS 3191), where high turbulence stimulated growth (0.31 ± 0.07), but reduced intracellular toxin content (PTXs) and had no influence on its toxin production rate. Turbulence did not have a measurable effect on the ingestion rates of *Dinophysis* on *Mesodinium* prey for any of the four isolates. Overall, species-specific responses to turbulence were observed, with indications that *D. ovum* and *D. caudata* might be the most sensitive to turbulence.

INTRODUCTION

The dinoflagellate genus *Dinophysis* has more than 100 described species, but only 12 have been shown to produce toxins (Reguera et al. 2011). *Dinophysis* is rare in phytoplankton assemblages, commonly occurring at concentrations less than 1 cell mL^{-1}, with blooms in the U.S. that range from 10 – 25 cells mL^{-1} (Trainer et al. 2013), while the highest cell density recorded in the U.S. was 2,120 cells mL^{-1} (Hattenrath-Lehmann et al. 2013). Even at relatively low cell concentrations, these mixotrophic dinoflagellates still produce two groups of lipophilic toxins called diarrhetic shellfish toxins (DSTs) and pectenotoxins (PTXs) that can accumulate in filter-feeding organisms (Trainer et al. 2013, Deeds et al. 2020). Okadaic acid (OA), dinophysistoxins (DTXs), and their derivatives are acidic polyethers that inhibit protein phosphatases (Cohen et al. 1990). Together, these toxins are the causative agents of global diarrhetic shellfish poisoning (DSP) in humans (Yasumoto et al. 1985, Dominguez et al. 2010). After consumption of contaminated shellfish, symptoms of DSP typically appear in 3 to 12 hours and are characterized by diarrhea, nausea, and vomiting; the recovery time is around 3 days (Hallegraeff, 2003, Blanco et al. 2005). Pectenotoxins (PTXs) are polyether-lactones that are also produced by some *Dinophysis* species and have been shown to be hepatoxic to mice via intraperitoneal injection (Miles et al. 2004), but no diarrheagenic effects via oral administration in mice have been observed (Terao et al. 1986, Reguera et al. 2012). Due to lack of proven human health effects, PTXs are not regulated in the U.S. or more recently, in the European Union (European Commission, 2021). PTXs may, however, pose a threat to shellfish health and aquaculture sustainability. Recent studies have shown that PTXs can exhibit toxicity on the early life stages of bivalves and fish (Rountos et al. 2019, Gaillard et al. 2020, Pease et al. 2022, Gaillard et al. 2023).

Dinophysis is globally distributed, with reported DSP events in Japan, Europe, Asia, Chile, Canada, New Zealand, and U.S. coasts (Campbell et al. 2010, Reguera et al. 2012, Trainer et al. 2013). In 2005, Park et al. (2006) were able to successfully establish the first *Dinophysis* monoculture (*D. acuminata*) through a three-step feeding regime. The cryptophyte *Teleaulax* sp. is fed to the mixotrophic ciliate *Mesodinium rubrum*, which is then fed to the kleptoplastidic mixotrophic dinoflagellate, *Dinophysis*. To acquire *M. rubrum* prey, *Dinophysis* displays a complex feeding behavior, in which a *Dinophysis* cell attaches itself to a *M. rubrum* cell through a peduncle or capture filament, and then transfers the cell contents, retaining the cryptophyte plastids (Park et al. 2006, Hansen et al. 2013, Jiang et al. 2018,). Since the pivotal work of Park et al. (2006), monocultures of *Dinophysis* isolated from around the world have been used to investigate the growth of these species in response to a variety of environmental conditions, such as nutrients, temperature, light, and salinity (Tong et al. 2011, Smith et al. 2012, Nielson et al. 2012, Tong et al. 2015, Hattenrath-Lehmann & Gobler, 2015, Fiorendino et al. 2020, Gaillard et al. 2021). In addition to growth, other laboratory studies have characterized toxin profiles and toxin production rates in relation to species, strain, or a variety of environmental conditions (Tong et al. 2011, Fux et al. 2011, Nielson et al. 2012, Smith et al. 2012, Tong et al. 2015, Smith et al. 2018, Ayache et al. 2023).

These studies lay the foundation for understanding *Dinophysis* physiology, but there is still a lack of knowledge regarding the role of turbulence in the growth, feeding, and production of toxins by *Dinophysis*. Turbulence is ubiquitous in aquatic systems and can thus potentially influence phytoplankton population dynamics (Guadayol et al. 2009). Margalef (1978) suggested a conceptual model or "Mandala" to explain the succession of phytoplankton species according to two factors: nutrients and turbulence. According to the theory, turbulent conditions with high

nutrient concentrations favor diatoms and coccolithophorids, while low turbulence, and nutrient-poor waters favor dinoflagellates. Building on Margalef's Mandala, Glibert (2016) proposed an updated mandala that incorporates twelve variables/traits that influence phytoplankton including preference for chemically reduced or oxidized nitrogen, adaptation to light and tendency to be autotrophic vs. mixotrophic, environmental turbulence, production of toxins or reactive oxygen species (ROS), growth rate, etc. The author asserts that it is important to include a distinction between nitrogen forms, as well as N:P ratios, due to increasing anthropogenic nutrient loading, and species preference for reduced or oxidized nutrient forms (Glibert, 2016). Additionally, this mandala accounts for mixotrophy, an important trait that is more widespread among phytoplankton than originally thought. These variables included in the new mandala are especially relevant to the genus *Dinophysis*, since it is now known that *Dinophysis* species are obligate mixotrophs that preferentially utilize reduced forms of nitrogen (ammonium and urea) over nitrate (Hattenrath-Lehmann & Gobler, 2015, Hattenrath-Lehmann et al. 2015, García-Portela et al. 2020, Hattenrath-Lehmann et al. 2021).

Phytoplankton cells are subject to both large-scale and small-scale turbulence either directly or indirectly, and changes in water column position due to turbulent mixing can result in different nutrient concentrations, light intensities, and prey availability (Mann & Lazier, 1991, Peters & Marrasé, 2000, García-Portela et al. 2019). Due to their size, phytoplankton interact more directly with small-scale turbulence (Kolmogorov scales) (Estrada & Berdalet, 1998). The kinetic energy generated by wind and waves is transferred to smaller eddies until viscous forces – "related to internal resistance of the fluid molecules" as explained by Estrada & Berdalet (1998), convert it to heat (Sullivan et al. 2003). Thus, phytoplankton in the water column perceive turbulence as laminar shear (Thomas et al. 1995, Estrada & Berdalet 1998). Given that

dinoflagellates, especially harmful algal bloom-forming species, are associated with a calm, stratified water column (Berdalet et al. 2007), several researchers have conducted laboratory and field studies to determine the response of dinoflagellates to small-scale turbulence. Many have found species-specific responses that may include changes in morphology (Zirbel et al. 2000), swimming behavior (Estrada et al. 1987, Chen et al. 1998, Karp-Boss et al. 2000), growth rates (Pollingher & Zemel, 1981, Havskum et al. 2005, Stoecker et al. 2006), and changes in intracellular toxin content (Juhl et al. 2001, Bolli et al. 2007). Recently, García-Portela et al. (2019) investigated the effect of small-scale turbulence on two species of *Dinophysis*: *D. acuminata* and *D. acuta* (isolated from Spain). The study demonstrated a species-specific growth response to turbulence, i.e., *D. acuta* was more sensitive to small-scale turbulence than *D. acuminata*. While both species had significantly lower growth rates in high turbulence treatments compared to controls, *D. acuminata* grew (i.e., positive growth rate) under high turbulence, while *D. acuta* did not grow (i.e., negative growth rate) when exposed to high turbulence, and did not resume growth during the 2-day recovery period. These different responses to turbulence likely explain their seasonal distribution *in situ*.

The current study continues along this important line of work, investigating the effects of small-scale turbulence on growth, feeding, and toxin production in three species (four isolates) of *Dinophysis* (*D. acuminata*, *D. ovum*, *D. caudata*). Isolates from the mid-Atlantic and Gulf of Mexico coasts were exposed to two levels of turbulence (high and low) and compared to a still control group with no turbulence. Over the 6-day experiment, samples were collected to measure cell concentration, growth rates, ingestion rates, toxin content, and production rates. Due to the complex feeding behavior of *Dinophysis*, it was hypothesized that exposure to low turbulence would increase predator-prey encounter rates, thus increasing *Dinophysis* ingestion, growth, and

toxin production rates, whereas exposure to high turbulence would disrupt *Dinophysis* feeding and negatively impact growth. Additionally, it was anticipated that exposure to high turbulence would stress or lyse cells, and lead to a higher release of extracellular toxins. Overall, this experiment will provide information about the response of *Dinophysis* to turbulent environmental conditions, which may affect bloom development and exposure of aquatic organisms to the associated toxins.

MATERIALS AND METHODS

This work included both a preliminary range-finding experiment and a 6-day turbulence experiment. In the preliminary range-finding experiment, an isolate of *Dinophysis acuminata* and an isolate of *Mesodinium rubrum* were each exposed to five levels of turbulence to determine levels at which both species survive. Following the range-finding experiment, a longer 6-day experiment with two levels of turbulence and a still control (no turbulence) was conducted with co-incubation flasks that included *Dinophysis* and *Mesodinium*, and prey-only flasks with just *Mesodinium*. The 6-day experiment was repeated using four isolates of *Dinophysis*. See below for more details.

2.1 Culture Maintenance

Four isolates of *Dinophysis* were used in the experiments: *D. acuminata* (DAVA 01) was isolated from Nassawadox, Chesapeake Bay, VA in 2017, *D. acuminata* (DANY1) was isolated from Meetinghouse Creek, Peconic Estuary, Long Island Sound, NY in 2013, *D. ovum* (DOSS 2206) and *D. caudata* (DCSS 3191), both were isolated from Surfside Beach, Gulf of Mexico, TX in 2020, and 2019, respectively. The two prey species used were *Mesodinium rubrum* (JAMR) and the cryptophyte *Teleaulax amphioxeia* (JATA), both isolated from Japan in 2007 (Nishitani et al. 2008). The cryptophyte, *T. amphioxeia*, was grown in f/2-Si media prepared with 0.22-µm filtered seawater from Wachapreague, VA and diluted to a salinity of 25. The ciliate, *M. rubrum*, was grown in f/6 media at salinity 25 and was given the cryptophyte as prey. For two of the experiments involving *D. ovum* and *D. caudata*, the *M. rubrum* cultures were acclimated to the appropriate temperature for a least two weeks before the experiment. *Dinophysis* cultures were also grown under temperature conditions representative of their geographical origin in preparation for the experiments. Both *D. acuminata* isolates, DAVA 01 and DANY1, were

grown at 15˚C, and *D. ovum* (DOSS 2206) and *D. caudata* (DCSS 3191) were growth at 20˚C. All cultures were maintained at the same light intensity (100 $\mu Em^{-2}s^{-1}$).

2.2 Experimental Design

2.2.1 Preliminary Range-Finding Experiment

The preliminary range-finding experiment was carried out individually on *D. acuminata* (DAVA 01) or *M. rubrum*. These cultures had been maintained under standard conditions: temperature, 15˚C, light, 100 $\mu Em^{-2}s^{-1}$ with a 14:10 light: dark cycle, and salinity 25. Triplicate cultures inoculated at 250 cells mL^{-1} for *Dinophysis* or 1,250 cells mL^{-1} for *Mesodinium* were subjected to five levels of turbulence: 0 rpm, 60 rpm, 80 rpm, 100 rpm, and 120 rpm. This range of settings was adopted from Zirbel et al. (2000).

Prior to this preliminary experiment, cultures of *D. acuminata* and *M. rubrum* were fed *M. rubrum* or *T. amphioxeia*, respectively, to prevent food depletion-induced stress. At the beginning of the experiment, however, *Dinophysis* culture was sieved through a 10-µm mesh to remove any remaining *Mesodinium* cells, and the cells were transferred to 125-mL Erlenmeyer flasks containing clean filtered seawater (0.22 µm). *Dinophysis* and *Mesodinium* monocultures were not fed during the experimental period. To determine *Dinophysis* and *Mesodinium* cell densities and calculate growth rates, a 1-mL culture sample was taken at day 1 (t_0), fixed with Lugol's solution (500 mL Carolina Biological Supply Co, Burlington, NC), and counted using a Sedgwick rafter cell chamber (S50 Counting cell, Electron Microscropy Sciences, Hatfield, PA), and a light microscope at 100x magnification (Olympus CX31 Olympus Corporation, Tokyo, Japan). The cultures were then placed on an orbital shaker for 48 hours in a temperature-controlled incubator with the desired turbulence setting. After 48 hours, another 1-mL subsample

(t_{48}) was taken from each treatment flask and counted. This same experiment was repeated for the *M. rubrum* culture.

2.2.2 Six-day Turbulence Experiments

Dinophysis acuminata (DAVA 01) growth rates did not differ between treatments in the range-finding experiment (ANOVA, $p > 0.05$), thus 60 and 120 rpm of turbulence in addition to a still control (no turbulence) were selected for this experiment. The experimental design included triplicate flasks containing both *Dinophysis* and *Mesodinium* cells (co-incubation flasks). To calculate the ingestion rates, triplicate control flasks containing only *Mesodinium* (prey-only flasks) were also used to compare *Mesodinium* growth in the absence or presence of *Dinophysis*.

Co-incubation flasks: *Dinophysis* cultures were inoculated at ~250 cells mL^{-1} in 60-mL of filtered seawater in 125-mL Erlenmeyer flasks, and *Mesodinium* was added at a predator: prey ratio of 1:5 (at ~1,250 cells mL^{-1}). All cultures were then placed on orbital shakers at 0, 60, and 120 rpm, and cells were grown in triplicate semi-continuous cultures for 6 consecutive days. The flasks exposed to 0rpm served as a still control for *Dinophysis* and *Mesodinium*, demonstrating feeding, growth, and toxin production in the absence of turbulence. On Days 0, 2, 4, and 6, a subsample from each flask was collected and preserved with Lugol's solution for cell enumeration using light microscopy; these cell counts were used to calculate growth rates. For toxin analysis, a 10-mL sample was collected from each flask every other day (i.e., on Days 2 and 4), and replaced with fresh *Mesodinium* culture to maintain a predator: prey ratio of 1: 5 and a total volume of 60-mL in the flask. In two instances, *D. acuminata* (DANY1) co-incubation flasks were recorded at a ratio of 1:3 or 1:4.

Prey-only flasks: On Day 2 of the experiment, triplicate flasks with just *Mesodinium* were inoculated in 60-mL of f/6 medium in 125-mL Erlenmeyer flasks at the same concentration of *Mesodinium* as in the co-incubation flasks (~1,250 cells mL^{-1}). After inoculation, the flasks were placed on the orbital shakers at 0, 60, and 120 rpm in the incubator and undisturbed for 48 hours. On Day 4, *Mesodinium* was enumerated using microscopy, and the prey-only flasks were terminated.

2.3 Turbulence calculations

Turbulence in these experiments was generated using two orbital shakers (VWR S-500 Orbital Shaker, Henry Troemner LLC, USA, VWR Standard Orbital Shaker, Model 3500, Troemner LLC, USA), with an oscillation diameter of 19 mm (0.75 in). To compare turbulence levels reported in this study with the those found in the literature, kinetic energy dissipation rates (ε), were included. Dissipation rates were calculated using the equation from Peters & Marrasé (2000) described by Arnott et al. (2021), and the following factors were applicable to an orbital shaker turbulence simulation:

$$\varepsilon = \frac{S(d \cdot f)^3}{V}$$

where S is the surface in contact with fluid (as derived from flask geometry, m^2), d is the distance the vessel travels in one oscillation (m), f is the frequency of oscillation (Hz), and V is the volume of fluid (m^3). To derive the surface in contact with fluid (S) in the above equation, the formula for the total surface area (TSA) of a frustrum of a cone was used, as this shape is representative of the culture vessel that was used during the experiments: 125-mL Erlenmeyer flasks filled with 60-mL of culture. The TSA of a frustrum equation is:

$$\text{TSA of frustrum} = \pi L(R + r) + \pi(R^2 + r^2)$$

where L is the height of the liquid in the flask, R is the radius of the bottom of the flask, and r is the radius of the top of the liquid in the flask. Ultimately, kinetic energy dissipation rates were calculated for four levels of turbulence used in the preliminary range-finding experiment: 60rpm, 80rpm, 100rpm, 120rpm. Their respective ε values were: 1.27×10^{-3} $m^2 s^{-3}$, 3.01×10^{-3} $m^2 s^{-3}$, 5.88×10^{-3} $m^2 s^{-3}$, 1.02×10^{-2} $m^2 s^{-3}$. Dissipation rates were an order of magnitude different between the selected turbulence levels of 60 and 120 rpm.

2.4 Growth rate and ingestion rate calculations

Growth rates were calculated for each species at each treatment level, using the formula by Guillard (1973):

$$\mu = \frac{\ln(\frac{C_2}{C_1})}{t_2 - t_1}$$

where C_1 and C_2 are the concentrations of cells at time (day) 1 and 2 (cells mL^{-1}) and μ is the growth rate (day^{-1}). Growth rates were calculated over a range of time intervals: Days 0-2 and 2-6. For Days 0-2, cell counts from Days 0-2 were used in the above equation. For Days 2-6, growth rates were calculated from Days 2-4 and 4-6 of the experiment, to capture the exponential growth of the cultures then, the average of these growth rates were used to calculate the growth rate from Days 2-6 of the experiment.

Subsamples were taken from each co-incubation flask after the addition of fresh *Mesodinium* prey. Cell counts for *Dinophysis* before the addition of prey were calculated for Days 2 and 4 by multiplying post-dilution counts with a dilution factor. These counts are referred to as “pre-dilution counts”.

The ingestion rates of *Dinophysis* were calculated based on cell counts (cells mL^{-1}) of *Dinophysis* and *Mesodinium* in the co-incubation and prey-only flasks. Ingestion rate equations

were adopted from Frost (1972). *Mesodinium* growth rates were calculated for each of the three runs of the prey-only flasks. These growth rates were then averaged together and used in the ingestion rate calculations for the four *Dinophysis* strains. The growth rate constant for *Mesodinium* growth, k, in the prey-only flasks is:

$$C_2 = C_1 e^{k(t_2-t_1)}$$

where C_1 and C_2 are cell concentrations (cells mL^{-1}) of *Mesodinium* in the prey-only flasks at t_1 and t_2. For the co-incubation flasks, the grazing coefficient, g (i.e., growth rate of *Mesodinium* when *Dinophysis* is present), is:

$$C_2^* = C_1^* e^{(k-g)(t_2-t_1)}$$

where C_2^* and C_1^* are cell concentrations of *Mesodinium* in the flasks with *Dinophysis* at time t_1 and t_2. The average cell concentration, [C], of *Mesodinium* in each co-incubation flask during time interval $t_2 - t_1$ is:

$$[C] = \frac{C_1^*[e^{(k-g)(t_2-t_1)}-1]}{(t_2-t_1)(k-g)}$$

The grazing rate, F, of *Dinophysis* is then calculated using the equation:

$$F = Vg/N \text{ (mL } \textit{Dinophysis} \text{ } hr^{-1})$$

where V is the volume (mL) of culture in the flask, g is defined as above, and N is the total number of *Dinophysis* cells in the flask. Finally, the ingestion rate, I, of *Dinophysis* can then be calculated using the equation:

$$I = [C] \times F \text{ (cells eaten } \textit{Dinophysis}^{-1} \text{ } day^{-1})$$

2.5 Toxin extraction and analysis

Toxins samples were collected from each treatment flask at two time points during the experiments: Days 2 and 4. The methods described below were adopted from Ayache et al. (2023). The cultures were gently homogenized, and 10-mL subsample was collected and

centrifuged (3200 x g, 12 min, 4˚C) to separate the cell pellet from the supernatant. The cell pellet was resuspended in 1-mL of 100% methanol, and the supernatant was transferred to a separate centrifuge tube. Both fractions were stored in a freezer at -20˚C until extraction.

Intracellular toxins The cell pellet was bath-sonicated for 15 minutes, and then centrifuged (3200 x g, 15 min, 4˚C). The methanol supernatant was filtered using a PVDF syringe filter (0.2-µm, 13-mm) into glass 1.5-mL maximum recovery LC vials and stored at -20˚C until analysis.

Extracellular toxins Extracellular (dissolved) toxins were extracted using a 60-mg Oasis HLB solid-phase extraction (SPE) cartridge (Waters, Milford, MA, USA) that was first equilibrated with 3 mL of 100% methanol, followed by 3 mL of water. The sample was then loaded onto the column, rinsed with 3 mL of water, and then dried. Toxins were then eluted with 1 mL of 100% methanol and filtered (PVDF syringe filter, 0.2 µm, 13 mm) into glass 1.5-mL maximum recovery LC vials and finally stored at -20˚C until analysis.

Base Hydrolysis In order to convert esterified toxin derivatives in the samples into the parent compounds (OA, DTXs), the intra- and extracellular samples underwent base hydrolysis (Suzuki et al. 2004). Therefore, 32 µl of 2.5M sodium hydroxide (NaOH) solution was added to 250 µl of culture sample. The samples were then heated for 40 minutes at 76˚C, cooled, and neutralized with the addition of 32 µl of 2.5M acetic acid (AcOH). Following syringe filtration (PVDF syringe filter, 0.2-µm, 13-mm), samples were stored at -20˚C until analysis. Samples were only base hydrolyzed for the experiments including *D. acuminata* (DAVA 01 and DANY1), since the *D. ovum* and *D. caudata* isolates were confirmed not to produce esterified forms, or OA or DTX analogs, respectively (Ayache et al. 2023).

Toxin quantification was performed using tandem quadrupole Xevo TQD Utra-performance liquid chromatography (Waters, Milford, MA, USA) coupled to an electrospray

ionization (ESI) source with a trapping dimension and at-column dilution (LC-MS/MS trap/ACD) (Onofrio et al. 2020); chromatography and mass spectrometry conditions, and analyte transitions followed Ayache et al. (2023). Certified reference materials for OA, DTX-1, DTX-2, and PTX-2 (NRC-CNRC, Halifax, Nova Scotia, Canada) were used for verification of retention times and quantification by comparison to standard curves; hydroxy-PTX2 was quantified based on the PTX-2 standard. The limit of detection (LOD) and limit of quantification (LOQ) for OA, DTX-1, DTX-2, and PTX-2 are described in Ayache et al. (2023). Any samples where toxin was not detected (i.e., at or below LOD) were reported as zero.

Intracellular toxin is expressed on a per cell basis (content), while extracellular toxin is expressed on a per mL of culture basis (concentration). To calculate total toxin (intra + extracellular), intracellular toxin was converted from toxin content (per cell) to toxin concentration (per mL of culture) and added to extracellular to allow for the determine of percent of toxin extracellular (extracellular toxin / total toxin * 100).

2.5.1 Toxin production rate equations

Net toxin production rate (R_{tox}, pg toxin cell^{-1} day^{-1}) considers growth rate and intracellular toxin data and was calculated for specific time intervals (Days 2 and 4 of the experiment) using the equation (Anderson et al. 1990):

$$R_{tox} = \frac{(T_1 - T_0)}{(\bar{N})(\Delta)}$$

where $\bar{N}$ is the ln average of the cell concentration for *Dinophysis*,

$$\bar{N} = \frac{N_1 - N_o}{\ln N_1 - \ln N_0}$$

2.6 Statistical analysis

The experiments were carried out in triplicate, and results were presented as mean values ± standard deviation (SD) in all text, figures, tables, and statistical analyses apart from the following exceptions due to loss of sample or non-detect: DCSS 3191, Day 2, 120 rpm – growth, ingestion rate, toxin production rate; DAVA 01, Days 0 and 2, 60 rpm – growth; DAVA 01, Day 4, 120 rpm – extracellular DST; DANY1, Day 4, 120rpm intracellular DST and all treatments, extracellular DST. Growth rate, ingestion rate, and multiple toxin metrics: toxin content and concentration, % extracellular toxin, and toxin production rate, were verified for normality and homogeneity of variance using the Shapiro and Bartlett tests, respectively, in preparation for statistical analysis. If the data met these assumptions, a one-way analysis of variance (ANOVA) with a pair-wise Tukey HSD multiple comparison test was performed. Residuals of each model were examined for autocorrelation, normality, and homogenous variance, as determined by the Durbin Watson, Shapiro, and Bartlett tests, respectively. When the raw data or model residuals did not meet these assumptions, data were either transformed to achieve normality, or a Kruskal-Wallis rank sum test for non-parametric data was used, followed by a pairwise comparison using Conover's all-pairs post hoc test. In two instances, ANOVA was performed on data that did not meet these assumptions (*D. ovum* – extracellular percent toxin and extracellular toxin concentration). Two toxin analogues, OA and DTX-1, were combined into one category (DSTs) for analysis of toxin content and toxin production rate data in *D. acuminata* (DAVA 01 and DANY1) and *D. ovum*. PTX-2 and hydroxyPTX-2 were also combined into one category (PTXs). The level of significance (α) was set to 0.05, and all statistical tests were performed in R studio, version 4.1.0.

RESULTS

3.1 *Dinophysis* growth rates in response to turbulence

During Days 0-2 post-inoculation, growth was variable, with no difference detected between the three treatments: control (no turbulence), low, and high turbulence. The exception was *D. acuminata*, isolate DANY1, which showed a significant decrease in growth rate at high turbulence after only 2 days of high turbulence (Table 1).

Growth response was calculated over Days 2 – 6 for each treatment and isolate (Table 1, Figure 1). The *D. acuminata,* isolate, DAVA 01, grown in the high turbulence treatment had a significantly lower growth rate (0.04 ± 0.19 d^{-1}) than both the control (0.29 ± 0.09 d^{-1}) and low turbulence treatment (0.30 ± 0.11 d^{-1}) ($p < 0.05$) (Table 1). Similarly, the growth rate of the second *D. acuminata* isolate, DANY1, grown in high turbulence treatment (-0.02 ± 0.12 d^{-1}) was significantly lower than the control (0.32 ± 0.10 d^{-1}) and low turbulence treatment (0.39 ± 0.04 d^{-1}) ($p < 0.05$) (Table 1). In addition. for *D. ovum* strain, DOSS 2206, the growth rate in the high turbulence treatment (0.02 ± 0.13 d^{-1}) was significantly lower than the control (0.19 ± 0.07 d^{-1}) and the low turbulence treatment (0.16 ± 0.08 d^{-1}) ($p < 0.05$) (Table 1). *Dinophysis caudata* isolate, DCSS 3191, showed however, a different response at both high and low turbulence, with significantly higher growth rates in the low and high turbulence treatments (0.34 ± 0.05 d^{-1} and 0.31 ± 0.07 d^{-1}, respectively) compared to the control (0.19 ± 0.05 d^{-1}) ($p < 0.05$) (Table 1).

Table 1 Average growth rates (d^{-1}) of the four *Dinophysis* species, across the three turbulence treatments. Growth rates are presented as averages over Days 0-2, the post-inoculation period, as well as an average over Days 2-6 (Day 2-4 and Day 4-6 cell counts used to calculate growth rates). Data are presented as mean ± SD, n = 3. Superscript letters that are different indicate significance between treatments, tested within an isolate.

Species	Treatment	Day 0-2	Overall Day 2-6
D. acuminata (DAVA 01)	Control	0.38 (0.27)[a]	0.29 (0.09)[a]
	Low	0.43 (0.20)[a]	0.30 (0.11)[a]
	High	0.34 (0.19)[a]	0.04 (0.19)[b]
D. acuminata (DANY1)	Control	0.29 (0.04)[a]	0.32 (010)[a]
	Low	0.31 (0.03)[a]	0.39 (0.04)[a]
	High	0.05 (0.05)[b]	- 0.02(0.12)[b]
D. ovum	Control	0.35 (0.04)[a]	0.19 (0.07)[a]
	Low	0.39 (0.09)[a]	0.16 (0.8)[ab]
	High	0.22 (0.11)[a]	0.02 (0.13)[b]
D. caudata	Control	0.11 (0.05)[a]	0.19 (0.05)[a]
	Low	0.12 (0.05)[a]	0.34 (0.05)[b]
	High	0.14 (0.12)[a]	0.31 (0.07)[b]

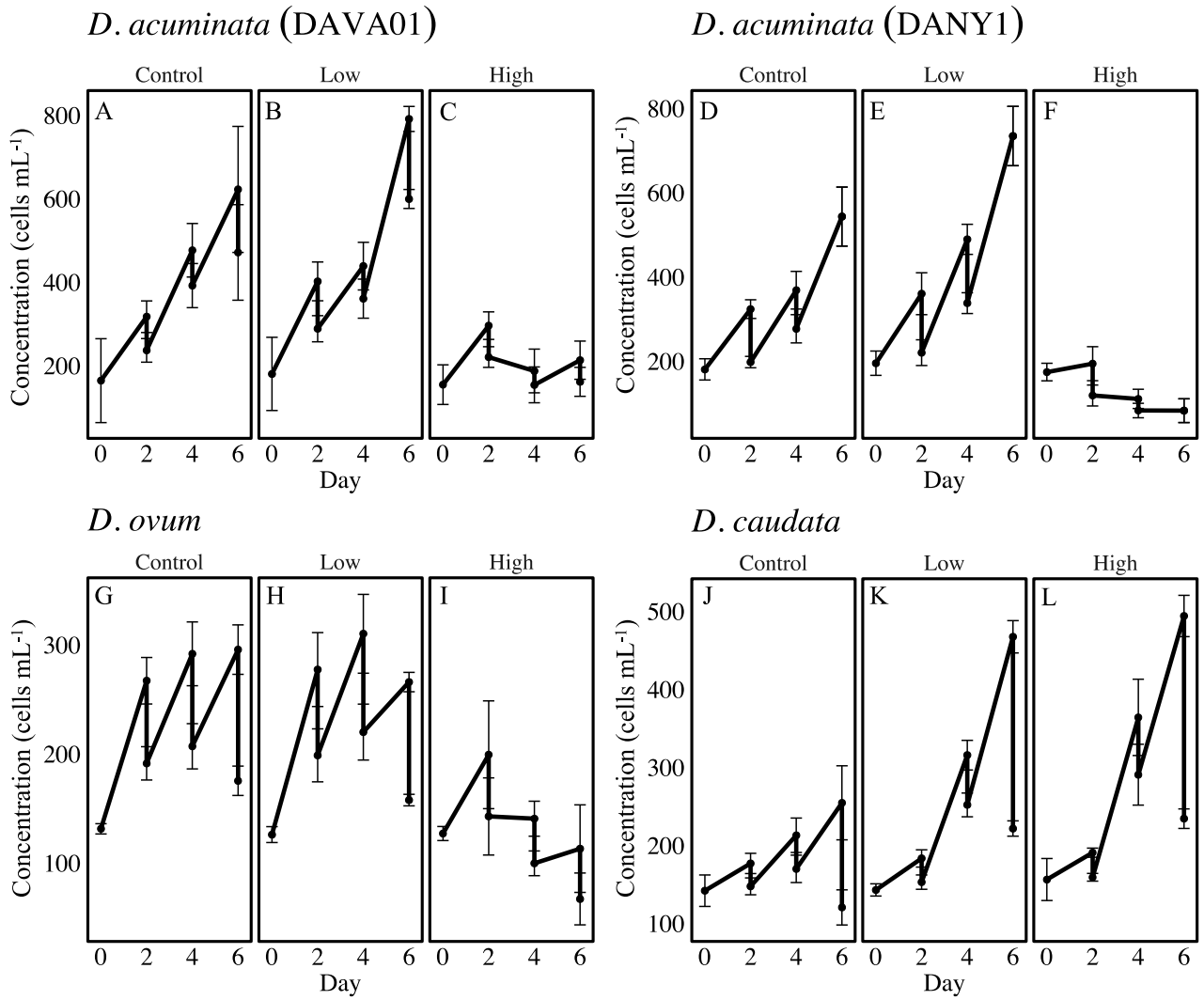

Figure 1 Average cell concentration (cells mL^{-1}) during semi-continuous culturing of *D. acuminata* (DAVA 01) (A, B, C), *D. acuminata* (DANY1) (D, E, F), *D. ovum* (G, H, I), and *D. caudata* (J, K, L) at three different turbulence levels: control (no turbulence), low (60 rpm), and high (120 rpm). Data points are mean ± SD, n = 3.

3.2 *Dinophysis* ingestion rates

Prey-only flask experiments were conducted three times, each in triplicate, and the growth rates averaged to obtain an overall growth rate for *Mesodinium* over two days in the absence of *Dinophysis*. In contrast to the preliminary range-finding experiment which found no effect of turbulence ranging from 0 – 120 rpm, *Mesodinium* growth was negatively impacted by turbulence in the prey-only flasks, with the average growth rate in the high turbulence treatment (-0.36 ± 0.23 d^{-1}) being significantly lower than the control (0.15 ± 0.05 d^{-1}) ($p < 0.05$). The growth rate in the low turbulence treatment (0.09 ± 0.02 d^{-1}) was lower than the control, but not significantly different from the control or high turbulence treatments.

Ingestion rates were calculated by comparing cell counts from co-incubation flasks (*Dinophysis* + *Mesodinium*) and prey-only flasks (*Mesodinium*) between Days 2-4 of the experiment. Overall, there was no difference detected for ingestion rates between any treatments within any isolate (Figure 2) ($p > 0.05$). The ingestion rates for *D. acuminata*, isolate DAVA 01, showed an increasing trend from the control (1.76 ± 1.15 cells *Mesodinium Dinophysis*$^{-1}$ day^{-1}); to low (2.20 ± 0.32 cells *Mesodinium Dinophysis*$^{-1}$ day^{-1}) turbulence treatments, but then decreased in the high turbulence treatment (0.65 ± 1.00 cells *Mesodinium Dinophysis*$^{-1}$ day^{-1}) (Figure 2). The ingestion rates for the *D. acuminata* (DANY1) strain were lowest in the low turbulence treatment (0.63 ± 0.43 cells *Mesodinium Dinophysis*$^{-1}$ day^{-1}), followed by the control (0.75 ± 1.14 cells *Mesodinium Dinophysis*$^{-1}$ day^{-1}), and highest in the high turbulence treatment (1.31 ± 0.69 cells *Mesodinium Dinophysis*$^{-1}$ day^{-1}) (Figure 2). For *D. ovum*, the low turbulence treatment had the lowest ingestion rate (1.38 ± 0.07 cells *Mesodinium Dinophysis*$^{-1}$ day^{-1}), followed by the control (2.09 ± 0.41 cells *Mesodinium Dinophysis*$^{-1}$ day^{-1}), and high turbulence treatment (3.07 ± 1.60 cells *Mesodinium Dinophysis*$^{-1}$ day^{-1}) (Figure 2). Lastly, ingestion rates

for *D. caudata* seemed to decrease with increasing turbulence, as the ingestion rate in the control was the highest (3.09 ± 0.51 cells *Mesodinium Dinophysis*$^{-1}$ day^{-1}) followed by the low and high turbulence treatments (2.21 ± 0.50 cells *Mesodinium Dinophysis*$^{-1}$ day^{-1}, 1.74 ± 0.81 cells *Mesodinium Dinophysis*$^{-1}$ day^{-1}, respectively) (Figure 2).

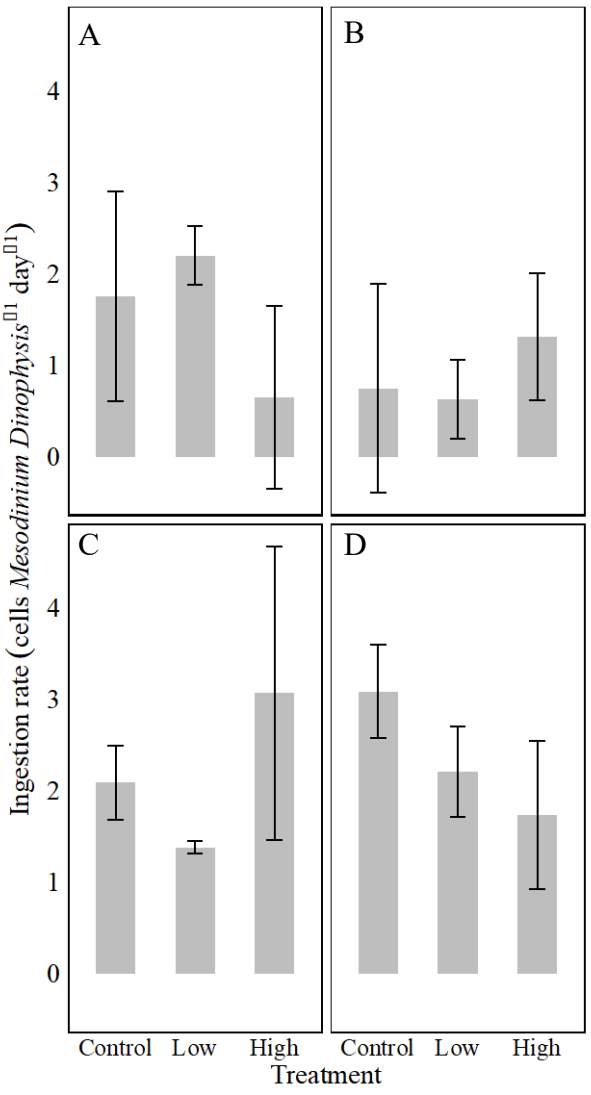

Figure 2 Average ingestion rates (cells *Mesodinium Dinophysis*$^{-1}$ day^{-1}) of *D. acuminata* (DAVA 01) (A), *D. acuminata* (DANY1) (B), *D. ovum* (C), and *D. caudata* (D) calculated between Days 2-4 of the experiment. Data points are mean ± SD, n = 3. No difference was detected between the treatments, within an isolate.

3.3 Toxin content (intracellular) and toxin concentration (extracellular)

Toxins OA, DTX-1, and PTX-2 were found in *D. acuminata* (DAVA 01) intracellular and extracellular fractions across all treatments (Figure 3). The intracellular fraction of *D. acuminata* (DANY1) contained OA, DTX-1, and PTX-2, while the extracellular fraction contained only PTX-2 and OA (Figure 3). OA and hydroxyPTX-2 were found in intracellular and extracellular fractions of *D. ovum* and *D. caudata* cultures, respectively.

Within *D. acuminata* (DAVA 01), the high turbulence treatment had significantly higher intracellular (4.02 ± 0.90 pg cell^{-1}, $p < 0.05$) DST content compared to the control (2.03 ± 0.13 pg cell^{-1}) and the low turbulence treatment (2.06 ± 0.34 pg cell^{-1}) (Figure 3). However, the intracellular PTX-2 content of DAVA 01 did not differ across any treatment ($p > 0.05$); the concentration of PTX-2 was equal to 18.40 ± 0.69, 16.39 ± 1.54, and 23.72 pg cell^{-1} in the control, low and high turbulence treatments, respectively (Figure 3). In addition, no significant differences in the extracellular DST or PTX-2 concentrations were detected in this species across treatments; the extracellular DST concentration in the control was 205.88 ± 46.33 pg mL^{-1}, compared to 222.22 ± 41.00 pg mL^{-1} in the low turbulence treatment, and 171.10 ± 4.25 pg mL^{-1} in the high turbulence treatment (Figure 3). The low turbulence treatment had the highest concentration of extracellular PTX-2 at 2308.72 ± 1007.06 pg mL^{-1}, followed by the control (2161.05 ± 1034.82 pg mL^{-1}) and the high turbulence treatment (1997.77 ± 1353.51 pg mL^{-1}).

For the second isolate of *D. acuminata* (DANY1), the intracellular PTX-2 content in the high turbulence treatment (39.89 ± 6.43 pg cell^{-1}) was significantly higher than the low turbulence treatment (17.05 ± 1.05 pg cell^{-1}) and the control (22.06 ± 3.00) ($p < 0.05$) (Figure 3). Conversely, the extracellular PTX-2 concentration in the high turbulence treatment (386.01 ± 97.08 pg mL^{-1}) was significantly lower than the control (726.13 ± 115.44 pg mL^{-1}, $p < 0.05$); the

extracellular PTX-2 concentration in the low turbulence treatment was 522.55 ± 111.02 pg mL^{-1} (Figure 3). In contrast to PTX-2, statistics were not performed using DANY1 intracellular or extracellular DST toxin values due insufficient data, i.e., many non-detects (see section 2.6). The average intracellular DST content was 0.37 ± 0.11 pg $cell^{-1}$ in the control and 0.28 ± 0.11 pg $cell^{-1}$ in the low turbulence treatment; in the high turbulence treatment, however, no DSTs were detected. Extracellular DSTs were only quantifiable in two samples across the three levels of turbulence, with one being 99.40 pg mL^{-1} in the low turbulence treatment, and the other being 99.97 pg mL^{-1} in the high turbulence treatment (Figure 3).

For *D. ovum*, intracellular OA content of the control, low and high turbulence treatments were comparable (3.75 ± 0.57, 3.50 ± 0.32, and 3.48 ± 0.12 pg $cell^{-1}$, respectively) with no significant difference detected between the three treatments (Figure 3). However, in the extracellular fraction, the high turbulence treatment had significantly more OA (586.71 ± 78.06 pg mL^{-1}) than the control (395.18 ± 35.20 pg mL^{-1}, $p < 0.05$) and the turbulence treatment (402.57 ± 97.76 pg mL^{-1}) (Figure 3).

The highest intracellular hydroxyPTX-2 content for *D. caudata* was detected in the control (20.18 ± 1.19 pg $cell^{-1}$, $p < 0.05$) and was significantly higher than the low and high turbulence treatments (12.51 ± 0.58 pg $cell^{-1}$, and 13.87 ± 1.26 pg $cell^{-1}$, respectively) (Figure 3). However, there was no significant difference detected in the concentration of extracellular hydroxyPTX-2 within the different treatments (636.10 ± 45.78, 846.00 ± 223.78, and 1189.4 ± 423.10 pg mL^{-1} in the control, low, and high turbulence treatments, respectively) (Figure 3).

Total toxin was calculated (intra + extra expressed as pg toxin per mL of culture) to allow for the percentage of extracellular toxins to be determined on day 4 and compared across the control, low, and high turbulence treatments. The percentage of extracellular OA in *D. ovum*

cultures significantly increased (2x) under high turbulence (54% ± 1) compared to the control (27% ± 2) and low turbulence treatments (27% ± 5). Although not significant, a similar trend was seen with (1) *D. caudata* culture, extracellular hydroxyPTX-2 was 13% ± 1 in the control and 19% ± 5 in the high turbulence treatment, and (2) *D. acuminata* (DAVA 01) culture, extracellular PTX-2 was 20% ± 10 in the control and 28% ± 10 under high turbulence. In contrast, there was little to no difference (≤ 2% difference) in percent extracellular DSTs between treatments for *D. acuminata*, DAVA 01, and percent extracellular PTXs for *D. acuminata*, DANY1, were significantly lower under turbulence (6% ± 1) than the control (8% ± 1).

3.4 Toxin production rates

The intracellular net toxin production rates (R_{tox}, pg toxin cell^{-1} day^{-1}) were calculated over Days 2-4 of the experiment. For the two *D. acuminata* isolates, DST R_{tox} rates were similar within an isolate, when compared across the control (0.19 ± 0.21 pg cell^{-1} day^{-1}, 0.03 ± 0.09 pg cell^{-1} day^{-1}), low (0.31 ± 0.24 pg cell^{-1}, 0.03 ± 0.07 pg cell^{-1} day^{-1}), and high treatments (-0.08 ± 0.19 pg cell^{-1} day^{-1}, -0.40 ± 0.13 pg cell^{-1} day^{-1}) respectively (Figure 4). As shown in Figure 4A and 4B, no difference was detected between DAVA 01 treatments, and non-detects prohibited statistical analysis of DANY1 DST R_{tox}. Similarly, the *D. caudata* strain exhibited no significant differences in the intracellular hydroxyPTX-2 R_{tox} across treatments, with the low turbulence treatment rate being 2.63 ± 0.86 pg cell^{-1} day^{-1}, followed by the control (2.69 ± 0.42 pg cell^{-1} day^{-1}) and high turbulence treatment (3.42 ± 0.19 pg cell^{-1} day^{-1}) (Figure 4F).

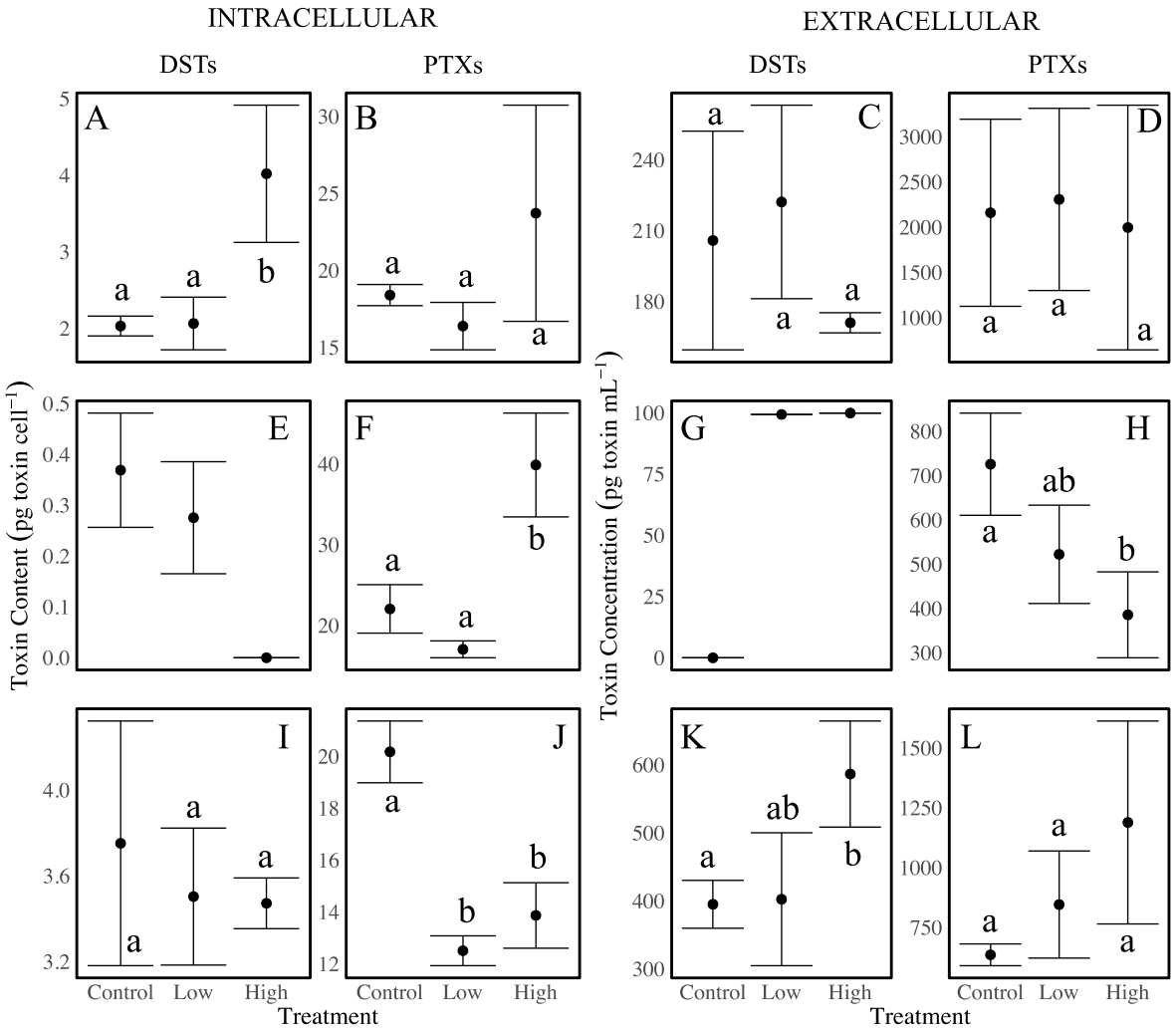

Figure 3 Intracellular (pg toxin cell^{-1}) and extracellular (pg toxin mL^{-1}) toxins measured in *D. acuminata* (DAVA 01) (A, B, C, D), *D. acuminata* (DANY1) (E, F, G, H), *D. ovum* (I, K), and *D. caudata* (J, L) on Day 4. Toxins include DSTs (OA + DTX-1) and PTXs (PTX-2 and HydroxyPTX-2). Data are mean ± SD, n = 3. No SDs are given for DANY treatments because the intra or extracellular DST contents/concentrations were below the limit of quantification or detection in one or two replicates. Superscript letters that are different indicate significance between treatments, tested within an isolate.

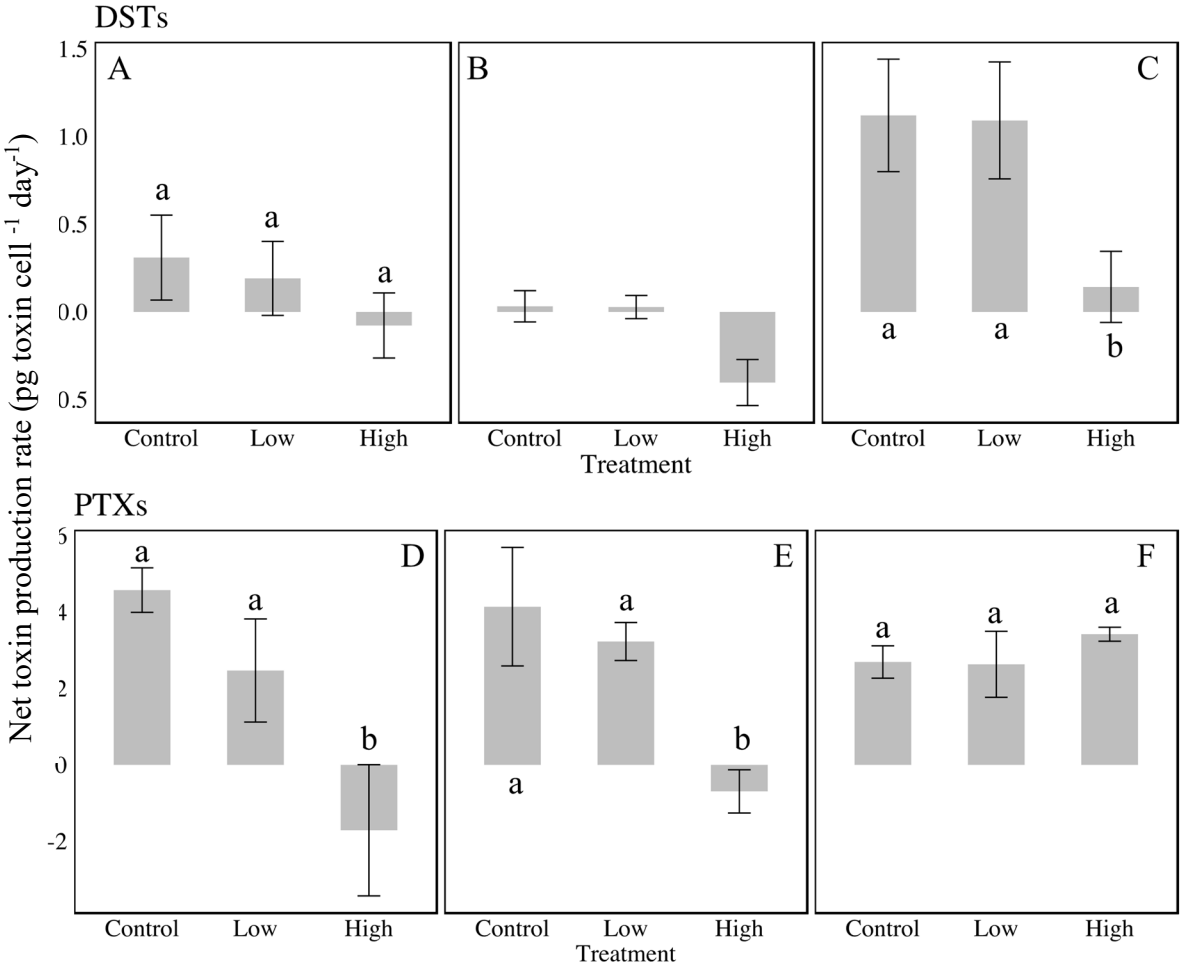

Figure 4 Intracellular net toxin production rates (pg cell^{-1} day^{-1}) for DSTs (top panel) and PTXs (bottom panel) for *D. acuminata*, DAVA 01 (A,D), *D. acuminata*, DANY1 (B,E), *D. ovum* (C) , and *D. caudata* (F) isolates calculated between Days 2-4 of the experiment. All PTX (PTX-2 and HydroxyPTX-2) or DST (OA + DTX-1) analogues were combined. Data are presented as mean ± SD, n = 3. Superscript letters that are different indicate significance between treatments, tested within an isolate.

Turbulence, however, did have a measurable effect on PTX-2 R_{tox} for both *D. acuminata* isolates and DST R_{tox} for *D. ovum*, with elevated turbulence significantly reducing toxin production. The high turbulence treatment for DAVA 01 had a significantly lower PTX-2 R_{tox} (-0.69 ± 0.56 pg cell^{-1} day^{-1}) compared to the low turbulence treatment (3.23 ± 0.50 pg cell^{-1} day^{-1}) and control (4.14 ± 1.55 pg cell^{-1} day^{-1}) ($p < 0.05$) (Figure 4D). Similarly, the high turbulence treatment had a significantly lower PTX-2 R_{tox} (-1.71 ± 1.72 pg cell^{-1} day^{-1}) than the control (4.58 ± 0.58 pg cell $^{-1}$ day^{-1}) and low turbulence treatments (2.47 ± 1.35 pg cell^{-1} day^{-1}) ($p < 0.05$) for strain DANY1 (Figure 4E). The high turbulence treatment for the *D. ovum* isolate had a significantly lower DST intracellular R_{tox} (0.14 ± 0.20 pg cell^{-1} day^{-1}) compared to the control and low turbulence treatments (1.12 ± 0.32 and 1.09 ± 0.33 pg cell^{-1} day^{-1}, respectively) ($p < 0.05$) (Figure 4C).

DISCUSSION

This study explored the impacts of turbulence on *Dinophysis* spp. ingestion and growth rates and provided complementary data on their toxin content, concentrations, and production rates. Similar to prior research regarding the impact of small-scale turbulence on *Dinophysis* cultures, species-specific responses to turbulence were observed. High turbulence seemed to be the most detrimental to *Dinophysis ovum*, with exposure to high turbulence significantly reducing growth, increasing extracellular toxin concentration, and reducing intracellular net toxin production rate, suggesting cell lysis and release of toxins into the culture medium. On the contrary, turbulence enhanced the growth of *Dinophysis caudata* but decreased its intracellular hydroxyPTX-2 toxin content.

4.1 Effect of turbulence on *Dinophysis* growth rates

Three of the four strains tested, including two *D. acuminata* strains, DAVA 01 and DANY1, and *D. ovum*, exhibited similar responses to turbulence: exposure to low turbulence had no effect on growth compared to the control, exposure to high turbulence severely inhibited growth. Some differences, however, were notable in the growth response of the three isolates of the *Dinophysis-acuminata* complex. A negative growth rate (i.e., mortality) was observed under high turbulence for *D. acuminata* (DANY1), and this isolate reacted to high turbulence faster than any other strain tested, with a significantly decreased growth rate after just 2 days of exposure. Together these results suggest that *D. acuminata*, DANY1 strain, may be more susceptible to turbulence than strain DAVA 01 or the *D. ovum* isolate. Unlike the other three strains, the growth of *D. caudata* appeared to be stimulated at both low and high turbulence levels relative to the no turbulence control.

The observed species-specific results are similar to previous studies that have demonstrated the varied impacts of turbulence on dinoflagellate species (Berdalet, 1992, Zirbel et al. 2000, Sullivan et al. 2003, Sullivan & Swift 2003, Berdalet et al. 2007). Dinoflagellates have been the dominant species used to study the effects of turbulence on phytoplankton due to their apparent sensitivity to small-scale turbulence (Estrada & Berdalet 1997). In fact, Peters and Marrasé (2000), summarized a variety of turbulence studies and found that there was a 121% bulk decrease in normalized (standardized across the studies) growth rate among dinoflagellate species when exposed to a wide range of kinetic energy dissipation rates (ε).With regards to *Dinophysis* specifically, García-Portela et al. (2019) exposed two species of *Dinophysis*, *D. acuminata* and *D. acuta* (both isolated from Spain), to different levels of turbulence to determine relative sensitivity. The authors found that the growth of both species was unaffected by low ($\varepsilon \approx 10^{-6}$ m^2s^3) and medium ($\varepsilon \approx 10^{-5}$ m^2s^3) levels of turbulence, but exposure to high turbulence ($\varepsilon \approx 10^{-4}$ m^2s^3) revealed different responses, with *D. acuta* ceasing growth, while *D. acuminata* continued to grow at a slower rate after an initial lag phase. Additionally, this species-specific response has also been observed in other harmful algal bloom (HAB) genera. For instance, Sullivan et al. (2003) exposed two species of HABs, *Lingulodinium polyedrum* and *Alexandrium catenella* to a range of five turbulence levels (between 10^{-8} to 10^{-4} m^2 s^{-3}) and found that the growth rate of *L. polyedrum* increased linearly with increasing turbulence intensity until a threshold was reached. Conversely, the growth rate of *A. catenella* was unaffected by low level of turbulence, but as turbulence increased, there was a reduction in the division rate, an increase in cell size, and an increase in chain length.

It is important to note that the dissipation rates (ε) used in these two previous laboratory experiments were generally lower than the rates used in the current study (10^{-3} m^2 s^{-3} and 10^{-2} m^2

s^{-3}, respectively), with previous studies conducted at dissipation rates that were one to five orders of magnitude lower. The most common experimental methods for generating turbulence in the laboratory include aeration systems, Couette cylinders, oscillating grid systems, and shaker tables (Arnott et al. 2021 and references therein). While both Sullivan et al. (2003) and García-Portela et al. (2019) both used oscillating grids to generate turbulence, Guadyol et al. (2009) compared turbulence generation suitability between oscillating grid systems and shaker tables and found that both systems produced fairly isotropic conditions (i.e., turbulent forces have no preferred direction) (McGillicuddy Jr. & Franks, 2019). The authors deemed both techniques sufficient for environmentally realistic turbulence generation, with a few stipulations for shaker tables. Isotropy can be lost while using shaker tables in low turbulence or energy conditions, so the authors recommended avoiding oscillation frequencies below 1 Hz (40rpm) to ensure isotropy is maintained. Additionally, there is the potential for a gradient of dissipation in the experimental flasks, where energy dissipation rates (ε) can vary by an order of magnitude between the wall and the center of the flask. To limit the interference of these two caveats, the current study avoided oscillation frequencies below 1 Hz, and used small and narrow cultures flasks (125-mL Erlenmeyer flasks, as used in Zirbel et al. 2000), to maintain homogeneity of turbulent forces. The preliminary range of shaker table settings and subsequent dissipation rates were adopted from Zirbel et al. (2000), who also performed preliminary tests with orbital shaker oscillation rates between 40 and 120rpm, using the same culture flasks (125 mL Erlenmeyer flasks) and volume of culture (60mL).

Additionally, environmentally relevant values of ε range from 10^{-10} m^2 s^{-3} for surface layers in the open ocean, to 10^2 m^2 s^{-3} for surf zones with frequent wave action (Arnott et al. 2021 and references therein). The low turbulence level, 60rpm ($\varepsilon = 3.01 \times 10^{-3}$ m^2 s^{-3}), used in the

current study is within the range of an inlet/estuary (≈ 10^{-10} to 10^{-1} m^2 s^{-3}) and the high turbulence level, 120rpm (ε = 1.02 x10^{-2} m^2 s^{-3}), is within the range of the surf zone (≈ 10^{-6} to 10^{2} m^2 s^{-3}) (Arnott et al. 2021 and references therein). Thus, the higher the value of ε, the more small-scale turbulence the phytoplankton cells experience. The dissipation rates used in Sullivan et al. (2003) and García-Portela et al. (2019) were both between 10^{-8} to 10^{-4} m^2 s^{-3}; this range of dissipation rates includes the open ocean, continental shelf, inlet/estuary, and surf zone (Arnott et al. 2021 and references therein) and are thus still captured in the environmental ranges of turbulence used in the current study.

In addition to laboratory studies, species-specific differences in response to turbulence have been documented in field populations of *Dinophysis* (Díaz et al. 2019, Baldrich et al. 2021, Baldrich et al. 2023). In the Galician Rías Baxias (NW Spain), changes in water column dynamics during a relaxation-upwelling transition revealed the growth rate of *D. acuminata* in the surface layer was halved following the onset of an upwelling pulse (Díaz et al. 2019). The researchers found, using turbulence profilers, that the dissipation rates (ε) within the surface layer changed by two orders of magnitude (10^{-6} to 10^{-4} m^2 s^{-3}) over time. Most of the *D. acuminata* population remained in the top 5 m of the water column throughout the sampling period (36-h), and thus the authors hypothesized that the rapid increase in turbulence and cooling surface waters associated with downwelling-upwelling transitions negatively impacted the population. Similar studies have been conducted in Southern Chile, in stratified fjords where Baldrich et al. (2021) used a range of environmental variables to identify the realized niches of two co-occurring *Dinophysis* species, *D. acuminata* and *D. acuta*. A 48-h sampling period revealed that these two species have distinct niches; *D. acuminata* was found in the upper 2 m of the water column, suggesting that it is more tolerant of the higher turbulence (ε = ~ 10^{-5} m^2 s^{-3}),

while *D. acuta* cells were found between 4 and 8 m depth, indicating that it is less tolerant of surface-level turbulence.

4.2 Effect of turbulence on *Dinophysis* ingestion rates

Previous studies showed that turbulence may have a positive influence on the ingestion rate of mixotrophic dinoflagellates, with the exception of the highest turbulence levels (Peters & Marrasé 2000). As a result, low levels of turbulence were predicted to increase *Dinophysis* and *Mesodinium* encounter rates, thus increasing ingestion rates. Whereas, high levels of turbulence were hypothesized to disrupt the complex feeding behavior of *Dinophysis*, thus decreasing ingestion rates. However, no significant differences in ingestion rates were detected for any of the four *Dinophysis* strains examined in this study, regardless of the turbulence level. These results are similar to those of Havskum et al. (2005), who examined the effect of turbulence on *Ceratium tripos*, and the predator-prey relationship between *C. tripos* and the mixotrophic dinoflagellate *Fragilidium subglobosum*. The authors found that the mixotrophic growth of the predator, *F. subglobosum*, when fed high cell densities of *C. tripos* (>> 10 cells mL^{-1}), was independent of the four turbulence levels. However, growth and ingestion rates of *F. subglobosum* were significantly higher in the highest turbulence treatment (10^{-3} m^2s^3) when cultures were fed low prey densities, around 5 to 8 cells mL^{-1} (Havskum et al. 2005). During the current study, *Mesodinium* was always present in the treatment flasks prior to the addition of supplemental feeding every two days, indicating that prey was in abundance throughout the experimental period. *Dinophysis* has been shown to be an obligate mixotroph, requiring both light and prey for continual survival (Kim et al. 2008), while *F. subglobosum* is considered a facultative mixotroph, and may thus rely solely on phototrophic or phagotrophic growth (Sanders et al. 1990, Holen & Boraas, 1995, Skovgaard 1996). Thus, the comparison between these two

dinoflagellates is not valid. A better comparison may be provided with a more recent study by García-Portela et al. (2019), where authors measured the ingestion rates of *D. acuminata* and *D. acuta* when exposed to three levels of turbulence ($\varepsilon = 10^{-6}$, 10^{-5}, and 10^{-4} $m^2 s^{-3}$). In contrast to the current study where no effect of turbulence was observed on ingestion (even at higher ε), the previous study found that, in general, exposure of *Dinophysis* spp. to turbulence raised ingestion rates on the first day of the experiment, but then the effect diminished. Together this suggests that the current study may have missed any effect of turbulence on ingestion rates by waiting for Days 2 to 4 to conduct those measurements; a decision originally made to allow cultures to stabilize after inoculation into treatment and control flasks.

4.3 Effect of turbulence on *Dinophysis* toxin content and production rates

To our knowledge, this is the first laboratory study that investigated the effects of turbulence on *Dinophysis* toxin production and release (Díaz et al. 2019). For both *D. acuminata* strains, DAVA 01 and DANY1, turbulence inhibited growth, which led to an increase in intracellular DSTs and/or PTX-2 content, as toxin accumulated overtime in the slower-growing cells. As growth and toxin production is often coupled in HAB species, turbulence and slowed growth also led to decreased toxin production per cell. While changes in toxin content or production were not notable for *D. ovum* strain, an effect of turbulence resulted in a higher concentration of extracellular OA and elevated percentage found extracellularly. This enhanced release of toxins into the medium could be attributed to cell leakiness under turbulent stress; less of the enhancement however is due to cell death and lysing as growth remained positive under the high turbulence treatment (Table 1, Figure 1). Thus, patterns in growth and toxin content observed for the *D. ovum* strain support the original hypothesis that high turbulence can reduce growth and lead to a release of extracellular toxins into the medium. Effects were species-

specific, however, as growth of *D. caudata* was instead stimulated by turbulence, and rapidly dividing cells accumulated significantly less toxin intracellularly.

Little data exist on the effect of turbulence on *Dinophysis* toxin content and production rates. For instance, Díaz et al. (2019) measured particulate and dissolved toxin quotas (OA) collected during a cruise in the Galician Rías of Vigo and Pontevedra and found an association between the growth rate of the *D. acuminata* isolate and turbulence, where the growth rate significantly decreased (from 0.65 to 0.33 d^{-1}) with increased turbulence ($\varepsilon < 10^{-4} m^2 s^{-3}$). However, the authors did not find any correlation between toxin accumulation per cell and the division rate of *D. acuminata* and suggested that this could be due to contamination of their net haul samples with other species. In a laboratory experiment, Juhl et al. (2001) exposed cultures of *Alexandrium catenella* to turbulence for 1-24 h d^{-1} over a period of 6-8 days using Couette flow chambers. The results showed that cultures exposed to more than 1 hour of turbulence every day had three times as much toxin per cell compared to the controls. The authors also found that as the growth rate of cultures decreased with increasing exposure to turbulence, the cellular toxin content significantly increased. In a different study, Bolli et al. (2007) exposed two species of the dinoflagellate *Alexandrium*, *A. minutum* and *A. catenella*, to two levels of turbulence to investigate its effects on cyst development and toxin dynamics using an orbital shaker at 120 rpm, or a vertically oscillating grid system. In contrast to the Juhl et al. (2001) study, the results showed that after 4 days of continuous turbulence exposure, the cellular gonyautoxin (GTX) (1+4) toxin contents were significantly lower than in the controls. The authors suggested that the discrepancies in data could be attributed to varying physiological states of the cultures, or differences in the experimental setup and design.

CONCLUSIONS

While *Dinophysis* spp. are known to form thin layers at depth (Reguera et al. 2012), it has also been hypothesized that blooms may originate offshore and be advected into coastal areas (Campbell et al. 2010), where cells could be subjected to higher levels of turbulence. Exposing four strains of *Dinophysis*, consisting of three species that were isolated from two different coasts of the U.S., to varying levels of disturbance elicited species-specific responses in growth, toxin content, release, and production. These growth and toxin production data can be incorporated into future modeling efforts to understand and predict *Dinophysis* blooms, toxicity, release of toxins into the environment, and threat of DSP. Additionally, incorporating other strains or species of *Dinophysis* from different U.S. coasts into future turbulence exposure studies will further characterize species-specific responses to turbulence.

Acknowledgements

Thank you to Nour Ayache for her guidance on experimental design and assistance, as well as Amy Menegey, Marta Sanderson, and Joshua Garber for their assistance with experiments and sample extractions. Thank you to Nicole Millette for her assistance with experimental design and analysis. Thank you to Lisa Campbell and Christopher Gobler for contributing *Dinophysis* strain DOSS2206 and DANY1, respectively. Many thanks to Dr. Claude Mallet (Waters, Inc.) for his valuable advice and generous donation of analytical instrumentation and Hunter Walker for lending a shaker table for the experiments. This work was funded by the National Oceanic and Atmospheric Administration (NOAA) National Centers for Coastal Ocean Science Competitive Research, ECOHAB Program under award #NA19NOS4780182 to JLS and a Student Research Grant from VIMS to VRS.

REFERENCES

Anderson, D. M., Kulis, D. M., Sullivan, J. J., Hall, S., & Lee, C. (1990). Dynamics and physiology of saxitoxin production by the dinoflagellates *Alexandrium* spp. *Marine Biology*, *104*(3), 511–524. https://doi.org/10.1007/BF01314358

Arnott, R. N., Cherif, M., Bryant, L. D., & Wain, D. J. (2021). Artificially generated turbulence: A review of phycological nanocosm, microcosm, and mesocosm experiments. *Hydrobiologia*, *848*(5), 961–991. https://doi.org/10.1007/s10750-020-04487-5

Aune, T., Yndestad, M., 1993. Diarrhetic shellfish poisoning. In: Falconer, I.R. (Ed.), Algal Toxins in Seafood and Drinking Water. Academic Press, New York, pp. 87–104.

Ayache, N., Bill, B. D., Brosnahan, M. L., Campbell, L., Deeds, J. R., Fiorendino, J. M., Gobler, C. J., Handy, S. M., Harrington, N., Kulis, D. M., McCarron, P., Miles, C. O., Moore, S. K., Nagai, S., Trainer, V. L., Wolny, J. L., Young, C. S., & Smith, J. L. (2023). A Survey of *Dinophysis* Spp. And Their Potential To Cause Diarrhetic Shellfish Poisoning In Coastal Waters Of The United States. *Accepted*.

Baldrich, Á. M., Pérez-Santos, I., Álvarez, G., Reguera, B., Fernández-Pena, C., Rodríguez-Villegas, C., Araya, M., Álvarez, F., Barrera, F., Karasiewicz, S., & Díaz, P. A. (2021). Niche differentiation of Dinophysis acuta and D. acuminata in a stratified fjord. *Harmful Algae*, *103*, 102010. https://doi.org/10.1016/j.hal.2021.102010

Baldrich, Á. M., Díaz, P. A., Álvarez, G., Pérez-Santos, I., Schwerter, C., Díaz, M., Araya, M., Nieves, M. G., Rodríguez-Villegas, C., Barrera, F., Fernández-Pena, C., Arenas-Uribe, S., Navarro, P., & Reguera, B. (2023). Dinophysis acuminata or Dinophysis acuta: What Makes the Difference in Highly Stratified Fjords? *Marine Drugs*, *21*(2), 64. https://doi.org/10.3390/md21020064

Berdalet, E. (1992). EFFECTS OF TURBULENCE ON THE MARINE DINOFLAGELLATE GYMNODINIUM NELSONII1. *Journal of Phycology*, *28*(3), 267–272. https://doi.org/10.1111/j.0022-3646.1992.00267.x

Berdalet, E., Peters, F., Koumandou, V. L., Roldán, C., Guadayol, Ò., & Estrada, M. (2007). Species-specific physiological response of dinoflagellates to quantified small-scale turbulence [1]. *Journal of Phycology*, *43*(5), 965–977. https://doi.org/10.1111/j.1529-8817.2007.00392.x

Blanco, J., Moroño, Á., & Fernández, M. L. (2005). *Toxic Episodes In Shellfish, Produced By Lipophilic Phycotoxins: An Overview*.

Bolli, L., Llaveria, G., Garces, E., Guadayol, O., van Lenning, K., Peters, F., & Berdalet, E. (2007). Modulation of ecdysal cyst and toxin dynamics of two *Alexandrium* (Dinophyceae) species under small-scale turbulence.

Campbell, L., Olson, R. J., Sosik, H. M., Abraham, A., Henrichs, D. W., Hyatt, C. J., & Buskey, E. J. (2010). First Harmful *Dinophysis* (Dinophyceae, Dinophysiales) Bloom In The U.S. Is Revealed By Automated Imaging Flow Cytometry1: *Dinophysis* Dynamics From Imaging Flowcytobot. *Journal of Phycology*, *46*(1), 66–75. https://doi.org/10.1111/j.1529-8817.2009.00791.x

Chen, D., K. Muda, K. Jones, J. Leftly & P. Stansby, 1998. Effect of shear on growth and motility of *Alexandrium minutum* Halim, a red-tide dinoflagellate. In Reguera, B., J. Blanco, M. L. Ferna´ndez & T. Wyatt (eds), Harmful algae. Xunta de Galicia and Intergovernmental Oceanographic Commision of UNESCO, Vigo: 352–355.

Cohen P, Holmes CF, Tsukitani Y. Okadaic acid: a new probe for the study of cellular regulation. Trends Biochem Sci. 1990 Mar;15(3):98-102. doi: 10.1016/0968-0004(90)90192-e. PMID: 2158158.

Deeds, J. R., Whitney L. Stutts, Mary Dawn Celiz, Jill MacLeod, Amy E. Hamilton, Bryant J. Lewis, David W. Miller, Kohl Kanwit, Juliette L. Smith, David M. Kulis, Pearse McCarron, Carlton D. Rauschenberg, Craig A. Burnell, Stephen D. Archer, Jerry Borchert, & Shelley K. Lankford. (2020). Dihydrodinophysistoxin-1 Produced by *Dinophysis norvegica* in the Gulf of Maine, USA and Its Accumulation in Shellfish. *Toxins*, *12*(533), 1–19.

Díaz, P. A., Ruiz-Villarreal, M., Mouriño-Carballido, B., Fernández-Pena, C., Riobó, P., & Reguera, B. (2019b). Fine scale physical-biological interactions during a shift from relaxation to upwelling with a focus on Dinophysis acuminata and its potential ciliate prey. *Progress in Oceanography*, *175*, 309–327. https://doi.org/10.1016/j.pocean.2019.04.009

Dominguez, H.J., Paz, B., Daranas, A.H., Norte, M., Franco, J.M., Fernández, J.J., 2010. Dinoflagellate polyether within the yessotoxin, pectenotoxin and okadaic acid toxin groups: Characterization, analysis and human health implications. Toxicon 56, 191–217. https://doi.org/10.1016/j.toxicon.2009.11.005

Estrada, M., Alcaraz, M., & Marrasé, C. (1987). Effects of turbulence on the composition of phytoplankton assemblages in marine microcosms. *Marine Ecology Progress Series*, *38*(3), 267–281.

Estrada, M., & Berdalet, E. (1997). Phytoplankton in a turbulent world. *Scientia Marina*, *61*, 125–140.

Estrada, M., & Berdalet, E. (1998). Effects of Turbulence on Phytoplankton. *Physiological Ecology of Harmful Algal Blooms*, *41*.

European Commission, 2021. Commission Implementing Regulation (EU) 2021/1709 of 23 September 2021 amending Implementing Regulation (EU) 2019/627 as regards uniform practical arrangements for the performance of official controls on products of animal origin.

Fiorendino, J. M., Smith, J. L., & Campbell, L. (2020). Growth response of *Dinophysis*, *Mesodinium*, and *Teleaulax* cultures to temperature, irradiance, and salinity. *Harmful Algae*, *98*, 101896. https://doi.org/10.1016/j.hal.2020.101896

Frost, B. W. (1972). Effects Of Size And Concentration Of Food Particles On The Feeding Behavior Of The Marine Planktonic Copepod *Calanus Pacificus* 1: Feeding Behavior Of *Calanus*. *Limnology and Oceanography*, *17*(6), 805–815. https://doi.org/10.4319/lo.1972.17.6.0805

Fuchs, H. L., & Gerbi, G. P. (2016). Seascape-level variation in turbulence- and wave-generated hydrodynamic signals experienced by plankton. *Progress in Oceanography*, *141*, 109–129. https://doi.org/10.1016/j.pocean.2015.12.010

Fux, E., Smith, J. L., Tong, M., Guzmán, L., & Anderson, D. M. (2011). Toxin profiles of five geographical isolates of *Dinophysis* spp. From North and South America. *Toxicon*, *57*(2), 275–287. https ://doi.org/10.1016/j.toxicon.2010.12.002

Gaillard, S., Le Goïc, N., Malo, F., Boulais, M., Fabioux, C., Zaccagnini, L., Carpentier, L., Sibat, M., Réveillon, D., Séchet, V., Hess, P., Hégaret, H. (2020). Cultures of *Dinophysis sacculus*, *D. acuminata* and pectenotoxin 2 affect gametes and fertilization success of the Pacific oyster, *Crassostrea gigas*. Environ. Pollut. 265. https://doi.org/10.1016/j.envpol.2020.114840

Gaillard, S., Réveillon, D., Danthu, C., Hervé, F., Sibat, M., Carpentier, L., Hégaret, H., Séchet, V., & Hess, P. (2021). Effect of a short-term salinity stress on the growth, biovolume, toxins,

osmolytes and metabolite profiles on three strains of the *Dinophysis acuminata*-complex (*Dinophysis* cf. Sacculus). *Harmful Algae*, *107*, 102009. https ://doi.org/10.1016/j.hal.2021.102009

Gaillard, S., Réveillon, D., Mason, P. L., Ayache, N., Sanderson, M., Smith, J. L., Giddings, S., McCarron, P., Séchet, V., Hégaret, H., Hess, P., & Vogelbein, W. K. (2023). Mortality and histopathology in sheepshead minnow (Cyprinodon variegatus) larvae exposed to pectenotoxin-2 and Dinophysis acuminata. *Aquatic Toxicology*, *257*.

García-Portela, M., Reguera, B., Ribera d'Alcalà, M., Rodríguez, F., & Montresor, M. (2019). Effects of small-scale turbulence on two species of *Dinophysis*. *Harmful Algae*, *89*, 101654. https://doi.org/10.1016/j.hal.2019.101654

García-Portela, M., Reguera, B., Gago, J., Le Gac, M., & Rodríguez, F. (2020). Uptake of Inorganic and Organic Nitrogen Sources by Dinophysis acuminata and D. acuta. *Microorganisms*, *8*(2), 187. https://doi.org/10.3390/microorganisms8020187

Guadayol, Ò., Peters, F., Stiansen, J. E., Marrasé, C., & Lohrmann, A. (2009). Evaluation of oscillating grids and orbital shakers as means to generate isotropic and homogeneous small-scale turbulence in laboratory enclosures commonly used in plankton studies: Turbulence in laboratory containers. *Limnology and Oceanography: Methods*, *7*(4), 287–303. https://doi.org/10.4319/lom.2009.7.287

Guillard RRL (1973) Division rates. In: Stein JR (ed) Handbook of phycological methods: culture methods and growth measurements. Cambridge University Press, Cambridge, p 289−312

Hallegraeff, G. M.,(2003). Harmful algal blooms: a global overview. In: Hallegraeff, G.M., Anderson, D.M., Cembella, A.D. (Eds.), *Manual on harmful marine microalgae* (2nd rev. ed). UNESCO Publishing, Landais, France, 25-40.

Harred, L. B., & Campbell, L. (2014). Predicting harmful algal blooms: A case study with *Dinophysis ovum* in the Gulf of Mexico. *Journal of Plankton Research*, *36*(6), 1434–1445. https://doi.org/10.1093/plankt/fbu070

Hattenrath-Lehmann, T. K., Marcoval, M. A., Berry, D. L., Fire, S., Wang, Z., Morton, S. L., & Gobler, C. J. (2013). The emergence of *Dinophysis acuminata* blooms and DSP toxins in shellfish in New York waters. *Harmful Algae*, *26*, 33–44. https://doi.org/10.1016/j.hal.2013.03.005

Hattenrath-Lehmann, T., & Gobler, C. J. (2015). The contribution of inorganic and organic nutrients to the growth of a North American isolate of the mixotrophic dinoflagellate, *Dinophysis acuminata*: The effects of nutrients on a culture of *Dinophysis. Limnology and Oceanography*, *60*(5), 1588–1603. https://doi.org/10.1002/lno.10119

Hattenrath-Lehmann, T. K., Marcoval, M. A., Mittlesdorf, H., Goleski, J. A., Wang, Z., Haynes, B., Morton, S. L., & Gobler, C. J. (2015). Nitrogenous Nutrients Promote the Growth and Toxicity of *Dinophysis acuminata* during Estuarine Bloom Events. *PLOS ONE*, 22.

Hattenrath-Lehmann, T. K., Nanjappa, D., Zhang, H., Yu, L., Goleski, J. A., Lin, S., & Gobler, C. J. (2021). Transcriptomic and isotopic data reveal central role of ammonium in facilitating the growth of the mixotrophic dinoflagellate, Dinophysis acuminata. *Harmful Algae*, *104*, 102031. https://doi.org/10.1016/j.hal.2021.102031

Havskum, H., Hansen, P. J., & Berdalet, E. (2005). Effect of turbulence on sedimentation and net population growth of the dinoflagellate *Ceratium tripos* and interactions with its predator, *Fragilidium subglobosum*. *Limnology and Oceanography*, *50*(5), 1543–1551. https://doi.org/10.4319/lo.2005.50.5.1543

Holen DA, Boraas ME (1995) Mixotrophy in chrysophytes. In: Sandgren CD, Smol JP , Kristiansen J (eds) Chrysophyte algae; ecology, phylogeny and development. Cambridge University Press, Cambridge, p 119-140.

Jiang, H., Kulis, D. M., Brosnahan, M. L., & Anderson, D. M. (2018). Behavioral and mechanistic characteristics of the predator-prey interaction between the dinoflagellate *Dinophysis acuminata* and the ciliate *Mesodinium rubrum*. *Harmful Algae*, *77*, 43–54. https ://doi.org/10.1016/j.hal.2018.06.007

Juhl, A. R., Trainer, V. L., & Latz, M. I. (2001). Effect of fluid shear and irradiance on population growth and cellular toxin content of the dinoflagellate *Alexandrium fundyense*. *Limnology and Oceanography*, *46*(4), 758–764.

Karp-Boss, L., Boss, E., & Jumars, P., A. (2000). Motion of dinoflagellates in a simple shear flow. *Limnology and Oceanography*, *45*(7), 1594–1602.

Kim, S., Kang, Y., Kim, H., Yih, W., Coats, D., & Park, M. (2008). Growth and grazing responses of the mixotrophic dinoflagellate *Dinophysis acuminata* as functions of light intensity and prey concentration. *Aquatic Microbial Ecology*, *51*, 301–310. https://doi.org/10.3354/ame01203

Mann, K.H., Lazier, J.R.N., 1991. Dynamics of Marine Ecosystems. Biological-physical Interactions in the Oceans. Blackwell Scientific Publications, Boston.

Margalef, R. (1978). Life-forms of phytoplankton as survival alternatives in an unstable environment. *Oceanol.*, *1*, 493–509.

McGillicuddy, D. J., & Franks, P. J. S. (2019). Models of Plankton Patchiness. In *Encyclopedia of Ocean Sciences* (pp. 536–546). Elsevier. https://doi.org/10.1016/B978-0-12-409548-9.11610-0

Miles, C.O., Wilkins, A.L., Munday, R., Dines, M.H., Hawkes, A.D., Briggs, L.R., Sandvik, M., Jensen, D.J., Cooney, J.M., Holland, P.T., Quilliam, M.A., MacKenzie, A.L., Beuzenberg, V., Towers, N.R. (2004). Isolation of pectenotoxin-2 from *Dinophysis acuta* and its conversion to pectenotoxin-2 seco acid, and preliminary assessment of their acute toxicities. Toxicon 43, 1–9. https://doi.org/10.1016/j.toxicon.2003.10.003

Nielsen, L., Krock, B., & Hansen, P. (2012). Effects of light and food availability on toxin production, growth and photosynthesis in *Dinophysis acuminata*. *Marine Ecology Progress Series*, *471*, 37–50. https://doi.org/10.3354/meps10027

Nishitani, G., Nagai, S., Sakiyama, S., & Kamiyama, T. (2008). Successful cultivation of the toxic dinoflagellate *Dinophysis caudata* (Dinophyceae). *Plankton and Benthos Research*, *3*(2), 78–85. https://doi.org/10.3800/pbr.3.78

Onofrio, M. D., Mallet, C. R., Place, A. R., & Smith, J. L. (2020). A Screening Tool for the Direct Analysis of Marine and Freshwater Phycotoxins in Organic SPATT Extracts from the Chesapeake Bay. *Toxins*, *12*(5), 322. https://doi.org/10.3390/toxins12050322

Park, M., Kim, S., Kim, H., Myung, G., Kang, Y., & Yih, W. (2006). First successful culture of the marine dinoflagellate *Dinophysis acuminata*. *Aquatic Microbial Ecology*, *45*, 101–106. https://doi.org/10.3354/ame045101

Pease, S. K. D., Brosnahan, M. L., Sanderson, M. P., & Smith, J. L. (2022). Effects of Two Toxin-Producing Harmful Algae, *Alexandrium catenella* and *Dinophysis acuminata* (Dinophyceae), on Activity and Mortality of Larval Shellfish. *Toxins*, *14*(5), 335. https://doi.org/10.3390/toxins14050335

Peters, F., & Marrasé, C. (2000). Effects of turbulence on plankton: An overview of experimental evidence and some theoretical considerations. *Marine Ecology Progress Series*, *205*, 291–306. https://doi.org/10.3354/meps205291

Pollingher, U., & Zemel, E. (1981). *In situ* and experimental evidence of the influence of turbulence on cell division processes of *Peridinium cinctum* forma *westii* (Lemm.) Lefèvre. *British Phycological Journal*, *16*(3), 281–287. https://doi.org/10.1080/00071618100650301

Reguera, B., Velo-Suárez, L., Raine, R., & Park, M. G. (2012). Harmful *Dinophysis* species: A review. *Harmful Algae*, *14*, 87–106. https://doi.org/10.1016/j.hal.2011.10.016

Reguera, B., Riobó, P., Rodríguez, F., Díaz, P., Pizarro, G., Paz, B., Franco, J., & Blanco, J. (2014). *Dinophysis* Toxins: Causative Organisms, Distribution and Fate in Shellfish. *Marine Drugs*, *12*(1), 394–461. https ://doi.org/10.3390/md12010394

Rountos, K. J., Kim, J. J., Hattenrath-Lehmann, T. K., & Gobler, C. J. (2019). Effects of the harmful algae, Alexandrium catenella and Dinophysis acuminata, on the survival, growth, and swimming activity of early life stages of forage fish. *Marine Environmental Research*, *148*, 46–56. https://doi.org/10.1016/j.marenvres.2019.04.013

Sanders, R. W., Porter, K. G., & Caron, D. A. (1990). Relationship between phototrophy and phagotrophy in the mixotrophic chrysophyte *Poterioochromonas malhamensis*. *Microbial Ecology*, *19*(1), 97–109. https://doi.org/10.1007/BF02015056

Skovgaard, A. (1996). Mixotrophy in *Fragilidium subglobosum* (Dinophyceae): growth and grazing responses as functions of light intensity. *Marine Ecology Progress Series*, *143*, 247–253. https://doi.org/10.3354/meps143247

Smith, J. L., Tong, M., Fux, E., & Anderson, D. M. (2012). Toxin production, retention, and extracellular release by *Dinophysis acuminata* during extended stationary phase and culture decline. *Harmful Algae*, *19*, 125–132. https://doi.org/10.1016/j.hal.2012.06.008

Stoecker, D. K., Long, A., Suttles, S. E., & Sanford, L. P. (2006). Effect of small-scale shear on grazing and growth of the dinoflagellate *Pfiesteria piscicida*. *Harmful Algae*, *5*(4), 407–418. https://doi.org/10.1016/j.hal.2005.11.009

Sullivan, J.M. & Swift, E. (2003). Effects of small-scale turbulence on net growth rate and size of ten species of marine dinoflagellates. *Journal of Phycology*, *39*, 83–94.

Sullivan, J. M., Swift, E., Donaghay, P. L., & Rines, J. E. B. (2003). Small-scale turbulence affects the division rate and morphology of two red-tide dinoflagellates. *Harmful Algae*, *2*(3), 183–199. https://doi.org/10.1016/S1568-9883(03)00039-8

Suzuki, T., Beuzenberg, V., Mackenzie, L., & Quilliam, M. A. (2004). Discovery of okadaic acid esters in the toxic dinoflagellate *Dinophysis acuta* from New Zealand using liquid chromatography/tandem mass spectrometry. *Rapid Communications in Mass Spectrometry*, *18*(10), 1131–1138. https://doi.org/10.1002/rcm.1455

Swanson, K. M., Flewelling, L. J., Byrd, M., Nunez, A., & Villareal, T. A. (2010). The 2008 Texas *Dinophysis ovum* bloom: Distribution and toxicity. *Harmful Algae*, *9*(2), 190–199. https://doi.org/10.1016/j.hal.2009.10.001

Terao, K., Ito, E., Yanagi, T., & Yasumoto, T. (1986). Histopathological studies on experimental marine toxin poisoning. I. Ultrastructural changes in the small intestine and liver of suckling mice induced by dinophysistoxin-1 and pectenotoxin-1. *Toxicon*, *24*(11–12), 1141–1151.

Thomas, W. H., Vernet, M., & Gibson, C. H. (1995). Effects Of Small-Scale Turbulence On Photosynthesis, Pigmentation, Cell Division, And Cell Size In The Marine Dinoflagellate *Gonyaulax Polyedra* (Dinophyceae)1. *Journal of Phycology*, *31*(1), 50–59. https://doi.org/10.1111/j.0022-3646.1995.00050.x

Tong, M., Kulis, D. M., Fux, E., Smith, J. L., Hess, P., Zhou, Q., & Anderson, D. M. (2011). The effects of growth phase and light intensity on toxin production by *Dinophysis acuminata* from the northeastern United States. *Harmful Algae*, *10*(3), 254–264. https://doi.org/10.1016/j.hal.2010.10.005

Tong, M., Smith, J., Kulis, D., & Anderson, D. (2015). Role of dissolved nitrate and phosphate in isolates of *Mesodinium rubrum* and toxin-producing *Dinophysis acuminata*. *Aquatic Microbial Ecology*, *75*(2), 169–185. https://doi.org/10.3354/ame01757

Trainer, V., Moore, L., Bill, B., Adams, N., Harrington, N., Borchert, J., da Silva, D., & Eberhart, B.-T. (2013). Diarrhetic Shellfish Toxins and Other Lipophilic Toxins of Human Health Concern in Washington State. *Marine Drugs*, *11*(6), 1815–1835. https://doi.org/10.3390/md11061815

Yasumoto, T., Murata, M., Oshima, Y., Sano, M., Matsumoto, G.K., Clardy, J. (1985). Diarrhetic shellfish toxins. Tetrahedron 41, 1019–1025. https://doi.org/10.1016/S0040-4020(01)96469-5

Zirbel, M. J., Veron, F., & Latz, M. I. (2000). The reversible effect of flow on the morphology of *ceratocorys horrida* (PERIDINIALES, DINOPHYTA) *. *Journal of Phycology*, *36*(1), 46–58. https://doi.org/10.1046/j.1529-8817.2000.98088.x

THESIS SUMMARY

Conclusions

Dinophysis and its production of diarrhetic shellfish toxins (DSTs) and pectenotoxins (PTXs) pose a threat to both human and shellfish health. The 2008 *D. ovum* bloom in Gulf of Mexico, Texas was the first shellfish bed closure in the U.S. due to DST concentrations in shellfish above regulatory levels. Since the 2008 bloom, *Dinophysis* cells and DSTs have been increasingly found on the East, West, and Gulf Coasts of the U.S. This apparent emergence of *Dinophysis* cells and toxins could be a product of changing environmental conditions, increased monitoring, or a combination of the two, and remains unresolved. *Dinophysis* is a unique harmful algal bloom (HAB) species because it can produce potent toxins at extremely low cell concentrations, and its mixotrophic nature, as well as the mixotrophic nature of its apparently obligate prey item, *Mesodinium rubrum*, means it is necessary to understand bloom dynamics of its prey and the dynamics of the cryptophyte spp. required by *M. rubrum*. Lab and field studies have also revealed a great deal of variability in both growth and toxin profiles between *Dinophysis* species, and even strains. As such, it is important to identify factors that promote or inhibit growth and toxin production on a region-to-region basis.

The main goals of this thesis were to use field and lab studies to identify abiotic and biotic factors that may be driving *Dinophysis* growth and toxin production. The first chapter was a field study that focused on *Dinophysis* bloom dynamics in Chesapeake Bay, while the second chapter was a lab study that included a cross-species and strain examination of *Dinophysis* from U.S. coastal waters. Both chapters were aimed at further understanding drivers of *Dinophysis* feeding, growth, and toxin production. Chapter 1 of this thesis identified both biotic and abiotic factors that are linked to *D. acuminata* abundance in the York River, Chesapeake Bay. The IFCB proved to be an invaluable monitoring tool because *D. acuminata* abundances did not exceed 1

cell mL^{-1} during any sampling season, which is below the limit of detection of traditional manual microscopy methods. *Dinophysis* would not have been detected without the IFCB. Important abiotic factors identified by statistical models included salinity and time of year (month), while significant biotic factors included a 14-day lagged *Mesodinium rubrum* abundance, and *Prorocentrum cordatum* abundance. The lagging of *M. rubrum* abundance agrees with previous literature for other systems, as several studies have found that lagging *M. rubrum* abundance by up to three months in predictive models adequately explains *Dinophysis* abundance. Here in Chesapeake Bay, average *Dinophysis acuminata* abundance was highest in April and May, with lower cell abundances in winter months. Additionally, *D. acuminata* abundance was significantly linked with *P. cordatum* abundance; this result suggests that there is the potential for *P. cordatum* to be used as a trigger for monitoring of *D. acuminata* out in the field, which could be useful for regulatory agencies.

The second chapter of this thesis expanded the focus from Chesapeake Bay to the Northeast and Gulf Coasts of the U.S., by incorporating three species, four strains of *Dinophysis* isolated from these locations. The effects of small-scale turbulence on dinoflagellates have been well-documented in the literature, but its effects on the genus *Dinophysis* specifically are scarce. Building off the only other study investigating the impacts of small-scale turbulence on *Dinophyssis* spp., this chapter exposed *D. acuminata* (2 strains), *D. ovum*, and *D. caudata* cultures to two levels of turbulence (high and low). Growth rates, ingestion rates, toxin content/concentration, and toxin production rates were measured or calculated for each of the four strains. Overall, a species-specific response to turbulence was observed, with *D. acuminata* strains and *D. ovum* growth being inhibited at the highest turbulence level, while *D. caudata* growth was stimulated by both low and high turbulence. There was a similar trend with net toxin

production rates; toxin production rates for *D. acuminata* strains and *D. ovum* were inhibited with higher turbulence, while *D. caudata* toxin production appeared to increase. Additionally, while an effect of turbulence on ingestion rates was not detected, turbulence did influence intra- and extracellular toxins in the cultures. Ultimately, the differential growth of the cultures because of exposure to turbulence was concluded to be the driving factor of toxin content and production rates.

Many previous studies have characterized *Dinophysis* spp. in response to a variety of environmental factors like light, temperature, salinity, and nutrients. The results of this thesis contribute to the standing knowledge of *Dinophysis* bloom dynamics and physiology in both the lab and culture setting. Due to the inherent complexity of *Dinophysis* feeding, growth, and toxin production, the results of this work can provide information to develop an early warning for *Dinophysis* blooms. Additionally, investigating predator-prey dynamics between *Dinophysis* and *Mesodinium* was important. The relationship between *Dinophysis* and another dinoflagellate, *Prorocentrum cordatum*, suggests that the correlation with the more abundant *P. cordatum* may provide an indicator of possible presence of *Dinophysis*. *Prorocentrum cordatum* can bloom at cell densities as high as 600 cells mL^{-1} in Chesapeake Bay, as evidenced by the cell abundances recorded in this study. The relationship between small-scale turbulence and several *Dinophysis* strains characterized in this study may provide information for the development of multi-factor experiments in the lab to address more realistic environmental conditions or incorporate turbulence and toxin content or production into future modeling efforts using *in situ* data. In Chesapeake Bay, *Dinophysis* cells and toxins have been found year-round, and this study provides the first steps to understanding some factors that may promote or inhibit *Dinophysis* growth in Chesapeake Bay and coasts of the U.S.

APPENDIX

APPENDIX A: CONTINUOUS TOXIN MONITORING IN YORK RIVER, VA

In addition to deployments of the IFCB off the VIMS pier to track HAB cell abundance, long-term sampling has also been conducted to track toxin concentration as part of the CBTOX (award #NA14OAR4170093) and DinoX projects (award #NA19NOS4780182). Two different sampling techniques, solid phase adsorption toxin tracking (SPATT) discs and sieved samples, were used to capture intra- and extracellular toxins in the water column from January 1 through July 1 for 2018-2022 sampling seasons.

Toxin Sampling: Methods

Toxin sampling occurred every 1-2 weeks from 2018 through 2022. At the time of sampling, two types of samples were collected: a solid phase adsorption toxin tracking (SPATT) disc, and a sieved sample, that will be referred to as a Sieve Tox sample herein. SPATTs were deployed for 1-2 weeks at a time. SPATTs were constructed and extracted based on methods from Onofrio et al. (2021). Briefly, SPATTs were constructed with HP-20 resin and stored in ultrapure water prior to deployment. After recovery of SPATTs, resin was extracted with 100% methanol and phycotoxins were quantified using ultra-performance liquid chromatography – tandem mass spectrometry, with a trapping dimension and at-column dilution (UPLC-MS/MS with trap/ACD; Onofrio et al. 2020).

To generate a Sieve Tox sample, 8-L of whole surface water were collected from the VIMS pier. The sample was then 15-μm sieved, backwashed into a 50-mL centrifuge tube, and frozen at -20˚C until analysis. To extract the Sieve Tox samples, the thawed samples were centrifuged (3200 g, 4˚C, 20 mins), and the supernatant was pipetted into a new 50-mL centrifuge tube. 1-mL of

100% methanol was then added to the remaining cell pellet and samples were vortexed for 5 seconds. The tube containing the cell pellet was bath sonified for 15 minutes, centrifuged (3200 g, 4˚C, 15mins), and the supernatant was pipetted into the 50-mL centrifuged tube with the water supernatant, and vortexed for 5 seconds. Then, a solid phase extraction (SPE) cartridge was equilibrated with 3mL of 100% methanol and 3mL of GenPure water. The sample was loaded onto the SPE cartridge, washed with another 3mL of GenPure water and 1mL of 35% methanol before being eluted in two 750-µL fractions. Samples were syringe filtered into clean mass spec vials, and a 500-µL fraction of the sample was transferred to a new autosampler vial to undergo base hydrolysis. Samples were then analyzed on the LC-MS/MS and phycotoxins quantified within methanol extracts.

Both SPATT and Sieve Tox samples were collected from 2018-2022 as part of the CBTOX and DinoX projects. All SPATT data as presented as non-base hydrolyzed, while Sieve Tox samples are presented as base hydolyzed (BH). DSTs are presented as the sum of OA and DTX-1.

Toxin Sampling: Results

Toxins on SPATTs

For all years of SPATT data, DST concentrations were always higher than PTX-2 (except early April 2020). The highest observed toxin concentration on SPATTs occurred in 2018, with a peak concentration of 13.88 ng DST g resin^{-1} day^{-1} (Figure A1). DSTs and PTX-2 did not show any strong peaks during the 2019 and 2021 sampling seasons; neither DST nor PTX-2 concentrations exceeded 5 ng toxin g resin^{-1} day^{-1} (Figure A1). In 2020, the concentration of PTX-2 exceeded 5 ng toxin g resin^{-1} day^{-1} once in early April, while DST concentration exceeded this threshold in late June (Figure A1). DSTs were elevated in 2018 and 2022 compared to the

other sampling seasons. In 2018, the peak in DST concentration occurred in late January, and steadily decreased to below 5 ng DST g resin^{-1} day^{-1} by the end of the sampling season. There was a small peak in PTX-2 concentration coincident with a marginal increase in DST concentrations on May 31, 2018 (Figure A1). Other than this small increase, PTX-2 concentrations were at background levels for the duration of the 2018 season. A similar trend was seen during the 2022 sampling season, with the peak in DST concentration occurring in mid-February, approximately a month later than 2018 (Figure A1). The peak DST concentration in 2022 was 10.21 ng DST g resin^{-1} day^{-1} (Figure A1). After the peak in DSTs, there was a steady decline until late May, followed by a slight increase in both DSTs and PTX-2 on the last day of sampling, June 1st (Figure A1).

Toxins in sieved samples

For all years of sieved data, PTX-2 was always higher than DSTs when both toxins were detected (Figure A2). The highest observed toxin concentration in sieved samples occurred in 2019, with a peak concentration of 9.39 ng PTX-2 L^{-1} (Figure A2). The PTX-2 concentration in 2020 and 2022 did not exceed 5 ng toxin L^{-1} (Figure A2). In 2020, there were two small peaks of PTX-2 at the beginning of March and beginning of April (Figure A2). There were also two small peaks in PTX-2 concentration in 2022, with one occurring mid-February and one at the end of March (Figure A2). The timing of the peak of PTX-2 was essentially identical in 2018 and 2019, occurring in mid-May of both years. Toxin concentrations abruptly increased for 1-3 sampling points, and then abruptly decreased back to background levels (Figure A2). DST concentrations in both years slightly increased during the peak in PTX-2 concentration. During 2021, the peak in PTX-2 concentrations occurred earlier in the year (January – March) compared to 2018 and

2019; there was a steady decline in PTX-2 to background concentrations following the peak (Figure A2).

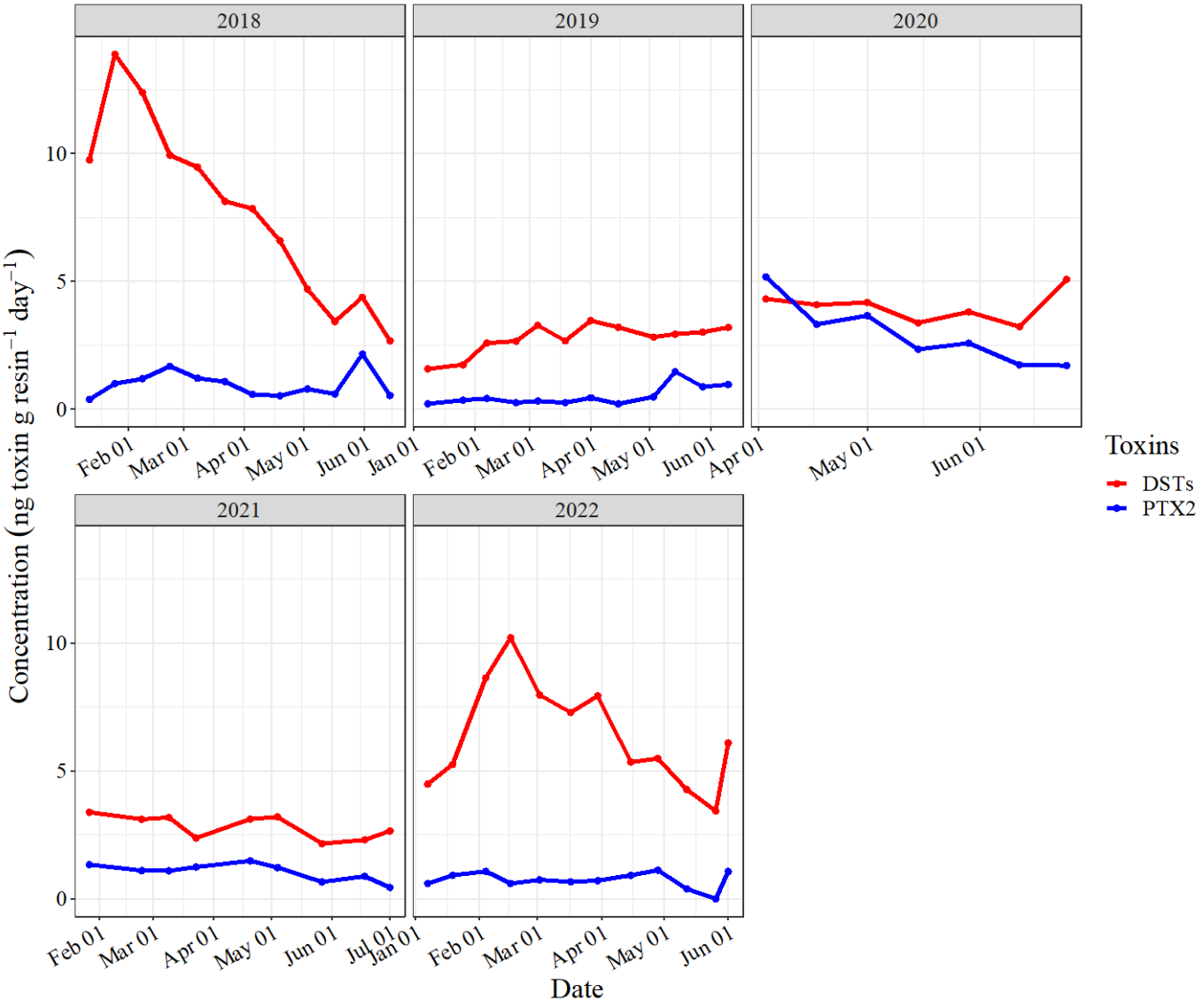

Figure A1 Concentration (ng toxin g resin^{-1} day^{-1}) of DSTs (OA + DTX-1) and PTX-2 on SPATTs collected from the York River from 2018 through 2022.

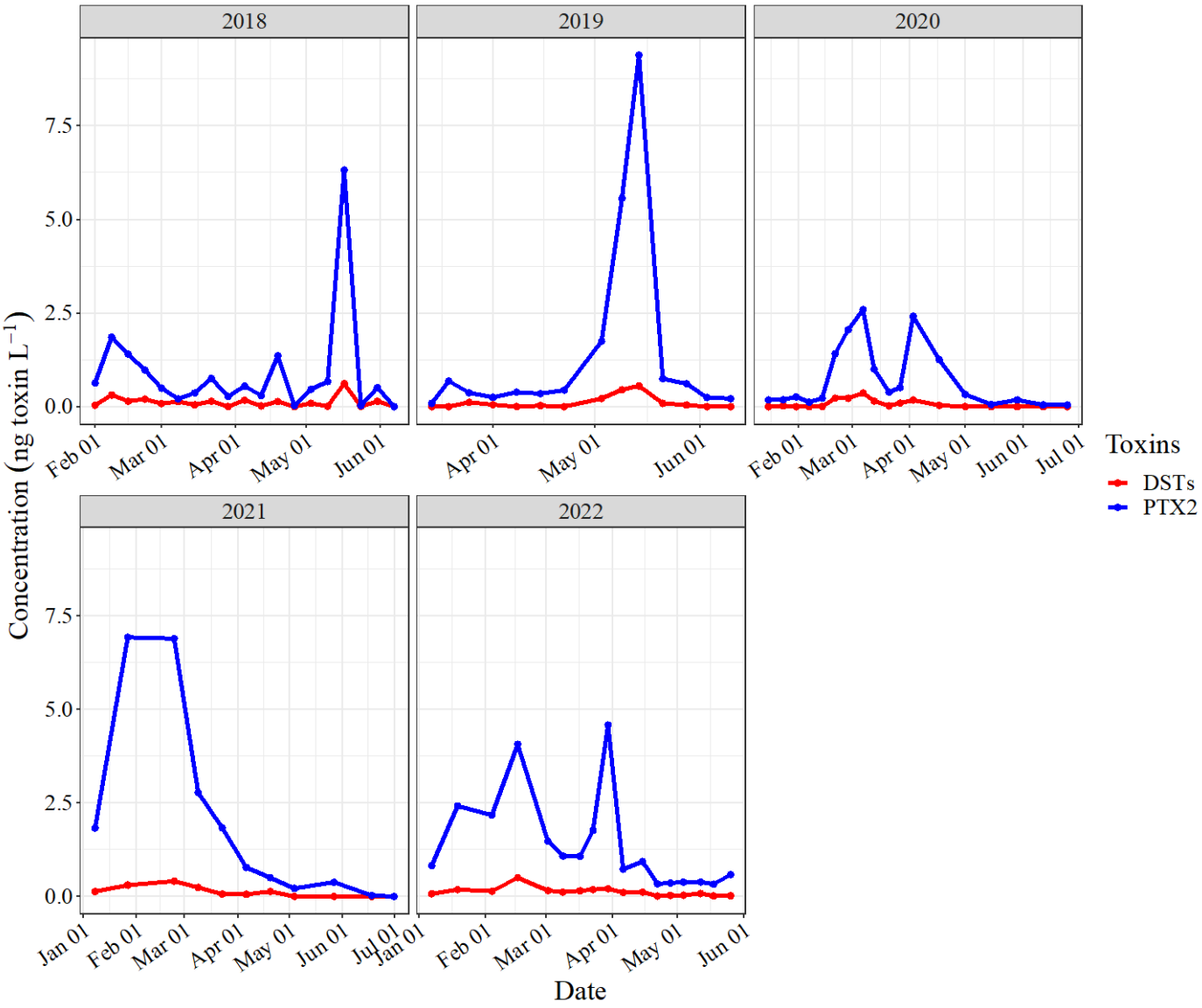

Figure A2 Concentration (ng toxin L^{-1}) of DSTs (OA + DTX-1) and PTX-2 from sieved samples collected from the York River from 2018 through 2022.